THE QUARTERLY JOURNAL OF MECHANICS AND APPLIED MATHEMATICS

VOLUME II PART 3

SEPTEMBER 1949

OXFORD

AT THE CLARENDON PRESS

1949

Price 12*s.* 6*d. net*

PRINTED IN GREAT BRITAIN BY CHARLES BATEY AT THE UNIVERSITY PRESS, OXFORD

THE QUARTERLY JOURNAL OF MECHANICS AND APPLIED MATHEMATICS

THE QUARTERLY JOURNAL OF MECHANICS AND APPLIED MATHEMATICS is published at 12*s.* 6*d.* net for a single number with an annual subscription (for four numbers) of 40*s.* post free.

NOTICE TO CONTRIBUTORS

1. *Communication.* Papers should be communicated to one or other of the Executive Editors, by name, at King's College, Strand, London, W.C. 2.

2. *Presentation.* Manuscripts should preferably be typewritten, and each paper should be preceded by a summary not exceeding 300 words in length. References to literature should be given in standard order, *author, title of journal, volume number, date, page.* These should be placed at the end of the paper and arranged according to the order of reference in the paper.

3. *Diagrams.* The number of diagrams should be kept to the minimum consistent with clarity. The lines of the figures should be drawn in ink either on draughtsman's paper or on good quality white paper. Each individual line in the figure should bear reducing to one-half of the size of the original, and great care should be exercised to see that the lines are regular in thickness, especially where they meet. Lettering of the figure should be in pencil and should be sufficient to define clearly the lines and curves in it. The writing of formulae or of explanations on the diagram itself should be avoided. All explanations of symbols, etc., should be given in underline. Contributors should indicate on their manuscripts where figures should be inserted.

4. *Tables.* Tables should preferably be arranged so that they can be printed with the columns parallel to the longer edge of the page.

5. *Vector Notation.* All single letters used to denote vectors in the manuscript should be marked by underlining with a wavy line. Scalar and vector products should be denoted by $\underset{\sim}{a} . \underset{\sim}{b}$ and $\underset{\sim}{a} \wedge \underset{\sim}{b}$ respectively.

6. *Offprints.* Authors of papers will be entitled to 25 free offprints.

7. All correspondence other than that dealing with contributions should be addressed to the Publisher:

GEOFFREY CUMBERLEGE
OXFORD UNIVERSITY PRESS
AMEN HOUSE, LONDON, E.C. 4

BUCKLING OF CONTINUOUS BEAMS ON ELASTIC SUPPORTS

By J. M. KLITCHIEFF (*High School of Technology, Belgrade*)

[Received 3 January 1949]

SUMMARY

It is sometimes necessary to select the rigidity of intermediate elastic supports of a beam so that they behave as though they were absolutely rigid when the beam buckles on being subjected to longitudinal compression. The usual method of solving the problem leads to the tedious work of developing a determinant of order $m-1$ and of solving an equation of degree $m-1$, m being the number of spans. The author represents the deflexion curve by trigonometric series and arrives at equation (6′), which is more convenient for practical use. The value of the rigidity obtained differs by less than 2·6 per cent. from the true value.

Introduction

Let us consider a continuous beam (Fig. 1) of constant cross-section simply supported at the ends on rigid supports 0 and m and having equally spaced intermediate elastic supports 1, 2,..., $m-1$ of equal rigidity. The

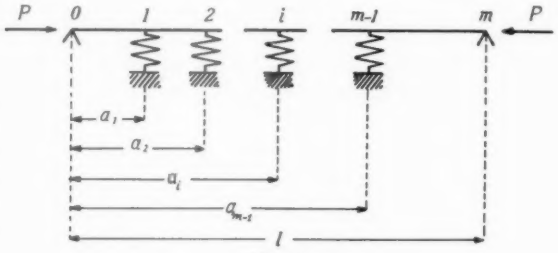

Fig. 1.

beam is subjected to longitudinal compression by forces P applied at the ends. It is sometimes necessary to select the common rigidity of the intermediate supports so that they will not deflect when the beam buckles and therefore be equivalent to absolutely rigid supports.

This problem was first discussed by I. G. Boobnov (**1**), who used the following method. Calculating the deflexion of a simple beam submitted to the simultaneous action of compressive force P and lateral reactions R_1, R_2,..., R_{m-1} of the elastic supports, and putting the deflexion of a support i equal to $\mathfrak{A}R_i$ ($\mathfrak{A}$ being the 'spring constant' of the support, that is, the deflexion produced in the support by the unit load), he arrived at $m-1$ equations with $i = 1, 2,..., m-1$.

[Quart. Journ. Mech. and Applied Math., Vol. II, Pt. 3 (1949)]
5092.7

The buckling of the beam becomes possible when these linear and homogeneous equations yield a solution for R_1, R_2,..., R_{m-1} different from zero. Hence the critical values of P are found by setting the determinant of the equations equal to zero. It leads to an equation of degree $m-1$ and the roots determine the values of P corresponding to the buckling of the beam into 1, 2,..., $m-1$ half-waves (shown on Figs. 2 and 3 for $m = 3$). If $\mathfrak{A}$ is a given number some of these values can become smaller

FIG. 2.

FIG. 3.

FIG. 4.

than the force P_m corresponding to the buckling into m half-waves (Fig. 4, for $m = 3$), when every intermediate support becomes an inflexion point.

To determine the limiting value of $\mathfrak{A}$ at which the intermediate supports still behave as though they were absolutely rigid, I. G. Boobnov introduced into the equation for P the value P_m and arrived at $m-1$ values of $\mathfrak{A}$ as roots of the equation. The smallest of them is the limiting value required.

This method of solving the problem is a logical one, but it leads to developing a determinant of order $m-1$ and to solving an equation of degree $m-1$. This work becomes tedious if the number of spans is not small. It was done by I. G. Boobnov for $m = 2, 3, 4, 5, 6, 7, 9$, and 11. From the numerical values obtained he concluded that $\mathfrak{A}$ approaches a certain limit as the number of spans increases; an explanation of this statement was given later by S. Timoshenko (**2**). The representation of the deflexion-curve in the form of trigonometric series is especially useful in this case and leads, as is shown below, to the very simple formula (6′) giving the general solution of the problem for any number of spans.

Details of numerical solution

We start from the known differential equation for the deflexion-curve of a beam submitted to the simultaneous action of a lateral load and of an

axial compressive force P (Fig. 5):

$$EIu''+\mathfrak{M} = -Pu. \tag{1}$$

Here EI denotes the flexural rigidity of the beam and $\mathfrak{M}$ the bending moment produced by the lateral force Q alone. It can be represented in the form of the trigonometric series

$$\mathfrak{M} = \frac{2}{\pi^2} Ql \sum_{k=1}^{\infty} \frac{1}{k^2} \sin\frac{k\pi a}{l} \sin\frac{k\pi x}{l},$$

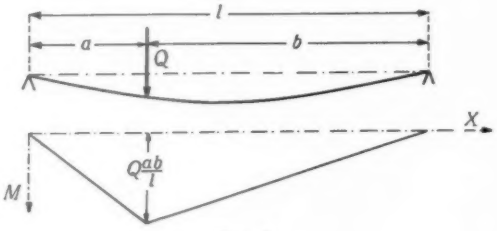

FIG. 5.

or, if we replace Q by $-u_i/\mathfrak{A}$ (u_i being the deflexion at $x = a_i$):

$$\mathfrak{M} = -\frac{2}{\pi^2} \frac{l}{\mathfrak{A}} u_i \sum_{k=1}^{\infty} \frac{1}{k^2} \sin\frac{k\pi a_i}{l} \sin\frac{k\pi x}{l}.$$

We assume that the deflexion-curve can also be represented by a trigonometric series

$$u = \sum_{n=1}^{\infty} c_n \sin\frac{n\pi x}{l}; \tag{2}$$

then

$$\mathfrak{M}_i = -\frac{2}{\pi^2} \frac{l}{\mathfrak{A}} \sum_{n=1}^{\infty} c_n \sin\frac{n\pi x}{l} \sum_{k=1}^{\infty} \frac{1}{k^2} \sin\frac{k\pi a_i}{l} \sin\frac{k\pi x}{l}.$$

The bending moment produced by the simultaneous action of the lateral forces $R_1, R_2, \ldots, R_{m-1}$ will be

$$\mathfrak{M} = \sum_{i=1}^{m-1} \mathfrak{M}_i = -\frac{2}{\pi^2} \frac{l}{\mathfrak{A}} \sum_{i=1}^{m-1} \sum_{n=1}^{\infty} c_n \sin\frac{n\pi a_i}{l} \sum_{k=1}^{\infty} \frac{1}{k^2} \sin\frac{k\pi a_i}{l} \sin\frac{k\pi x}{l},$$

or

$$\mathfrak{M} = -\frac{2}{\pi^2} \frac{l}{\mathfrak{A}} \sum_{k=1}^{\infty} c_k \sum_{i=1}^{m-1} \sin\frac{k\pi a_i}{l} \sum_{n=1}^{\infty} \frac{1}{n^2} \sin\frac{n\pi a_i}{l} \sin\frac{n\pi x}{l}. \tag{3}$$

Introducing the expressions (2) and (3) into (1)

$$EI\left(\frac{n\pi}{l}\right)^2 c_n + \frac{2}{\pi^2} \frac{l}{\mathfrak{A}} \frac{1}{n^2} \sum_{k=1}^{\infty} c_k \sum_{i=1}^{m-1} \sin\frac{k\pi a_i}{l} \sin\frac{n\pi a_i}{l} = Pc_n,$$

we get
$$n^4c_n+2\Omega\sum_{k=1}^{\infty}c_k\sum_{i=1}^{m-1}\sin\frac{k\pi a_i}{l}\sin\frac{n\pi a_i}{l}=\gamma n^2c_n, \tag{4}$$

where the following notations are introduced,

$$\Omega=\frac{l^3}{\pi^4EI\mathfrak{A}}, \qquad \gamma=\frac{Pl^2}{\pi^2EI}.$$

If the intermediate supports are equally spaced, $a_i=il/m$, and it follows from (4) that

$$n^4c_n+\Omega\sum_{k=1}^{\infty}c_kK(n,k)=\gamma n^2c_n, \tag{5}$$

where
$$K(n,k)=2\sum_{i=1}^{m-1}\sin\frac{ni\pi}{m}\sin\frac{ki\pi}{m}.$$

This coefficient vanishes when k or n are integral multiples of m. If they are not, then

$$K(n,k)=\sum_{i=1}^{m-1}\left\{\cos\frac{i(k-n)\pi}{m}-\cos\frac{i(k+n)\pi}{m}\right\}.$$

Using the known expression for trigonometric polynomials

$$\sum_{i=1}^{m-1}\cos i\theta=-\frac{1}{2}+\frac{1}{2}\frac{\sin(m-\frac{1}{2})\theta}{\sin\frac{1}{2}\theta},$$

it is easy to prove that $K(n,k)=m$, if $k=n+2jm$ $(j=1,2,\ldots)$ and that $K(n,k)=-m$, if $k=-n+2jm$. For all other values of k the coefficient K vanishes.

Thus for values of n which are integral multiples of m we obtain from (5) a group of independent equations

$$1^2m^2=\gamma,$$
$$2^2m^2=\gamma,$$
$$\ldots\ldots$$
$$\ldots\ldots$$

corresponding to the buckling of the beam into m, $2m$,... half-waves. The smallest value of the critical force P_m is given by the first of them

$$\gamma_m=m^2,$$

which corresponds to the buckling into m half-waves.

For values of n which are not integral multiples of m we obtain homogeneous linear equations in the coefficients c_n. These equations can be divided into $m-1$ independent systems. Setting their determinants equal to zero, we obtain $m-1$ values of the critical force, corresponding to buckling into

1, 2,..., $m-1$ half-waves. For example, the equation corresponding to the buckling into $m-r$ half-waves would be

$$\begin{vmatrix} (m-r)^4-(m-r)^2\gamma+m\Omega & -m\Omega & m\Omega & . & . \\ -m\Omega & (m+r)^4-(m+r)^2\gamma+m\Omega & -m\Omega & . & . \\ m\Omega & -m\Omega & (3m-r)^4-(3m-r)^2\gamma+m\Omega & . & . \\ . & . & . & . & . \\ . & . & . & . & . \end{vmatrix} = 0.$$

We impose the condition that this force must not be smaller than the force required for buckling into m half-waves and replace γ by m^2

$$\begin{vmatrix} [(m-r)^2-m^2](m-r)^2+m\Omega & -m\Omega & m\Omega & . & . \\ -m\Omega & [(m+r)^2-m^2](m+r)^2+m\Omega & -m\Omega & . & . \\ m\Omega & -m\Omega & [(3m-r)^2-m^2](3m-r)^2+m\Omega & . & . \\ . & . & . & . & . \\ . & . & . & . & . \end{vmatrix} = 0.$$

We retain $2n$ columns and $2n$ rows in the determinant and add every column to the foregoing one. Then, developing the determinant in terms of the constituents of the last column and increasing n to ∞, we obtain

$$m\Omega \sum_{s=1,3,5\ldots}^{\infty} \left\{ \frac{1}{[(sm-r)^2-m^2](sm-r)^2} + \frac{1}{[(sm+r)^2-m^2](sm+r)^2} \right\} = -1, \tag{5'}$$

or

$$\Omega(1-R) = \frac{(4m^2-r^2)(m^2-r^2)^2}{2m(5m^2+r^2)}, \tag{6}$$

where

$$R = \frac{(4m^2-r^2)(m^2-r^2)^2}{2(5m^2+r^2)} \sum_{s=3}^{\infty} \left\{ \frac{1}{[(sm-r)^2-m^2](sm-r)^2} + \right.$$
$$\left. + \frac{1}{[(sm+r)^2-m^2](sm+r)^2} \right\}.$$

The greatest value of R corresponds to $r = 1$, and

$$R < \sum_{s=3}^{\infty} \frac{(4m^2-1)(m^2-1)^2}{(5m^2+1)[(sm-1)^2-m^2](sm-1)^2}$$

$$< \sum_{s=3}^{\infty} \frac{2m(2m+1)(m+1)^2}{5m^2(s^2m^2-2sm+1-m^2)s^2} = \frac{2}{5m} \sum_{s=3}^{\infty} \frac{m^3\left(2+\frac{5}{m}+\frac{4}{m^2}+\frac{1}{m^3}\right)}{s^4m^2\left(1-\frac{2}{sm}-\frac{1}{s^2}\right)}$$

$$< \frac{2}{5} \sum_{s=3}^{\infty} \frac{2+\frac{5}{2}+1+\frac{1}{8}}{s^4(1-\frac{1}{3}-\frac{1}{9})} = \frac{81}{20} \sum_{s=3}^{\infty} \frac{1}{s^4} = \frac{81}{20}\left(\frac{\pi^4}{96}-1\right) = 0{\cdot}059,$$

so that it can be omitted from (6). Thus the greatest value of Ω is

$$\Omega = \frac{(4m^2-1)(m^2-1)^2}{2m(5m^2+1)}, \tag{6'}$$

and

$$\mathfrak{A} = \frac{l^3}{\pi^4 EI\Omega}.$$

Instead of $\mathfrak{A}$, I. G. Boobnov used

$$\Phi = \pi^2 m^3 \frac{EI}{l^3}\mathfrak{A} = \frac{2}{\pi^3}\frac{m^4(5m^2+1)}{(m^2-1)^2(4m^2-1)}. \tag{7}$$

Conclusion

The comparative table appended below gives the results of equation (7) and the values of Φ as calculated by I. G. Boobnov. Increasing m to ∞ we obtain from equation (7) the value 0·253; but if we also retain the second term of the series (5′), the value 0·250 is obtained, which agrees with the value indicated by I. G. Boobnov.

$m =$	2	3	4	5	6	7	9	11
I. G. Boobnov	0·500	0·333	0·293	0·276	0·268	0·263	0·258	0·255
Equation (7)	0·504	0·337	0·296	0·280	0·271	0·265	0·261	0·259

REFERENCES

1. I. G. Boobnov, *Theory of Structure of Ships*, p. 259 (St. Petersburg, 1912).
2. S. Timoshenko, *Theory of Elastic Stability*, p. 108 (New York, 1936).

ANALYSIS OF CONTINUOUS STRUCTURES BY THE STIFFNESS FACTORS METHOD

By LEROY A. BEAUFOY *and* A. F. S. DIWAN

(*College of Estate Management, 11 Great George Street, London, S.W.1*)

[Received 16 October 1948]

SUMMARY

The paper presents an 'exact' method of analysis of highly redundant two-dimensional continuous structures. No simultaneous equations are used, and all calculations may be done by slide rule. The method is a mathematical analogue of the experimental one using unloaded models. The general case is considered, but for ordinary use considerable simplification is possible. The procedure is illustrated by an example of a three-span continuous-arch system involving nine redundancies.

Introduction

THE stiffness factors method was developed using the concept of a hypothetical unloaded model imagined to be manipulated in the same way as an actual model (**1**); influence lines may be found, or moments and forces for a given loading computed directly. The distinctive characteristic of the experimental method is retained, that is, a structural analysis is first made of the unloaded structure. This analysis, which yields information about the deformation of the structure as a whole due to any given imposed distortion, is viewed as an expression of the elastic properties of the structure, which are independent of the loading carried by it. Once these are known the effect of any loading which does not strain the structure beyond the elastic range is easily investigated. Joint displacements in rotation and translation are found. For a loaded structure, these are obtained as direct displacements due to unbalanced fixed-end reactions on a joint plus displacements induced at the joint by balancing other joints. The total joint displacement being known, end moments and forces acting on members can be computed without using simultaneous equations or successive approximations.

Definitions

Stiffness factors

The stiffness factors for a member end or joint are the moment and the horizontal and vertical forces required at that end, or joint, to produce unit displacement there. These factors are called *horizontal displacement,*

vertical displacement, or *rotation* stiffness factors according to the direction of the displacement.

The stiffness factors for the end A of a member AB in a structure are called *restrained* or *actual* respectively when the far end B is assumed fixed or free to move (together with all other joints in the structure on the same side of A as B) to the extent which the stiffness of the members permits.

Stiffness factors for joint B are called *modified* or *actual* respectively when they give the stiffness of joint B when joint A is assumed fixed or free to move in conformity with the stiffness characteristics of the structure as a whole.

Displacement coefficients

The displacement coefficients for a member end or joint are the displacements due to unit moment or unit horizontal or vertical force applied at the end or joint. The displacement coefficients for joint B are called *modified* or *actual* respectively when the neighbouring joint A is assumed fixed or free to move in conformity with the stiffness characteristics of the structure as a whole.

Induced movements

A unit rotational, horizontal, or vertical displacement applied at joint A will, in general, induce a movement of joint B, which can be resolved into rotational, horizontal, and vertical components; these are called *induced movements*. In turn, they induce further movements at the next joint C, and so on.

Notation and sign convention

Symbols used without subscripts

ϕ	rotational displacements
Δ	horizontal displacements
λ	vertical displacements
m, M	moment
h, H	horizontal force
v, V	vertical force
x, y	horizontal and vertical coordinate distances, respectively
$\bar{x}, \bar{y}$	horizontal and vertical coordinates respectively of the elastic centre
EI	flexural rigidity of a structural member or unit
$\bar{S}$	elastic area of a structural member or unit
ds	elementary length of a member
AB	member AB; end A of member AB
k	a determinant

Subscripts

ϕ denotes that the quantity is in respect of applied rotational displacements

Δ denotes that the quantity is in respect of applied horizontal displacements

λ denotes that the quantity is in respect of applied vertical displacements

m denotes that the quantity is in respect of applied moment

h denotes that the quantity is in respect of applied horizontal force

v denotes that the quantity is in respect of applied vertical force

Superscripts

bc denotes that the quantity is in respect of the member BC

B denotes that the quantity is in respect of the joint B

Symbols used with subscripts ϕ, Δ, λ

m, h, v Moment, horizontal force, and vertical force respectively, acting simultaneously on one end of a member to produce unit displacement there when the other end of the member is restrained in the same manner as in the structure (actual stiffness factors for member ends)

m', h', v' As for m, h, v but when the other end of the member is considered fixed (restrained stiffness factors for member ends)

M, H, V Moment, horizontal force, and vertical force respectively, acting simultaneously at a joint to produce unit displacement there when all the other joints are restrained in the same manner as in the structure (actual stiffness factors for joints)

M', H', V' As for M, H, V but when the far end of one of the members connected to the joint is considered fixed (modified stiffness factors for joints)

ϕ, Δ, λ Rotational, horizontal, and vertical displacement respectively, produced at one joint of a structure by unit displacement applied elsewhere in the structure (induced movements)

Symbols used with subscripts m, h, v

ϕ, Δ, λ Rotational, horizontal, and vertical displacement respectively, produced at one joint of a structure by unit moment or force applied at the joint (actual displacement coefficients)

ϕ', Δ', λ' (Modified displacement coefficients corresponding to the above)

Others

c Carry-over factor for moments or forces

I_x Centroidal moment of inertia of a member or structural unit about the x-axis

I_y Centroidal moment of inertia of a member or structural unit about the y-axis

I_{xy} Centroidal product of inertia about axes x, y

$I'_x = I_x - (I^2_{xy}/I_y)$

$I'_y = I_y - (I^2_{xy}/I_x)$

Sign convention

Moments and rotational displacements are taken as positive when clockwise; horizontal and vertical forces, displacements, and coordinate distances as positive when measured to the right and upwards respectively.

Displacements of an elastic member

Let Fig. 1 represent a member AB, of flexural rigidity EI, fixed at B.

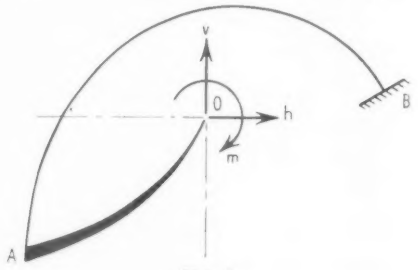

FIG. 1.

Imagine a rigid arm to extend from end A to the elastic centre O; at O let there be a vertical force v, a horizontal force h, and a moment m; take O as the origin of axes Ox and Oy.

When m is unity and acts alone we have

$$\phi = \int ds/EI = \bar{S} \tag{1a}$$

$$\Delta = -\int y\, ds/EI = 0 \tag{1b}$$

$$\lambda = \int x\, ds/EI = 0. \tag{1c}$$

When h is unity and acts alone we have

$$\phi = -\int y\, ds/EI = 0 \tag{2a}$$

$$\Delta = \int y^2\, ds/EI = I_x \tag{2b}$$

$$\lambda = -\int xy\, ds/EI = -I_{xy}. \tag{2c}$$

When v is unity and acts alone we have

$$\phi = \int x\, ds/EI = 0 \tag{3a}$$

$$\Delta = -\int xy\, ds/EI = -I_{xy} \tag{3b}$$

$$\lambda = \int x^2\, ds/EI = I_y. \tag{3c}$$

When m, h, and v are given any values and act simultaneously the total displacements of the elastic centre are given by

$$\phi = m\bar{S} \tag{4a}$$

$$\Delta = hI_x - vI_{xy} \tag{4b}$$

$$\lambda = vI_y - hI_{xy}. \tag{4c}$$

Transfer the origin of the x- and y-axes to end A and let the coordinates of the elastic centre O be $\bar{x}$ and $\bar{y}$. Then the displacements of end A are given by

$$\phi = m\bar{S} \tag{5a}$$

$$\Delta = hI_x - vI_{xy} - \phi\bar{y} \tag{5b}$$

$$\lambda = vI_y - hI_{xy} + \phi\bar{x}. \tag{5c}$$

The quantities $\bar{S}$, I_x, I_y, and I_{xy} above, together with the coordinates $\bar{x}, \bar{y}$ of the elastic centre with respect to end A, are called the *elastic constants*.

Restrained stiffness factors

Suppose (Fig. 2) that a moment m and forces h and v are required at O

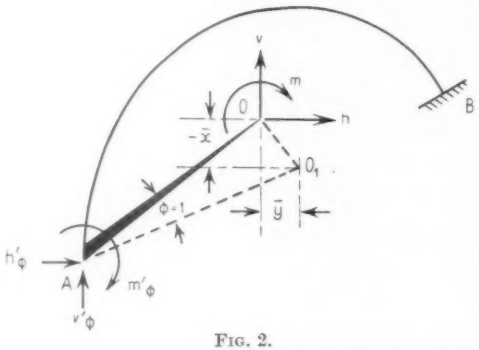

FIG. 2.

to produce a unit rotation of end A without translation, that point O moves to O_1, and that the horizontal translation of O is $\bar{y}$, and the vertical translation is $(-\bar{x})$. From equations (4) we have

$$\phi = m\bar{S} = 1 \tag{6a}$$

$$\Delta = hI_x - vI_{xy} = \bar{y} \tag{6b}$$

$$\lambda = vI_y - hI_{xy} = -\bar{x}, \tag{6c}$$

from which we deduce that

$$m = 1/\bar{S} \tag{7a}$$

$$h = \frac{\bar{y}}{I'_x} - \frac{\bar{x}I_{xy}}{I'_x I_y} \tag{7b}$$

$$v = \frac{\bar{y}I_{xy}}{I'_y I_x} - \frac{\bar{x}}{I'_y}. \tag{7c}$$

The corresponding values at A are given by

$$m'_\phi = \frac{1}{\bar{S}} + \frac{\bar{y}^2}{I'_x} + \frac{\bar{x}^2}{I'_y} - \frac{2\bar{x}\bar{y}I_{xy}}{I'_x I_y} \tag{8a}$$

$$h'_\phi = \frac{\bar{y}}{I'_x} - \frac{\bar{x}I_{xy}}{I'_x I_y} \tag{8b}$$

$$v'_\phi = \frac{\bar{y}I_{xy}}{I'_y I_x} - \frac{\bar{x}}{I'_y}. \tag{8c}$$

These values are the restrained rotation stiffness factors for end A of member AB.

Horizontal displacement

Suppose that a unit horizontal displacement is imposed on end A without permitting rotation or vertical translation there; the moment m'_Δ, and forces h'_Δ and v'_Δ required at A, viz. the restrained horizontal displacement stiffness factors there, may be shown to be

$$m'_\Delta = \frac{\bar{y}}{I'_x} - \frac{\bar{x}I_{xy}}{I'_x I_y} \tag{9a}$$

$$h'_\Delta = 1/I'_x \tag{9b}$$

$$v'_\Delta = I_{xy}/I'_x I_y. \tag{9c}$$

Vertical displacement

Similarly the restrained vertical displacement stiffness factors are given by

$$m'_\lambda = \frac{\bar{y}I_{xy}}{I'_y I_x} - \frac{\bar{x}}{I'_y} \tag{10a}$$

$$h'_\lambda = I_{xy}/I'_x I_y \tag{10b}$$

$$v'_\lambda = 1/I'_y. \tag{10c}$$

As the far end B is fixed, the restrained stiffness factors given above are also the actual stiffness factors for end A.

Horizontal prismatic member

For a straight horizontal prismatic member AB of length L and constant flexural rigidity EI, the elastic constants and stiffness factors for three particular cases are given in Tables 1 and 2 respectively.

TABLE 1. *Elastic constants for a horizontal prismatic member*

Elastic constant	*Condition of right-hand end*					
	Fixed		*Hinged*		*Freely supported*	
$\bar{S}$	L/EI		∞		∞	
$\bar{x}$	$L/2$	$-L/2$	L	0	L	0
I_x	0		0		∞	
I_y	$L^3/12EI$		$L^3/3EI$		$L^3/3EI$	
I_{xy}	0		0		0	

TABLE 2. *Stiffness factor values for left-hand end of a horizontal prismatic member*

Stiffness factors for left-hand end	*Condition of right-hand end*		
	Fixed	*Hinged*	*Freely supported*
m'_ϕ	$4EI/L$	$3EI/L$	$3EI/L$
$h'_\phi = m'_\Delta$	0	0	0
$v'_\phi = m'_\lambda$	$-6EI/L^2$	$-3EI/L^2$	$-3EI/L^2$
h'_Δ	∞	∞	0
$h'_\lambda = v'_\Delta$	0	0	0
v'_λ	$12EI/L^3$	$3EI/L^3$	$3EI/L^3$

Joint stiffness factors and balancing equations

The actual stiffness factors for a joint are the sums of the relevant stiffness factors for the ends of all members connected with the joint, since any unit displacement imposed on the joint also imposes unit displacements on all such ends. Thus, for example, the actual rotation stiffness factors are

$$M_\phi = \sum m_\phi; \qquad H_\phi = \sum h_\phi; \qquad V_\phi = \sum v_\phi.$$

To determine the induced movements at the joint B and the actual stiffness factors for the end A of member AB (Fig. 4), modified stiffness factors for the joint B, which give the stiffness of that joint when the joint A is assumed fixed, are used. They are equal to the sums of the actual factors for the ends of all members connected to the joint B, excluding BA, plus the restrained factor for BA. Thus

$$M'_\phi = m^{bc}_\phi + m^{bf}_\phi + m'^{ba}_\phi \tag{11a}$$

$$H'_\phi = h^{bc}_\phi + h^{bf}_\phi + h'^{ba}_\phi. \tag{11b}$$

The modified stiffness factors for a joint therefore depend on whether it is approached from the left or the right.

Since the actual stiffness factors for a joint represent the moment and forces required to produce a unit displacement there, it follows that if the joint has simultaneous movements ϕ, Δ, and λ, the required values M, H, and V are given by the following balancing equations

$$M = \phi M_\phi + \Delta M_\Delta + \lambda M_\lambda \tag{12a}$$

$$H = \phi H_\phi + \Delta H_\Delta + \lambda H_\lambda \tag{12b}$$

$$V = \phi V_\phi + \Delta V_\Delta + \lambda V_\lambda. \tag{12c}$$

Displacement coefficients

When M is unity and acts alone we have

$$\phi_m M_\phi + \Delta_m M_\Delta + \lambda_m M_\lambda = 1 \tag{13a}$$

$$\phi_m H_\phi + \Delta_m H_\Delta + \lambda_m H_\lambda = 0 \tag{13b}$$

$$\phi_m V_\phi + \Delta_m V_\Delta + \lambda_m V_\lambda = 0. \tag{13c}$$

If
$$k = \begin{vmatrix} M_\phi & M_\Delta & M_\lambda \\ H_\phi & H_\Delta & H_\lambda \\ V_\phi & V_\Delta & V_\lambda \end{vmatrix}$$
$$= M_\phi(H_\Delta V_\lambda - H_\lambda^2) - H_\phi(H_\phi V_\lambda - H_\lambda V_\phi) + V_\phi(H_\phi H_\lambda - H_\Delta V_\phi),$$

in which use is made of the reciprocal relations $M_\Delta = H_\phi$, $M_\lambda = V_\phi$, $V_\Delta = H_\lambda$, the solution of equations (13), representing the displacement coefficients for moment, can be written

$$\phi_m = (H_\Delta V_\lambda - H_\lambda^2)/k \tag{14a}$$

$$\Delta_m = -(H_\phi V_\lambda - H_\lambda V_\phi)/k \tag{14b}$$

$$\lambda_m = (H_\phi H_\lambda - H_\Delta V_\phi)/k. \tag{14c}$$

These values, together with those for the displacement coefficients for vertical and horizontal forces, which can be found in a similar manner, are collected together in Table 3 (column 2). Expressions for special cases

TABLE 3. *Displacement coefficients in terms of stiffness factors*

Displacement coefficient (1)	*Nature of joint displacement*			
	Rotation and translation in any direction (2)	*Rotation and vertical translation only* (3)	*Rotation and horizontal translation only* (4)	*Rotation only* (5)
ϕ_m	$A/(AM_\phi - BH_\phi + CV_\phi)$	V_Δ/D	H_Δ/E	$1/M_\phi$
$\lambda_m = \phi_v$	$C/(AM_\phi - BH_\phi + CV_\phi)$	$-V_\phi/D$	0	0
$\Delta_m = \phi_h$	$-B/(AM_\phi - BH_\phi + CV_\phi)$	0	$-H_\phi/E$	0
Δ_h	$D/(AM_\phi - BH_\phi + CV_\phi)$	0	M_ϕ/E	0
λ_v	$E/(AM_\phi - BH_\phi + CV_\phi)$	M_ϕ/D	0	0
$\Delta_v = \lambda_h$	$F/(AM_\phi - BH_\phi + CV_\phi)$	0	0	0

$A = H_\Delta V_\lambda - H_\lambda^2$; $B = H_\phi V_\lambda - H_\lambda V_\phi$; $C = H_\phi H_\lambda - H_\Delta V_\phi$; $D = M_\phi V_\lambda - V_\phi^2$;
$E = M_\phi H_\Delta - H_\phi^2$; $F = H_\phi V_\phi - M_\phi H_\lambda$

of restricted movements of joints are easily obtained from them (columns 3–5). If actual stiffness factors are used in this table, the resulting displacement coefficients give the actual displacements of the joints; if modified stiffness factors are used, the resulting displacement coefficients give the displacements of the joint for the condition to which the modified stiffness factors apply.

When M, H, and V are given any values and act simultaneously, the balancing movements at the joint are

$$\phi = M\phi_m + H\phi_h + V\phi_v \tag{15a}$$

$$\Delta = M\Delta_m + H\Delta_h + V\Delta_v \tag{15b}$$

$$\lambda = M\lambda_m + H\lambda_h + V\lambda_v. \tag{15c}$$

Actual stiffness factors and induced movements

When the end B of the member AB is not fixed, but is connected to one or more members for which the actual stiffness factors are known, the actual stiffness factors for the end A are obtained as follows: First fix the end B and impose the desired unit displacement at the end A. Next, fix the end A in this position and release joint B so that it takes up a position of equilibrium determined by the modified stiffness characteristics of joint B with respect to the end A. Then the forces and moment acting at the end A are the actual stiffness factors for AB.

Rotation

When the end B is fixed (Fig. 3) a moment m'_ϕ and forces h'_ϕ and v'_ϕ are required at the end A to cause unit rotation there. These set up an unbalanced condition at B, due to a moment m and forces h and v such that

$$m = m'^{ab}_\phi - h'^{ab}_\phi y_1 + v'^{ab}_\phi x_1 \tag{16a}$$

$$h = h'^{ab}_\phi \tag{16b}$$

$$v = v'^{ab}_\phi. \tag{16c}$$

Further, $m = -c^{ab}m'^{ab}_\phi$, in which c is the carry-over factor for moment from end A to end B due to rotation at A. (For prismatic beams, $c = \frac{1}{2}$.) Lock the joint A in this position and release joint B; the balancing movements there are the induced movements at B due to unit rotation imposed at A. These induced movements are found by substituting the values obtained from equations (16) in equations (15), giving

$$\phi_\phi = -c^{ab}m'^{ab}_\phi\phi'_m + h'^{ab}_\phi\phi'_h + v'^{ab}_\phi\phi'_v \tag{17a}$$

$$\Delta_\phi = -c^{ab}m'^{ab}_\phi\Delta'_m + h'^{ab}_\phi\Delta'_h + v'^{ab}_\phi\Delta'_v \tag{17b}$$

$$\lambda_\phi = -c^{ab}m'^{ab}_\phi\lambda'_m + h'^{ab}_\phi\lambda'_h + v'^{ab}_\phi\lambda'_v. \tag{17c}$$

These movements at B require the action on member BA of a moment m and forces h and v given by

$$m = \phi_\phi m'^{ba}_\phi + \Delta_\phi m'^{ba}_\Delta + \lambda_\phi m'^{ba}_\lambda \tag{18a}$$

$$h = \phi_\phi h'^{ba}_\phi + \Delta_\phi h'^{ba}_\Delta + \lambda_\phi h'^{ba}_\lambda \tag{18b}$$

$$v = \phi_\phi v'^{ba}_\phi + \Delta_\phi v'^{ba}_\Delta + \lambda_\phi v'^{ba}_\lambda. \tag{18c}$$

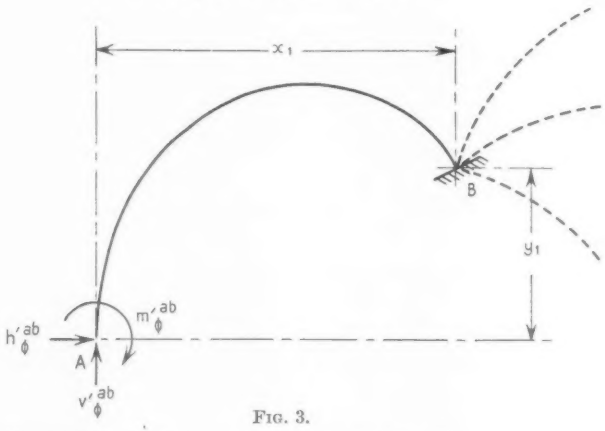

FIG. 3.

These actions at B produce reactions at A given by

$$m = c^{ba}\phi_\phi m'^{ba}_\phi - \Delta_\phi m'^{ab}_\Delta - \lambda_\phi m'^{ab}_\lambda \tag{19a}$$

$$h = -\phi_\phi h'^{ba}_\phi - \Delta_\phi h'^{ab}_\Delta - \lambda_\phi h'^{ab}_\lambda \tag{19b}$$

$$v = -\phi_\phi v'^{ba}_\phi - \Delta_\phi v'^{ab}_\Delta - \lambda_\phi v'^{ab}_\lambda. \tag{19c}$$

Hence, the total forces at A which, since B has now been released and A has been rotated through unit angle, are the actual stiffness factors for the end A of member AB, are given by

$$m_\phi = m'_\phi\left(1 + c^{ba}\phi_\phi \frac{m'^{ba}_\phi}{m'_\phi} - \Delta_\phi \frac{m'_\Delta}{m'_\phi} - \lambda_\phi \frac{m'_\lambda}{m'_\phi}\right) \tag{20a}$$

$$h_\phi = h'_\phi\left(1 - \phi_\phi \frac{h'^{ba}_\phi}{h'_\phi} - \Delta_\phi \frac{h'_\Delta}{h'_\phi} - \lambda_\phi \frac{h'_\lambda}{h'_\phi}\right) \tag{20b}$$

$$v_\phi = v'_\phi\left(1 - \phi_\phi \frac{v'^{ba}_\phi}{v'_\phi} - \Delta_\phi \frac{v'_\Delta}{v'_\phi} - \lambda_\phi \frac{v'_\lambda}{v'_\phi}\right). \tag{20c}$$

Horizontal displacement

Similarly, the induced movements at B due to a unit imposed horizontal displacement at A are

$$\phi_\Delta = m'^{ba}_\Delta \phi'_m + h'^{ab}_\Delta \phi'_h + v'^{ab}_\Delta \phi'_v \tag{21a}$$

$$\Delta_\Delta = m'^{ba}_\Delta \Delta'_m + h'^{ab}_\Delta \Delta'_h + v'^{ab}_\Delta \Delta'_v \tag{21b}$$

$$\lambda_\Delta = m'^{ba}_\Delta \lambda'_m + h'^{ab}_\Delta \lambda'_h + v'^{ab}_\Delta \lambda'_v, \tag{21c}$$

while the actual stiffness factors for end A are

$$m_\Delta = m'_\Delta\left(1+c^{ba}\phi_\Delta\frac{m'^{ba}_\phi}{m'_\Delta}-\Delta_\Delta-\lambda_\Delta\frac{m'_\lambda}{m'_\Delta}\right) \tag{22a}$$

$$h_\Delta = h'_\Delta\left(1-\phi_\Delta\frac{h'^{ba}_\phi}{h'_\Delta}-\Delta_\Delta-\lambda_\Delta\frac{h'_\lambda}{h'_\Delta}\right) \tag{22b}$$

$$v_\Delta = v'_\Delta\left(1-\phi_\Delta\frac{v'^{ba}_\phi}{v'_\Delta}-\Delta_\Delta-\lambda_\Delta\frac{v'_\lambda}{v'_\Delta}\right). \tag{22c}$$

Vertical displacement

The induced movements at B due to a unit imposed vertical displacement at A are

$$\phi_\lambda = m'^{ba}_\lambda\phi'_m+h'^{ab}_\lambda\phi'_h+v'^{ab}_\lambda\phi'_v \tag{23a}$$

$$\Delta_\lambda = m'^{ba}_\lambda\Delta'_m+h'^{ab}_\lambda\Delta'_h+v'^{ab}_\lambda\Delta'_v \tag{23b}$$

$$\lambda_\lambda = m'^{ba}_\lambda\lambda'_m+h'^{ab}_\lambda\lambda'_h+v'^{ab}_\lambda\lambda'_v, \tag{23c}$$

while the actual stiffness factors for end A are

$$m_\lambda = m'_\lambda\left(1+c^{ba}\phi_\lambda\frac{m'^{ba}_\phi}{m'_\lambda}-\Delta_\lambda\frac{m'_\Delta}{m'_\lambda}-\lambda_\lambda\right) \tag{24a}$$

$$h_\lambda = h'_\lambda\left(1-\phi_\lambda\frac{h'^{ba}_\phi}{h'_\lambda}-\Delta_\lambda\frac{h'_\Delta}{h'_\lambda}-\lambda_\lambda\right) \tag{24b}$$

$$v_\lambda = v'_\lambda\left(1-\phi_\lambda\frac{v'^{ba}_\phi}{v'_\lambda}-\Delta_\lambda\frac{v'_\Delta}{v'_\lambda}-\lambda_\lambda\right). \tag{24c}$$

Axial deformations

When axial deformation of members is disregarded, and a vertical member is connected to a joint, $\lambda = 0$, the induced movements, from equations (17) and (21), are

$$\phi_\phi = -c^{ab}m'^{ab}_\phi\phi'_m+h'^{ab}_\phi\phi'_h \tag{25a}$$

$$\Delta_\phi = -c^{ab}m'^{ab}_\phi\Delta'_m+h'^{ab}_\phi\Delta'_h \tag{25b}$$

$$\phi_\Delta = m'^{ba}_\Delta\phi'_m+h'^{ab}_\Delta\phi'_h \tag{25c}$$

$$\Delta_\Delta = m'^{ba}_\Delta\Delta'_m+h'^{ab}_\Delta\Delta'_h, \tag{25d}$$

in which the displacement coefficients in terms of the modified stiffness factors are as given in Table 3, column 4.

The actual stiffness factors, from equations (20) and (22), are

$$m_\phi = m'_\phi\left(1+c^{ba}\phi_\phi\frac{m'^{ba}_\phi}{m'_\phi}-\Delta_\phi\frac{m'_\Delta}{m'_\phi}\right) \tag{26a}$$

$$h_\phi = h'_\phi\left(1-\phi_\phi\frac{h'^{ba}_\phi}{h'_\phi}-\Delta_\phi\frac{h'_\Delta}{h'_\phi}\right) \tag{26b}$$

$$m_\Delta = m'_\Delta\left(1+c^{ba}\phi_\Delta\frac{m'^{ba}_\phi}{m'_\Delta}-\Delta_\Delta\right) \tag{26c}$$

$$h_\Delta = h'_\Delta\left(1-\phi_\phi\frac{h'^{ba}_\phi}{h'_\Delta}-\Delta_\Delta\right). \tag{26d}$$

Symmetrical members

For symmetrical arches and bents, when the restrained stiffness factors for the two terminals are equal (except in the cases of m'_Δ and v'_ϕ, when the signs will be reversed), if the span AB is written as L and the height of the centroid O above the (horizontal) springings AB as $\bar{y}$, then

$$c^{ab} = \frac{-(m'_\phi + v'_\phi{}^{ab} L)}{m'_\phi} = c,$$

$$\frac{h'_\Delta}{h'_\phi} = \frac{1}{\bar{y}},$$

and equations (26) reduce to the following:

$$m_\phi = m'_\phi\left(1 + c\phi_\phi - \Delta_\phi \frac{m'_\Delta}{m'_\phi}\right) \tag{27a}$$

$$h_\phi = h'_\phi\left(1 - \phi_\phi - \frac{\Delta_\phi}{\bar{y}}\right) \tag{27b}$$

$$m_\Delta = m'_\Delta\left(1 + c\phi_\Delta \frac{m'_\phi}{m'_\Delta} - \Delta_\Delta\right) \tag{27c}$$

$$h_\Delta = h'_\Delta(1 - \phi_\phi \bar{y} - \Delta_\Delta). \tag{27d}$$

Total end reactions on a member

For a member AB subject to imposed distortion let the displacements at A be ϕ^A, Δ^A, λ^A, and those at B be ϕ^B, Δ^B, λ^B. Then the moment and forces required at A are

$$M^A = \phi^A m'_\phi{}^{ab} + \phi^B c^{ba} m'_\phi{}^{ba} + (\Delta^A - \Delta^B) m'_\Delta{}^{ab} + (\lambda^A - \lambda^B) m'_\lambda{}^{ab} \tag{28a}$$

$$H^A = \phi^A h'_\phi{}^{ab} - \phi^B h'_\phi{}^{ba} + (\Delta^A - \Delta^B) h'_\Delta{}^{ab} + (\lambda^A - \lambda^B) h'_\lambda{}^{ab} \tag{28b}$$

$$V^A = \phi^A v'_\phi{}^{ab} - \phi^B v'_\phi{}^{ba} + (\Delta^A - \Delta^B) v'_\Delta{}^{ab} + (\lambda^A - \lambda^B) v'_\lambda{}^{ab}, \tag{28c}$$

while those at B are

$$M^B = \phi^B m'_\phi{}^{ba} + \phi^A c^{ab} m'_\phi{}^{ab} + (\Delta^B - \Delta^A) m'_\Delta{}^{ba} + (\lambda^B - \lambda^A) m'_\lambda{}^{ba} \tag{29a}$$

$$H^B = \phi^B h'_\phi{}^{ba} - \phi^A h'_\phi{}^{ab} + (\Delta^B - \Delta^A) h'_\Delta{}^{ba} + (\lambda^B - \lambda^A) h'_\lambda{}^{ba} = -H^A \tag{29b}$$

$$V^B = \phi^B v'_\phi{}^{ba} - \phi^A v'_\phi{}^{ab} + (\Delta^B - \Delta^A) v'_\Delta{}^{ba} + (\lambda^B - \lambda^A) v'_\lambda{}^{ba} = -V^A. \tag{29c}$$

If, in addition to imposed distortion, the member AB carries external loading, the fixed-end reactions due to this loading must be added to the above values.

Description of the method

Direct analysis consists of three distinct steps as follows:

Step 1

Divide the structure into units which are first considered as fixed-ended. Find their elastic constants and restrained stiffness factors. Then

determine the actual stiffness factors and induced movements of the joints. The structure is considered unloaded, but subject to the restraint conditions obtaining at its supports, so that its deformation depends only on the elastic properties of the structure itself. This step constitutes the structural analysis.

Step 2

Assuming all joints locked, determine the unbalanced moments and forces at the joints due to the given loading. Then release all joints and find the balancing movements at each one in turn due to its own previously unbalanced moments and forces (the other joints being unrestrained), together with the resulting induced movements at other joints. The total displacements at any joint are then the sum of balancing movements at the joint plus movements induced there by balancing movements elsewhere.

Step 3

Compute moments and forces throughout the structure as follows:

Moment = ($m'_\phi \times$ total rotation at joint) + ($m'_\Delta \times$ total horizontal displacement at joint) + moments carried over from the far end of the member due to rotation and horizontal translation there.

Horizontal force = ($h'_\phi \times$ total rotation at joint) + ($h'_\Delta \times$ total horizontal displacement at joint) + horizontal forces carried over from the far end of the member due to rotation and horizontal translation there.

These expressions follow from equations (28) and (29) and refer to the case where there is no vertical translation of the joint.

Steps 2 and 3 together constitute the process of stress analysis.

Example

The method will be applied to the continuous-arch system shown in Fig. 4 which has been solved elsewhere (**2**) by the method of successive approximations. The system is composed of three similar elliptical arches of 60-ft. span and 15-ft. central rise, carried on piers 20 ft. high. The arches and the piers are of the same constant cross-section.

Assume the curved length of the elliptical arch to be divided into eleven equal lengths each of 6·8 ft., and the coordinates of the mid-points of these lengths to be as follows:

x	0·70	4·90	10·65	16·90	23·45	30·0	36·55	43·10	49·35	55·10	59·30 ft.
y	3·2	8·2	11·5	13·5	14·6	15·0	14·6	13·5	11·5	8·2	3·2 ft.

The distributions of moments and of horizontal forces throughout the structure are to be found for a uniformly-distributed loading of 1,000 lb. per ft. run covering one of the end spans, neglecting axial deformation.

The complete solution is given in Tables 4, 5, and 6, to which the following explanation refers.

Step 1

Calculate the elastic constants for a single arch. Since ds/EI for the eleven equal lengths referred to above is 6·8, if unit value is assumed for

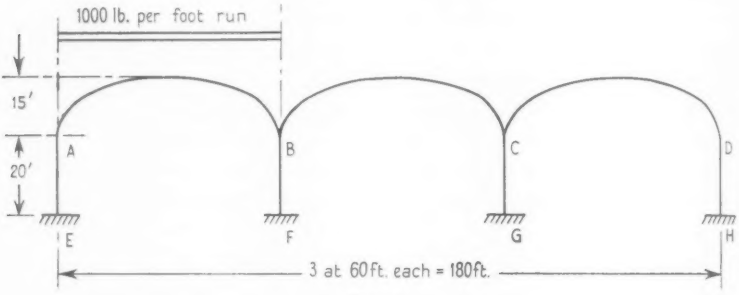

FIG. 4.

EI, then $\bar{S} = 74{\cdot}8$, the total curved length of the arch. The coordinates of the elastic centre are $\bar{x} = \pm 30$ ft. by inspection, and

$$\bar{y} = \sum y/11 = 10{\cdot}63 \text{ ft.}$$

Transfer the x-axis to pass through the elastic centre and obtain coordinates corresponding to those given above. Then $I_x = 6{\cdot}8 \sum y^2 = 1{,}300$; $I_y = 6{\cdot}8 \sum x^2 = 28{,}300$; $I_{xy} = 0$, since the arch is a symmetrical section. The elastic constants are now known for the arch and are entered in Table 4, item (1), columns CD and DC. For any pier such as DH, the elastic area $= L/EI = 20$; $\bar{x}$ by inspection $= 0$, and $\bar{y} = -10$;

$$I_x = L^3/12EI = 667;$$

I_y and I_{xy} are both equal to 0; these values appear in item (1), column DH of the table. Using equations (8) and (9), obtain values for the restrained stiffness factors for the separate arches and piers and record them in item (2). The flexural rigidity of the arch and pier sections was taken as 1 kip-ft.^{2}, which keeps the units consistent, but does not otherwise affect the solution.

Starting at the right-hand end of the structure, obtain by summation the modified stiffness factors for joint D as follows:

$$M'_\phi = 0{\cdot}20 + 0{\cdot}1324 = 0{\cdot}3324$$
$$H'_\phi = -0{\cdot}015 + 0{\cdot}0082 = -0{\cdot}0068$$
$$V'_\phi = 0{\cdot}0015 + 0{\cdot}00077 = 0{\cdot}00227,$$

and enter these values in the table in item (3), column DH. Next calculate

STRUCTURAL ANALYSIS

TABLE 4. *Stiffness factors, displacement coefficients, and induced movements*

Item	*AE*	*AB*	*BA*	*BF*	*BC*	*CB*	*CG*	*CD*	*DC*	*DH*
(1) Elastic constants	S Ξ φ I_x I_y I_{xy}							30	74·8 −30 10·63 1300 28300 0	20 0 −10 667 0 0
(2) Restrained stiffness factors (members) .	m'_1 k'_1 k'_2								0·1324 0·0082 0·00077	0·30 −0·015 0·0015
(3) Modified stiffness factors (joints) . . .	M'_1 H'_1 H'_2			0·419 −0·00324 0·002562			0·4074 −0·00153 0·0024425			0·3324 −0·0068 0·00227
(4) Modified displacement coefficients . .	ϕ'_m Δ'_m Δ'_h			2·48 3·21 394			2·5 4·68 422			3·22 9·65 471
(5) Induced movements	ϕ_0 Δ_0 ϕ_1 Δ_1	$\phi = 1$ ⟶ $\Delta = 1$ ⟶		0·100 3·44 0·0222 0·330	$\phi = 1$ ⟶ $\Delta = 1$ ⟶		0·212 3·80 0·0243 0·364	$\phi = 1$ ⟶ $\Delta = 1$ ⟶		0·30 4·52 0·034 0·44
(6) Actual stiffness factors (members) . . .	m_0 k_0 k_1	0·0907 0·00398 0·000336			0·0865 0·00356 0·000292			0·075 0·00227 0·000154		0·20 −0·015 0·0015
(7) Actual stiffness factors (joints) . . .	M_0 H_0 H_1						0·3615 −0·00917 0·001946			0·2907 −0·01102 0·001836
(8) Actual displacement coefficients . . .	ϕ_m Δ_m Δ_h						3·15 14·38 585			4·44 26·7 705

(9) Unit displacement table	ϕ	Δ	ϕ	Δ	ϕ	Δ	ϕ	Δ
	0·1928 0·0197	2·63 0·270	0·212 0·0243	3·80 0·364	1·0 —	— 1·0	0·30 0·034	4·52 0·44
	0·30 0·034	4·52 0·44	1·0 —	— 1·0	0·212 0·0243	3·80 0·364	0·1928 0·0197	2·63 0·270
	1·0 —	— 1·0	0·100 0·0222	3·44 0·330	0·1237 0·0127	1·972 0·204	0·1042 0·01077	1·424 0·1472

STRESS ANALYSIS

TABLE 5. *Total joint displacements*

Item	*A*			*B*			*C*			*D*	
(1) Fixed-end moment (ft.-kips)		126	−126		o	o		o	o		
Fixed-end thrust (kips)		36	−36		o	o		o	o		
(2) Unbalanced moment	−126			126			o			o	
Unbalanced thrust	−36			36			o			o	
	ϕ	Δ		ϕ	Δ		ϕ	Δ		ϕ	Δ
(3) Balancing movements at joint *A*, and resulting induced movements elsewhere	−1525 —	— −28850	→ →	−290 −640	−5220 −9500	→ →	−188 −365	−3000 −5900	→ →	−160 −310	−2170 −4250
(4) Balancing movements at joint *B*, and resulting induced movements elsewhere	280 780	4220 10120	← ←	935 —	— 23000	→ →	198 557	3550 8350	→ →	180 452	2460 6200
(5) Total joint displacements	−465	−14510		5	8280		202	3000		162	2240

TABLE 6 (*a*). *Computation of moments*

TABLE 6 (*a*). *Computation of moments*

Item	*AE*	*AB*	*BA*	*BF*	*BC*	*CB*	*CG*	*CD*	*DC*	*DH*
F.E.M.		126	−126		0	0		0	0	
$m'_a \times$ total ϕ	−93·0	−61·6	0·6	1·0	0·6	26·7	40·5	26·7	21·4	32·4
C.O. ($c = -0{\cdot}517$)		−0·3	32		−13·9	0·3		−11·1	−13·8	
$m'_a \times$ total Δ	216	−119	68	−124	68	24·6	−45	24·6	18·6	−34
C.O. ($c = -1{\cdot}0$)		−68	119		−24·6	−68		−18·6	−24·6	
Final moments	123	−122·9	93·6	−123	30·1	−17	−4·5	21·6	1·6	−1·6
(*Maugh*	*122·6*	*−122·6*	*92·4*	*−122*	*29·3*	*−16·4*	*−4·7*	*21·0*	*1·8*	*−1·8)*

	EA	*FB*	*GC*	*HD*
C.O. ($c = +0{\cdot}5$)	−46·5	0·5	20·3	16·2
C.O. ($c = +1{\cdot}0$)	216	−124	−45	−34
	169·5	−123·5	−24·7	−17·8
(*Maugh*	*170·4*	*−121·8*	*−24·0*	*−17·4)*

TABLE 6 (*b*). *Computation of horizontal forces*

Item	*AE*	*AB*	*BA*	*BF*	*BC*	*CB*	*CG*	*CD*	*DC*	*DH*
F.E.T.		36	−36		0	0		0	0	
$h'_a \times$ total ϕ	6·98	−3·82	0·05	−0·075	0·05	1·66	−3·03	1·66	1·33	−2·43
C.O. ($c = -1{\cdot}0$)		−0·05	3·82		−1·66	−0·05		−1·33	−1·66	
$h'_a \times$ total Δ	−21·6	−11·15	6·35	12·4	6·35	2·31	4·50	2·31	1·74	3·40
C.O. ($c = -1{\cdot}0$)		−6·35	11·15		−2·31	−6·35		−1·74	−2·31	
Final horizontal forces	−14·63	14·63	−14·63	12·33	2·43	−2·43	1·47	0·90	−0·90	0·97
(*Maugh*	*−14·65*			*12·19*			*1·44*			*0·96)*

	EA	*FB*	*GC*	*HD*
C.O. ($c = -1{\cdot}0$)	14·63	−12·33	−1·47	−0·97
(*Maugh*	*14·65*	*−12·19*	*−1·44*	*−0·96)*

the modified displacement coefficients for joint D from Table 3, column 4, substituting the modified stiffness factors, and enter them in Table 4, item (4), column DH.

Now calculate, from equations (25 a and b), the rotation ϕ_ϕ and translation Δ_ϕ induced at D by imposing unit positive rotation at C. Thus, $\phi_\phi = 0{\cdot}30$; $\Delta_\phi = 4{\cdot}52$. Enter these values in the table in item (5), column DH. (The value of the carry-over factor c for the arch, to be used in these equations, is obtained as follows: Consider the arch CD with a fixed end at D. A moment m'_ϕ and forces h'_ϕ, v'_ϕ are required at C to produce unit rotation there; a moment m^D is set up at D. The value of $m'_\phi = 0{\cdot}1324$ is known (Table 4, item (2)), and $v'_\phi = -0{\cdot}001063$ can be found from equation (8c). Then moments about D give

$$m^D = 0{\cdot}1324 - 0{\cdot}001063 \times 60 = 0{\cdot}0684.$$

Hence $c = -m^D/m'_\phi = -0{\cdot}0684/0{\cdot}01324 = -0{\cdot}517$).

Similarly, calculate from equations (25 c and d) the movements ϕ_Δ and Δ_Δ induced at D by imposing unit positive horizontal translation at C. Thus $\phi_\Delta = 0{\cdot}034$; $\Delta_\Delta = 0{\cdot}44$. Enter these values in the table under item (5), column DH. Now derive values of the actual stiffness factors for CD from equations (27 a, b, d) as follows:

$$m_\phi = 0{\cdot}1324[1 - 0{\cdot}517 \times 0{\cdot}30 - 4{\cdot}52(0{\cdot}0082/0{\cdot}1324)] = 0{\cdot}075$$

$$h_\phi = 0{\cdot}0082[1 - 0{\cdot}30 - 4{\cdot}52(0{\cdot}00077/0{\cdot}0082)] = 0{\cdot}00227$$

$$h_\Delta = 0{\cdot}00077[1 - 0{\cdot}44 - 0{\cdot}034(0{\cdot}0082/0{\cdot}00077)] = 0{\cdot}000154.$$

Enter these values in the table in item (6), column CD.

Note that the actual stiffness factors for DH, CG, BF, AE are the same as the restrained stiffness factors since in each case the far end of the member is fixed.

Next calculate the modified stiffness factors for joint C. They are:

$$M'_\phi = m_\phi^{cd} + m_\phi^{cg} + m'^{cb}_\phi = 0{\cdot}075 + 0{\cdot}20 + 0{\cdot}1324 = 0{\cdot}4074$$

$$H'_\phi = h_\phi^{cd} + h_\phi^{cg} + h'^{cb}_\phi = 0{\cdot}00227 - 0{\cdot}015 + 0{\cdot}0082 = -0{\cdot}00453$$

$$H'_\Delta = h_\Delta^{cd} + h_\Delta^{cg} + h'^{cb}_\Delta = 0{\cdot}000154 + 0{\cdot}0015 + 0{\cdot}00077 = 0{\cdot}002425.$$

Enter these values in the table in item (3), column CG.

The cycle of operations performed above may be described as follows: Starting with the modified stiffness factors for joint D, find the modified displacement coefficients and then the induced movements at the joints and hence the actual stiffness factors for CD, which enable the modified stiffness factors for joint C to be found. This cycle is repeated, giving in turn the modified displacement coefficients and the induced movements at joint C, the actual stiffness factors for BC, and the modified stiffness

factors for joint B. A final cycle gives the modified displacement coefficients and induced movements at joint B and the actual stiffness factors for AB. This enables items (3), (4), (5), and (6) in the table to be completed as shown.

The actual stiffness factors for the joints, item (7), follow by summation of values in item (6), and all required stiffness factors are known. Item (8) gives the actual displacement coefficients, which are obtained from Table 3 by substituting in it the actual stiffness factors.

Next prepare the unit displacement table, item (9), which shows the displacements ϕ and Δ at all joints due to unit imposed rotation or translation at any joint. This part of the analysis is now complete, and it may be used to determine the effect of any particular loading.

Step 2

Consider the uniformly-distributed loading of 1,000 lb. per horizontal ft. on the end span AB. The fixed-end reactions are:

Fixed-end moments (ft.-kips), 126 at AB; -126 at BA

Fixed-end thrusts (kips), 36 at AB; -36 at BA.

Elsewhere they are zero (see Table 5, item (1)). Hence, the unbalanced components at the joints are:

For joint A: Moment -126; thrust -36

For joint B: Moment 126; thrust 36.

These values constitute item (2) in the table.

Find the balancing movements at the joints from equations (15 a and b). Thus, for joint A:

$$\phi = -126\times 4{\cdot}44 - 36\times 26{\cdot}7 = -1525$$

$$\Delta = -126\times 26{\cdot}7 - 36\times 705 = -28850.$$

Enter these values in Table 5, item (3). Next use the unit displacement table to obtain by proportion the movements induced at other joints by these balancing movements at joint A and enter the results in item (3) in the table. Apply the same process to the unbalanced components at joint B, and enter the values as item (4). Sum the values in items (3) and (4) to obtain total joint displacements, item (5).

Step 3

The total joint displacements known, computation of moments and thrusts may be made, using equations (28). This is done in Table 6, which will not require further explanation. It will be seen that agreement with

Maugh's results is very close indeed, although calculations were made only with a 10-in. slide rule.

Advantages of the method

Principal among these are:

1. The total elimination of simultaneous equations, coupled with the fact that the method is an exact one; as a result, computations may be performed throughout by slide rule.

2. A single structural analysis, independent of the loading, is first made. From this, the effects of any loading are readily found.

3. Translation, as well as rotation, of the joints is considered, so that the effect of side sway is automatically taken into account.

4. Frames containing curved members of variable cross-section are readily analysed.

REFERENCES

1. G. E. Beggs, 'An accurate mechanical solution of statically indeterminate structures by use of paper models and special gages', *Proc. Amer. Concrete Inst.* **18** (1922), 58.
2. L. C. Maugh, *Statically Indeterminate Structures* (Wiley, 1946).

THE INDUCTION OF ELECTRIC CURRENTS IN NON-UNIFORM THIN SHEETS AND SHELLS

By A. T. PRICE (*Imperial College, London*)

[Received 12 October 1948]

SUMMARY

General equations are obtained for the induction of electric currents in any thin-sheet distribution of conducting material by periodic or aperiodic fields. Methods of solving the equations for non-uniform plane sheets and spherical shells are considered. Numerical calculations for a special case of the plane sheet are made to illustrate some important features. The case of the spherical shell is considered in some detail, with a view to geomagnetic applications. Methods of approximating to the solution when the conductivity is given as an empiric function are described.

1. Introduction

THE theory of the induction of electric currents in non-uniform thin-sheet distributions of conducting material is of importance in several geomagnetic applications. When, for example, attempts are made to infer the distribution of electrical conductivity within the earth from analyses of the observed daily variations or storm-time variations of the earth's magnetic field, on the assumption that the part of the varying field of internal origin is due to currents induced in the earth by the part of external origin, it is found that the oceans, which are relatively good conductors, must have some appreciable influence on the internal part (Chapman and Price, **1**, 1930; Lahiri and Price, **2**, 1939). To determine the exact nature of this influence it is desirable to calculate the currents induced in a thin spherical shell having a suitable non-uniform distribution of conductivity. The general theory of thin spherical shells is dealt with in § 9 of this paper, and the analytic solution for a special case is obtained in §§ 10 and 11. Methods for approximating to the solution for other distributions of conductivity are described in §§ 12 and 13.

Similar calculations relating to non-uniform plane distributions would be useful in investigations relating to earth currents, including those flowing in sea channels (Barber, **3**, 1948), when account is taken of the local variations in resistivity of the earth's crust. The theory of plane sheets is dealt with in §§ 4 to 6, and numerical solutions which illustrate some important features are obtained in §§ 7 and 8.

Another important application of the theory is the investigation of the effects of the non-uniform distribution of conductivity in the ionosphere on various geomagnetic phenomena, including sudden commencements, micropulsations, and short-period fluctuations of the earth's field during

magnetic storms. These have recently been discussed in a joint paper by A. A. Ashour and the writer (**4**, 1948), and the numerical calculations therein described are based on the formulae obtained in §§ 9 and 10 of the present paper.

2. Statement of the general problem

We consider any non-uniform thin-sheet distribution of conducting material, the medium on both sides being non-conducting and the magnetic permeability everywhere unity. A varying magnetic field in the surrounding medium, having its origin in sources external to the sheet, e.g. produced by electric currents in a region not in contact with the sheet, induces electric currents in the sheet. It is required to find the magnitude and distribution of these currents, and also their magnetic field.

We assume that the variations of the field are sufficiently slow to enable us to ignore the displacement current and treat the velocity of propagation of electromagnetic effects in the dielectric as infinite. The permissible rapidity of variation of the field will then be limited by the average conductivity of the conductor and by its linear dimensions.

3. General equations for any thin-sheet distribution of conducting material

Let **H**, **E**, and **i** denote the magnetic intensity, electric intensity, and the conduction current density, respectively, all measured in electromagnetic units. Neglecting the displacement current, the conduction current is non-divergent and the field equations therefore reduce to

$$\operatorname{curl} \mathbf{H} = 4\pi \mathbf{i}, \tag{1}$$

$$\operatorname{curl} \mathbf{E} = -\mu \, \partial \mathbf{H}/\partial t, \tag{2}$$

$$\mathbf{i} = \kappa \mathbf{E}, \tag{3}$$

where κ is the specific conductivity, and is a function of the space variables. The magnetic permeability μ is assumed to be unity everywhere, so that $\operatorname{div} \mathbf{H}$ is zero. In the dielectric $\operatorname{curl} \mathbf{H}$ is zero, hence

$$\mathbf{H} = -\operatorname{grad} \Omega, \tag{4}$$

where the potential Ω satisfies Laplace's equation.

On passing from the dielectric into the conducting material, the normal component H_n of **H** is continuous, since **H** is everywhere non-divergent. It follows that, if the thickness d is infinitesimal, the normal component H_n will have the same value at corresponding points on opposite sides of the sheet.

By applying the circuital relation (2) to a small rectangular circuit, having two sides parallel to the surface of the conductor, one being in the

conductor and one in the dielectric, it is seen that the tangential components of $\mathbf{E}$ are continuous at the interface. Hence, for an infinitesimally thin conducting sheet the component $\mathbf{E}_s$ of $\mathbf{E}$, parallel to the sheet, has the same magnitude and direction at corresponding points on opposite sides of the sheet.

Integrating equation (3) over the thickness d of the sheet at any point, we obtain

$$\int_0^d \mathbf{i}\, d\zeta = \int_0^d \kappa \mathbf{E}\, d\zeta,$$

where the integral on the right may be replaced by $\mathbf{E}_s \int_0^d \kappa\, d\zeta$ to the first order of small quantities, when d is small. The integrals $\int_0^d \mathbf{i}\, d\zeta$ and $\int_0^d \kappa\, d\zeta$ represent, respectively, the total sheet-current intensity per unit length of surface at the point, and the total conductivity per unit length; denoting these by $\mathbf{i}_s$ and $1/\rho$ respectively, we have

$$\mathbf{E}_s = \rho \mathbf{i}_s. \tag{5}$$

Applying equation (2) to a small circuit in the surface of the sheet, we obtain

$$\operatorname{curl} \mathbf{E}_s = -\mathbf{n}\, \partial H_n/\partial t = \mathbf{n}\, \partial^2\Omega/\partial t \partial n,$$

where $\mathbf{n}$ is a unit vector normal to the surface from the negative to the positive side. Substituting for $\mathbf{E}_s$ from (5), this becomes

$$\rho \operatorname{curl} \mathbf{i}_s + \operatorname{grad} \rho \wedge \mathbf{i}_s = -\mathbf{n}\, \partial H_n/\partial t = \mathbf{n}\, \partial^2\Omega/\partial t \partial n. \tag{6}$$

If we now apply the circuital relation (1) to a small rectangular circuit, having two sides of length δs parallel to the conducting sheet, with one on each side of it, we obtain

$$(H_s)_+ \delta s - (H_s)_- \delta s = 4\pi i_s \delta s \sin\theta,$$

where the $+$ and $-$ suffixes indicate values at the positive and negative faces of the sheet, and θ is the angle between $\delta\mathbf{s}$ and $\mathbf{i}_s$. Since this relation is true for any direction of $\delta\mathbf{s}$ tangential to the sheet, we can write

$$\mathbf{i}_s = \frac{1}{4\pi} \mathbf{n} \wedge (\mathbf{H}_+ - \mathbf{H}_-) = -\mathbf{n} \wedge \operatorname{grad} \Psi, \tag{7}$$

where

$$\Psi = \frac{1}{4\pi}(\Omega_+ - \Omega_-). \tag{8}$$

Equation (7) shows that Ψ is the stream-line function for the currents flowing in the sheet.

Substituting the value of $\mathbf{i}_s$ from (7) in equation (6), we get

$$\rho \operatorname{curl}\{\mathbf{n} \wedge (\mathbf{H}_+ - \mathbf{H}_-)\} + \operatorname{grad} \rho \wedge \{\mathbf{n} \wedge (\mathbf{H}_+ - \mathbf{H}_-)\} = -4\pi \mathbf{n}\, \partial H_n/\partial t,$$

which is easily reduced to the form

$$\rho \operatorname{div}(\mathbf{H}_+ - \mathbf{H}_-) + \operatorname{grad}\rho . (\mathbf{H}_+ - \mathbf{H}_-) = -4\pi\, \partial H_n/\partial t. \tag{9}$$

This equation gives the relation between the varying total magnetic fields on two sides of any sheet distribution of conducting material, irrespective of how these fields are produced. When there is a varying magnetic field of external origin, the total field will consist of this inducing field together with the field of the currents induced in the sheet. Let the potentials of these two parts be denoted by $\Omega^{(e)}$ and $\Omega^{(i)}$, respectively, so that

$$\Omega = \Omega^{(e)} + \Omega^{(i)}.$$

$\Omega^{(i)}$ will satisfy Laplace's equation and, in general, will tend to zero at great distances from the conducting sheet; $\Omega^{(e)}$ will satisfy Laplace's equation in the immediate neighbourhood of the sheet, and the corresponding field intensity ($-\operatorname{grad}\Omega^{(e)}$) will be continuous on passing through the sheet. Since the normal component of the total field ($-\partial\Omega/\partial n$) is continuous at the sheet, it follows that the normal component of the induced field ($-\partial\Omega^{(i)}/\partial n$) is also continuous. Further

$$\mathbf{H}_+ - \mathbf{H}_- = -\operatorname{grad}(\Omega_+^{(i)} - \Omega_-^{(i)}), \tag{10}$$

so that equation (9) may be written in the form

$$\rho \operatorname{div}\operatorname{grad}(\Omega_+^{(i)} - \Omega_-^{(i)}) + \operatorname{grad}\rho . \operatorname{grad}(\Omega_+^{(i)} - \Omega_-^{(i)}) = -4\pi \frac{\partial}{\partial t}\left(\frac{\partial\Omega^{(e)}}{\partial n} + \frac{\partial\Omega^{(i)}}{\partial n}\right). \tag{11}$$

If the inducing field is known, $\Omega^{(e)}$ will be a given function of the time and space variables. To find the induced field it is necessary to determine the function $\Omega^{(i)}$ which satisfies Laplace's equation, together with the appropriate conditions at infinity and the boundary condition (11) at the conducting sheet. When $\Omega^{(i)}$ has been found, the induced current distribution may be obtained from (7) and (10).

4. The non-uniform plane sheet

When the conducting sheet lies in one plane, say the plane $z = 0$ in Cartesian coordinates, the symmetrical properties of the field of the induced current-system show that

$$\Omega^{(i)}(x, y, z) = -\Omega^{(i)}(x, y, -z). \tag{12}$$

Hence, at $z = 0$,

$$\Omega_+^{(i)} = -\Omega_-^{(i)}, \tag{13}$$

and therefore

$$\Psi = \Omega_+^{(i)}/2\pi, \tag{14}$$

so that equation (11) reduces to

$$-\rho\left(\frac{\partial^2\Omega^{(i)}}{\partial z^2}\right)_+ + \operatorname{grad}\rho . \operatorname{grad}\Omega_+^{(i)} + 2\pi \frac{\partial}{\partial t}\left(\frac{\partial\Omega^{(i)}}{\partial z}\right)_+ = -2\pi \frac{\partial}{\partial t}\left(\frac{\partial\Omega^{(e)}}{\partial z}\right)_+. \tag{15}$$

It is therefore necessary in this case to find the function $\Omega^{(i)}$ which (i) satisfies Laplace's equation in the region $z > 0$, (ii) tends to zero as z tends to $+\infty$, and (iii) satisfies equation (15) at $z = 0$ if the sheet is of infinite extent. If it is of finite extent, (15) must be satisfied over that part of the plane $z = 0$ occupied by the sheet and $\Omega^{(i)}$ must be zero or constant over the remaining part.

When the sheet is *uniform* and of infinite extent, the second term on the left of (15) is zero, and the solution is very simple. We note here, for purposes of comparison, the solution when the inducing field is of the form $\Omega^{(e)}(z+vt, x, y)$, where v is real or imaginary. When v is real we have the well-known case treated by Maxwell (**5**) of a magnetic system approaching the sheet with velocity v; when v is imaginary we have the case of a periodic inducing field, having a simple-harmonic time factor. Taking the inducing field as originating in the region $z > 0$, so that $\Omega^{(e)} \to 0$ as $z \to -\infty$, it is easily seen that the potential of the induced field in the region $z > 0$ is given by

$$\Omega^{(i)} = k\Omega^{(e)}(-z+vt, x, y), \tag{16}$$

where

$$k = 2\pi v/(\rho+2\pi v). \tag{17}$$

On the other side of the sheet ($z < 0$) we have, by (12),

$$\Omega^{(i)} = -k\Omega^{(e)}(z+vt, x, y), \tag{18}$$

so that the total field on this side is

$$\Omega = (1-k)\Omega^{(e)} = \frac{\rho}{\rho+2\pi v}\Omega^{(e)}, \tag{19}$$

showing that the screening effect of the sheet is simply a reduction of the intensity of the magnetic field without any change of distribution. When v is real (Maxwell's case) the intensity is reduced in the ratio $\rho/(\rho+2\pi v)$. When v is imaginary (periodic field), the modulus of the complex number $\rho/(\rho+2\pi v)$ gives the reduction in amplitude, and its argument gives the change of phase.

These simple results cannot be extended to a *non-uniform* sheet, where the distribution as well as the intensity of the field will always be affected. To obtain an *analytic solution* in this case it is necessary to assume an appropriate series or integral expression for $\Omega^{(i)}$, say $\sum_s I_s(t)f_s(x, y, z)$ or $\int I(t, u)f(x, y, z, u)\,du$, where the functions f_s or f satisfy conditions (i) and (ii) above. The coefficients $I_s(t)$ or $I(t, u)$ are then evaluated by substituting in equation (15). This leads to a set of difference-differential equations to determine the coefficients $I_s(t)$, or to an integro-differential equation to determine $I(t, u)$.

The case where a series expression is the appropriate form for $\Omega^{(i)}$ is

treated in §§ 5 to 8 of this paper. An illustrative case which requires the integral form for $\Omega^{(i)}$, and leads to an integral equation for $I(t, u)$, has been discussed by A. A. Ashour in a paper now in preparation.

A quite different method of obtaining the solution by successive numerical approximations is briefly indicated in § 13. This method seems likely to be of considerable value in geophysical applications.

5. Plane sheet with ρ and $\Omega^{(e)}$ doubly-periodic functions of x and y

If ρ and $\Omega^{(e)}$ are periodic functions with the same period-rectangles, then $\Omega^{(i)}$ will also be periodic. We take the case where

$$\rho = 2\pi\sigma\{1-\epsilon(\cos px+\cos qy)\}, \quad \text{with} \quad \epsilon < 1 \tag{20}$$

and assume that the inducing field is an even function of x and y, and originates in the region $z > 0$, so that its potential is expressible in the form

$$\Omega^{(e)} = \sum_{m=0}^{\infty}\sum_{n=0}^{\infty} E_{m,n}\cos mpx\cos nqy\exp\{z\sqrt{(m^2p^2+n^2q^2)}\}, \tag{21}$$

where the coefficients $E_{m,n}$ are given functions of the time; the coefficient $E_{0,0}$, corresponding to a constant term in $\Omega^{(e)}$, may be taken to be zero.

The potential of the induced field for the region $z > 0$ will then be of the form

$$\Omega^{(i)} = \sum_{m=0}^{\infty}\sum_{n=0}^{\infty} I_{m,n}\cos mpx\cos nqy\exp\{-z\sqrt{(m^2p^2+n^2q^2)}\}, \tag{22}$$

where the coefficients $I_{m,n}$ are unknown functions of the time. This expression for $\Omega^{(i)}$ satisfies conditions (i) and (ii) of the previous section. Substituting the above expressions into the boundary condition (15), we obtain

$$\begin{aligned}\sum_{m=0}^{\infty}\sum_{n=0}^{\infty}\Big\{&\sigma\epsilon I_{m,n}(mp^2\sin px\sin mpx\cos nqy+nq^2\sin qy\cos mpx\sin nqy)+\\&+\sigma I_{m,n}(m^2p^2+n^2q^2)(1-\epsilon\cos px-\epsilon\cos qy)\cos mpx\cos nqy+\\&+\frac{dI_{m,n}}{dt}\sqrt{(m^2p^2+n^2q^2)}\cos mpx\cos nqy\Big\}\\ =\sum_{m=0}^{\infty}\sum_{n=0}^{\infty}&\frac{dE_{m,n}}{dt}\sqrt{(m^2p^2+n^2q^2)}\cos mpx\cos nqy.\end{aligned} \tag{23}$$

The expression on the left of (23) is easily reduced, by means of trigonometrical identities and a rearrangement of the terms, to a double Fourier series, so that (23) may be written in the form

$$\begin{aligned}\sum_{m=0}^{\infty}\sum_{n=0}^{\infty}\cos mpx\cos nqy\big[&\{\sigma(m^2p^2+n^2q^2)+\sqrt{(m^2p^2+n^2q^2)}(d/dt)\}I_{m,n}-\\&-\tfrac{1}{2}\sigma\epsilon\{m(m-1)p^2+n^2q^2\}I_{m-1,n}-\tfrac{1}{2}\sigma\epsilon\{m(m+1)p^2+n^2q^2\}I_{m+1,n}-\\&-\tfrac{1}{2}\sigma\epsilon\{m^2p^2+n(n-1)q^2\}I_{m,n-1}-\tfrac{1}{2}\sigma\epsilon\{m^2p^2+n(n+1)q^2\}I_{m,n+1}\big]\\=\sum_{m=0}^{\infty}\sum_{n=0}^{\infty}&\cos mpx\cos nqy\sqrt{(m^2p^2+n^2q^2)}(d/dt)E_{m,n},\end{aligned} \tag{24}$$

where, for the sake of generality in the notation, we introduce the two additional sets of coefficients $I_{-1,n}$ and $I_{m,-1}$, all these coefficients being defined to be zero; this gives correct values for the terms corresponding to $m = 0$ and to $n = 0$.

Since equation (24) holds over the whole period-rectangle, we may equate coefficients of $\cos mpx \cos nqy$ on the two sides, thus obtaining the doubly-infinite system of simultaneous linear differential equations of the form

$$-b_{m,n} I_{m-1,n} - c_{m,n} I_{m,n-1} + \left(1 + a_{m,n} \frac{d}{dt}\right) I_{m,n} - d_{m,n} I_{m,n+1} - e_{m,n} I_{m+1,n}$$

$$= \frac{1}{\sigma\sqrt{(m^2p^2 + n^2q^2)}} \frac{d}{dt} E_{m,n} \quad (m \geqslant 1,\ n \geqslant 1), \qquad (25)$$

to determine the unknown functions $I_{m,n}$. The values of the coefficients $a_{m,n}$, $b_{m,n}$,... in (25) are readily found by comparison with equation (24).

Since the double Fourier series on the right of (22) when $z = 0$ represents a function which is finite and continuous for all x and y, it follows that $I_{m,n}$ tends to zero when m tends to infinity and also when n tends to infinity. These conditions together with the conditions that $I_{-1,n}$, $I_{m,-1}$, and $I_{0,0}$ are all zero, are just sufficient to determine the required functions $I_{m,n}$ uniquely. The labour of solving the difference-equations (25) subject to the above boundary conditions is evidently considerable. Thus to obtain the Nth-convergents of the $I_{m,n}$'s (that is, the values of $I_{m,n}$ for $m \leqslant N$ and $n \leqslant N$, on the assumption that $I_{m,n} = 0$ for all $m > N$ or $n > N$), it is necessary to solve $(N+1)^2 - 1$ simultaneous equations. It is, however, possible to devise iterative methods in which the Nth-convergents can be obtained from the $(N-1)$th-convergents. This is illustrated by the relatively simple problem which we now consider.

6. Plane sheet with ρ a periodic function of x

Some important features of the induced current systems which flow in non-uniform sheets can be illustrated by considering a case where the inducing field is such that, in a uniform sheet, it would induce currents flowing in a direction which is perpendicular to the ridges of high resistance in the non-uniform sheet. One obvious feature would be a deflexion of the current lines by the ridges of high resistance, but other interesting features of the current system also emerge. We therefore consider the case where the potential of the inducing field is

$$\Omega^{(e)} = E(t) e^{qz} \cos qy, \qquad (26)$$

and the resistance of the sheet is given by

$$\rho = 2\pi\sigma(1 - \epsilon \cos px). \qquad (27)$$

In this case we can evidently assume that the potential of the induced field is of the form

$$\Omega^{(i)} = \cos qy \sum_{m=0}^{\infty} I_m(t) \cos mpx \exp\{-z\sqrt{(q^2+m^2p^2)}\}. \tag{28}$$

Following the general method indicated in § 5, it is found that the coefficients $I_m(t)$ of the Fourier series on the right of (28) satisfy the following recurrence relations

$$I_1 = 2\epsilon^{-1}(1+D)I_0 - 2\epsilon^{-1}DE, \tag{29}$$

$$(s+\tfrac{1}{2})I_2 = \epsilon^{-1}(s+1)\{1+(s+1)^{-\frac{1}{2}}D\}I_1 - I_0, \tag{30}\dagger$$

$$\frac{(m+1)ms+1}{m(m-1)s+1} I_{m+1} = \frac{2\epsilon^{-1}(m^2s+1)}{m(m-1)s+1}\left\{1+\frac{D}{\sqrt{(m^2s+1)}}\right\} I_m - I_{m-1} \quad (m>1), \tag{31}$$

where $s = p^2/q^2$ and D denotes the operator $\dfrac{1}{\sigma q}\dfrac{d}{dt}$.

Between these equations we may eliminate I_1, I_2,..., in succession to obtain a differential equation of the mth degree connecting I_m, I_0 and the known function $E(t)$. Writing the equations in the abbreviated forms

$$I_1 = a_1\epsilon^{-1}I_0 - b_1 E, \tag{32}$$

$$I_m = a_m\epsilon^{-1}I_{m-1} - b_m I_{m-2} \quad \text{for} \quad m>1, \tag{33}$$

where the a's and b's are easily determined by comparison with (29), (30), and (31), we find that

$$I_m = q_m(D)I_0 - p_m(D)E, \tag{34}$$

where

$$p_m = a_m\epsilon^{-1}p_{m-1} + b_m p_{m-2}, \qquad p_1 = b_1, \qquad p_0 = 0, \tag{35}$$

$$q_m = a_m\epsilon^{-1}q_{m-1} + b_m q_{m-2}, \qquad q_1 = a_1\epsilon^{-1}, \qquad q_0 = 1. \tag{36}$$

It follows that p_m and q_m are polynomials of degree m in the differential operator D, so that (34) is a differential equation of degree m. The ratio p_m/q_m is easily seen to be the mth convergent of the infinite continued fraction in the expression

$$I_0 = \left\{\frac{b_1}{a_1\epsilon^{-1}-}\ \frac{b_2}{a_2\epsilon^{-2}-}\ \frac{b_3}{a_3\epsilon^{-3}-}\ \ldots\right\}E, \tag{37}$$

which may be obtained formally from (32) and (33) by writing (32) in the form

$$I_0 = \frac{b_1 E}{a_1\epsilon^{-1} - I_1/I_0},$$

and making successive substitutions for I_1/I_0, I_2/I_1,..., using (33).

When $z = 0$, the Fourier series on the right of (28) represents a function which is finite and continuous for all x. Hence $I_m \to 0$ as $m \to \infty$. It

† Note that (30) differs slightly from (31) with $m = 1$.

follows from (34) that I_0 must satisfy the limiting form of the differential equation

$$q_m(D)I_0 = p_m(D)E, \tag{38}$$

as $m \to \infty$.

7. Numerical solution for a periodic inducing field

To determine the steady state solution when the inducing field has a simple harmonic time variation, we may take $E(t)$ as the real part of $E_1 e^{i\alpha t}$ and replace the operator D in the above by $i\alpha/\sigma q$. The value of the complex ratio I_0/E_1 is then found from the infinite continued fraction (37), and the values of I_1/E_1, I_2/E_1,..., are determined in succession from (32) and (33). The potential of the induced field is then the real part of the resulting expression (28) when $I_m(t)$ is replaced by $I_m e^{i\alpha t}$.

To illustrate with a numerical example, we take

$$\left.\begin{aligned} p = q, \quad &\text{so that} \quad s = 1, \\ \epsilon = \tfrac{2}{3}, \quad &\alpha/\sigma q = \tfrac{1}{3}, \end{aligned}\right\} \tag{39}$$

so that the resistance of the sheet is given by

$$\rho = \frac{6\pi\alpha}{p}(1 - \tfrac{2}{3}\cos px). \tag{40}$$

With these values, the successive convergents to the continued fraction (37) for I_0/E are

$$\frac{p_1}{q_1} = 0{\cdot}10000 + 0{\cdot}30000i \qquad \frac{p_2}{q_2} = 0{\cdot}12853 + 0{\cdot}32112i,$$

$$\frac{p_3}{q_3} = 0{\cdot}13261 + 0{\cdot}32171i \qquad \frac{p_4}{q_4} = 0{\cdot}13315 + 0{\cdot}32160i,$$

and

$$\frac{p_5}{q_5} = 0{\cdot}13321 + 0{\cdot}32155i.$$

These are evidently tending to a limit which is not very different from p_5/q_5. Taking this as the value of I_0/E_1 the values of I_m/E_1 were calculated for $m = 0$ to $m = 4$, and are given in Table 1.

TABLE 1

m	I_m/E_1	$\beta_m = \mathrm{mod}(I_m/E_1)$	$\epsilon_m = \arg(I_m/E_1)$
0	$0{\cdot}13321 + 0{\cdot}32155i$	0·3482	67·5°
1	$0{\cdot}07808 + 0{\cdot}09786i$	0·1252	51·4°
2	$0{\cdot}02128 + 0{\cdot}01807i$	0·0279	40·4°
3	$0{\cdot}00618 + 0{\cdot}00377i$	0·0069	31·4°
4	$0{\cdot}00181 + 0{\cdot}00048i$	0·0019	14·9°

We deduce that a magnetic field, whose potential is

$$\Omega^{(e)} = E_1 e^{pz} \cos \alpha t \cos py, \tag{41}$$

will induce a current-system in the sheet, whose magnetic field in the region $z > 0$ has the potential

$$\Omega^{(i)} = E_1 \cos py \sum_{m=0}^{\infty} \beta_m \cos(\alpha t + \epsilon_m) \cos mpx \exp\{-pz\sqrt{(m^2+1)}\}, \quad (42)$$

where the values of β_m and ϵ_m are given in Table 1.

This result may be compared with that which would be obtained if the sheet were uniform with the mean conductivity

$$\kappa_0 = \frac{p}{2\pi} \int_0^{2\pi/p} \frac{dx}{2\pi\sigma(1-\epsilon\cos px)} = \frac{3}{2\pi\sigma\sqrt{5}}. \quad (43)$$

In this case the potential of the induced field for the region $z > 0$ is given by

$$\Omega^{(i)} = 0{\cdot}4082 E_1 \cos(\alpha t + 66^\circ) e^{-pz} \cos py. \quad (44)$$

Since the stream-line function for the induced current is given by (14), the current lines will be the curves $\Omega_+^{(i)} = C$, a constant, where $\Omega_+^{(i)}$ is obtained from (42) by putting $z = 0$. Also from (7) the induced current density is given by

$$i_x = -\frac{1}{2\pi}\frac{\partial}{\partial y}\Omega_+^{(i)}, \qquad i_y = \frac{1}{2\pi}\frac{\partial}{\partial x}\Omega_+^{(i)}. \quad (45)$$

The current lines for the three epochs $\alpha t = 0$, 60°, and 120°, $\alpha t = 360^\circ$ corresponding to a complete period of the inducing field, are shown in Fig. 1. At $\alpha t = 180^\circ$ the current lines will be the same as at $\alpha t = 0$, except that they are reversed in direction. During the second half of the period the current distribution will pass through the same sequence of changes as in the first half, but the currents will flow in the opposite direction. The distribution of currents, which would be induced by the same field in a uniform sheet of the same mean conductivity, are shown on the right-hand side of the diagrams in Fig. 1. All the current lines are drawn for values of C increasing from zero by increments of 0·05.

One obvious result of the non-uniform distribution of conductivity is the deflexion of the currents away from the region of high resistance, so that they form circuits whose centres are, in general, in the region of low resistance. Fig. 1 shows that this is true at any rate for the greater part of the time.

The current density reaches a maximum value when $\alpha t = 114^\circ$, the distribution being then practically the same as that shown in Fig. 1*c*. The minimum current density occurs when $\alpha t = 24^\circ$, which is between the two epochs corresponding to Figs. 1*a* and 1*b*; it will be observed that the current flow has changed in direction during the interval between these two epochs. In the case of the uniform sheet the induced currents simply decrease to zero intensity at time $\alpha t = 24^\circ$, and then start to flow

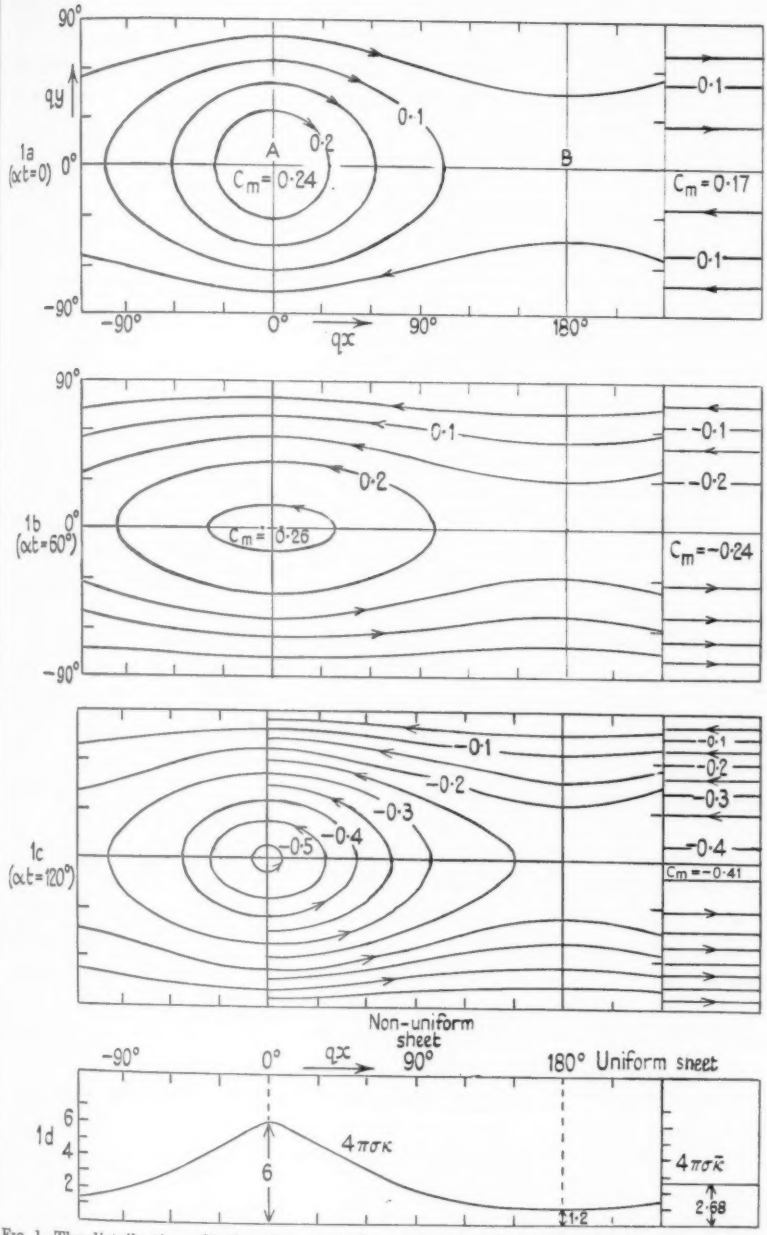

FIG. 1. The distribution of induced currents for a periodic inducing field at the three epochs (*a*) $\alpha t = 0$, (*b*) $\alpha t = 60°$, (*c*) $\alpha t = 120°$. The distribution of conductivity is shown in 1(*d*). The distribution of currents in a uniform sheet of the same mean conductivity ($\bar{\kappa}$) is shown on the right.

again in the opposite direction. But, in the case of the non-uniform sheet, some remarkable changes of distribution occur during the period when the current flow is being reversed. To illustrate these changes, the current distribution was found for the epochs $\alpha t = 17°$, $24°$, $30°$, and $40°$, and the corresponding current lines are shown in Fig. 2. These current lines are drawn for equal increments of 0·01 in C, except for the broken lines in Fig. 2*a*, which correspond to the much smaller increments of 0·0002 in C.

Fig. 2*a* shows that the vortex-system of current, which is centred at A on the line of highest conductivity, and which was of strength $C_m = 0{\cdot}240$ at time $t = 0$, has decreased in strength to $C_m = 0{\cdot}100$ at time $\alpha t = 17°$. Also a new vortex-system, of opposite polarity from that at A, has just come into existence at B, on the line of lowest conductivity. The strength of this new vortex is only $-0{\cdot}0004$ at time $\alpha t = 17°$.

At epoch $\alpha t = 24°$ (Fig. 2*b*) the vortex-system centred at A has decreased still further in strength to the value 0·040. It has also shrunk in dimensions, its outer boundary being a rectangle which is gradually closing up in the x-direction. The new vortex-system, which came into existence at B at time $\alpha t = 17°$, is now seen to be actually a double system with a pair of centres which have now moved apart. The strength of this vortex-system has increased (numerically) to the value $-0{\cdot}032$. Evidently there will not be in this case a particular instant at which the current density is everywhere zero (as there is when the sheet is uniform), because, while the vortex at A is decreasing, the one which started at B is increasing. The exact epoch of minimum total current occurs very shortly after $\alpha t = 24°$, at the instant when the strengths of the two vortices (of opposite polarity) become numerically equal, their values being in fact about $\pm 0{\cdot}036$.

At epoch $\alpha t = 30°$ (Fig. 2*c*) the vortex-system which was centred at A has closed up and disappeared completely, while the new twin vortex-system has increased in strength to $-0{\cdot}057$, and has spread out so as to occupy the entire region. The two centres of this new system have also moved still farther apart. Most of the current still circulates right round the pair of centres, which are of the same polarity, but some of it now passes through the region of high conductivity (cf. the current line $C = -0{\cdot}01$), to link up with the adjacent vortex-systems.

At epoch $\alpha t = 40°$ (Fig. 2*d*) the greater part of the current is flowing nearly parallel to the x-direction. But the most noticeable feature is now the complete separation of the twin vortex-systems which originated at B; one of the vortex centres is approaching the point A, and the corresponding vortex-system is beginning to coalesce with an exactly similar system on the other side of A. The centres of these two systems will continue to move closer together and will eventually coincide at A. The current

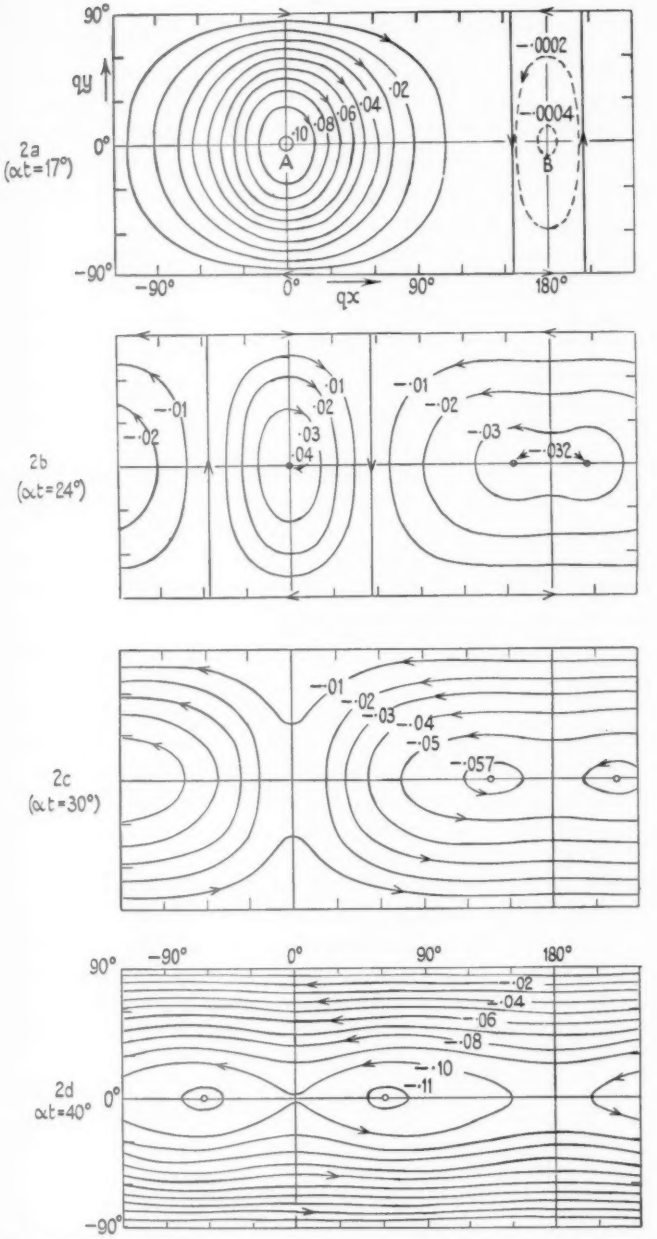

FIG. 2. The distribution of currents at the epochs (*a*) $\alpha t = 17°$, (*b*) $\alpha t = 24°$, (*c*) $\alpha t = 30°$, (*d*) $\alpha t = 40°$, showing how the distribution changes as the current flow is reversed.

distribution will then be as in Fig. 1*b* (epoch $\alpha t = 60°$) where the centres have nearly but not quite coincided.

The changes which take place in the current distribution during the general reversal of current flow can now be summarized as follows. Firstly, new vortex-systems of current, of polarity opposite from the old ones, appear in the regions of *low* conductivity. These new systems each split in two, and the new vortex centres move apart and migrate towards the regions of high conductivity. Pairs of vortex-systems coming from adjacent regions of low conductivity approach each other and coalesce in the regions of high conductivity. Thus new vortex-systems are built up in the regions of high conductivity in which the currents are flowing in the direction opposite from that of the previous systems.

It is evident that similar changes of current distribution will occur in any non-uniform sheet if the inducing field is periodic or fluctuating, since, when the field changes from an increasing one to a decreasing one (or vice versa) the new currents which are induced will be opposed by the old currents which linger in the regions of high conductivity. Consequently the new currents will be deflected so as to form closed circuits, which are initially in the regions of low conductivity.

The time taken up by the above changes in the current distribution is about one-eighth of the half-period for the particular case considered above. In general this time will depend partly on the difference between the maximum and minimum values of the conductivity, and partly on the rate of decay of free current-systems in the sheet, which in turn is largely determined by the mean conductivity. The decay of free current-systems is considered in the next section.

8. Aperiodic inducing fields: the effect of sudden changes

If the inducing field changes instantaneously by some finite amount, and afterwards remains constant, there will be induced in the sheet a system of currents, which subsequently decays freely. To examine this case, we take the time-factor $E(t)$ in the expression (26) for the inducing field to be of the form

$$E(t) = EH(t), \tag{46}$$

where E is a constant and $H(t)$ is Heaviside's discontinuous function, defined by $H(t) = 0$ when $t < 0$ and $H(t) = 1$ when $t \geqslant 0$. The field of the induced currents is then given by (28), where the time-factor $I_0(t)$ is given, from (38), by

$$I_0(t) = E \lim_{m\to\infty} \frac{p_m(D)}{q_m(D)} H(t), \tag{47}$$

which can be evaluated by the methods of the operational calculus. The

remaining time-factors $I_m(t)$ in (28) may then be found from (34) with the last term on the right of this equation taken as zero. This process is in fact equivalent to solving the differential equations (29) to (31) for $I_m(t)$ with the initial conditions $I_0(0) = E$ and $I_m(0) = 0$ for $m > 0$. The result therefore corresponds, as it should do, to the free decay of currents in the sheet, the initial distribution of these currents having a magnetic field given by

$$\Omega^{(i)} = Ee^{-qz}\cos qy. \tag{48}$$

When the effect of a sudden change in the inducing field has been found in the way indicated above, the result for any other aperiodic variation of the field can be deduced by the application of well-known theorems in the operational calculus.

To correspond with the case of the periodic field already treated in § 7, calculations have been made for the aperiodic case when the distribution of conductivity in the sheet is given by (40), and with $p = q$. To determine $I_0(t)$, the successive convergents

$$I_{0,n}(t) = E\frac{p_n(D)}{q_n(D)}H(t), \tag{49}$$

where $n = 1, 2,\ldots$, to the expression (47) for $I_0(t)$ were calculated, using Heaviside's partial fraction rule, since $p_n(D)$ and $q_n(D)$ are polynomials each of degree n in the operator $D = (1/\sigma q)\,d/dt$. The first three convergents are respectively

$$I_{0,1} = Ee^{-\sigma qt}, \tag{50}$$

$$I_{0,2} = E\{0{\cdot}7316e^{-0{\cdot}7599\sigma qt} + 0{\cdot}2684e^{-1{\cdot}6543\sigma qt}\}, \tag{51}$$

$$I_{0,3} = E\{0{\cdot}5977e^{-0{\cdot}6946\sigma qt} + 0{\cdot}3871e^{-1{\cdot}4120\sigma qt} + 0{\cdot}0152e^{-2{\cdot}544\sigma qt}\}. \tag{52}$$

Although the above *expressions* for $I_{0,2}$ and $I_{0,3}$ are quite different, it is remarkable how little the *values* of $I_{0,2}$ and $I_{0,3}$ differ throughout the range $t = 0$ to $t = 4/\sigma q$, by which time $I_0(t)$ has decayed to 0·039 of its initial value. This will be seen from the second and third lines of Table 2. It is evident that $I_{0,4}$ will differ still less from $I_{0,3}$; we therefore assume that $I_{0,3}$ is a good approximation to I_0, and we use (52) together with (34) to calculate I_1 and I_2; to this degree of approximation, the values of I_m for $m > 2$ are all zero. The values of I_1 and I_2 are shown in the last two lines of Table 2.

TABLE 2

σqt	0·1	0·2	0·4	0·6	0·8	1·0	2·0	3·0	4·0
$I_{0,2}/E$	0·9054	0·8212	0·6784	0·5632	0·4699	0·3935	0·1698	0·0767	0·0350
$I_{0,3}/E$	0·9053	0·8209	0·6783	0·5633	0·4698	0·3939	0·1721	0·0800	0·0386
I_1/E	0·0408	0·0741	0·1174	0·1406	0·1503	0·1513	0·1077	0·0612	0·0324
I_2/E	0·0022	0·0044	0·0098	0·0158	0·0207	0·0241	0·0248	0·0162	0·0090

We conclude that a sudden change at time $t = 0$ in the inducing field, of amount represented by the term

$$\Omega^{(e)} = EH(t)e^{qz}\cos qy \quad (z > 0) \tag{53}$$

in its potential, will give rise to a system of currents in the sheet, whose potential in the region $z > 0$ is given, for any subsequent time, by

$$\Omega^{(i)} = \{I_0 e^{-qz} + I_1 e^{-qz\sqrt{2}}\cos qx + I_2 e^{-qz\sqrt{5}}\cos 2qx\}\cos qy, \tag{54}$$

where I_0, I_1, and I_2 are given in Table 2.

The current lines at any particular instant are given by $\Omega^{(i)}_+ = C$, where $\Omega^{(i)}_+$ is obtained from (54) on putting $z = 0$. Fig. 3 shows the current lines corresponding to equal increments of 0·1 in C, for the three epochs, $\sigma qt = 0{\cdot}2$, 1, and 2. This figure shows the expected deflexion of the currents by the ridges of high resistance $\{x = (2n+1)\pi\}$ where $n = 0, 1, 2, \ldots$, so that they form closed circuits centred at points on the lines $(x = 2n\pi)$ of maximum conductivity.

The total current circulating in the sheet at any time is determined by the maximum value of $\Omega^{(i)}_+$ at that time. From (54) the maximum value of $\Omega^{(i)}_+$ at time t is $I_0(t)+I_1(t)+I_2(t)$, and is attained at the vortex centres $(x = 2n\pi,\ y = 2n\pi)$. Hence from Table 2 we see that the total current will be reduced to about 0·3 of its initial value in the time $t = 2/\sigma q$. We may conclude that, in the case of a periodic inducing field of sufficiently long period, the time taken up by the changes in distribution, described in § 7, which occur during the general reversal of flow of the current, will be roughly of the same order. Thus, in the case worked out in § 7, the time taken was about one-sixteenth of the complete period $2\pi/\alpha$, and, from (39), $\alpha = \sigma q/3$, so that the time taken is approximately $1{\cdot}2/\sigma q$.

9. Thin spherical shell with non-uniform conductivity

We now consider the case of a thin spherical shell of radius a for which the resistance ρ at any point is a function of the angular coordinates (θ, λ). The equation (11) in polar coordinates (r, θ, λ) becomes

$$\frac{1}{a^2}\left\{\frac{\partial\rho}{\partial\theta}\frac{\partial}{\partial\theta} + \frac{1}{\sin^2\theta}\frac{\partial\rho}{\partial\lambda}\frac{\partial}{\partial\lambda} + \frac{\rho}{\sin\theta}\frac{\partial}{\partial\theta}\left(\sin\theta\frac{\partial}{\partial\lambda}\right) + \frac{\rho}{\sin^2\theta}\frac{\partial^2}{\partial\lambda^2}\right\}(\Omega^{(i)}_+ - \Omega^{(i)}_-)$$

$$= -4\pi\frac{\partial^2}{\partial t\partial r}(\Omega^{(e)} + \Omega^{(i)}) \quad \text{at} \quad r = a. \tag{55}$$

Since $\Omega^{(e)}$ satisfies Laplace's equation in the neighbourhood of the shell, we may analyse it into spherical harmonics in the form

$$\Omega^{(e)} = a\sum_{m,n}(\zeta^n E^m_n + \zeta^{-n-1}I^m_n)e^{im\lambda}P^m_n(\cos\theta), \tag{56}$$

where $\zeta = r/a$, $\sum_{m,n}$ denotes the double summation $\sum_{n=1}^{\infty}\sum_{m=0}^{n}$ and E^m_n, I^m_n are

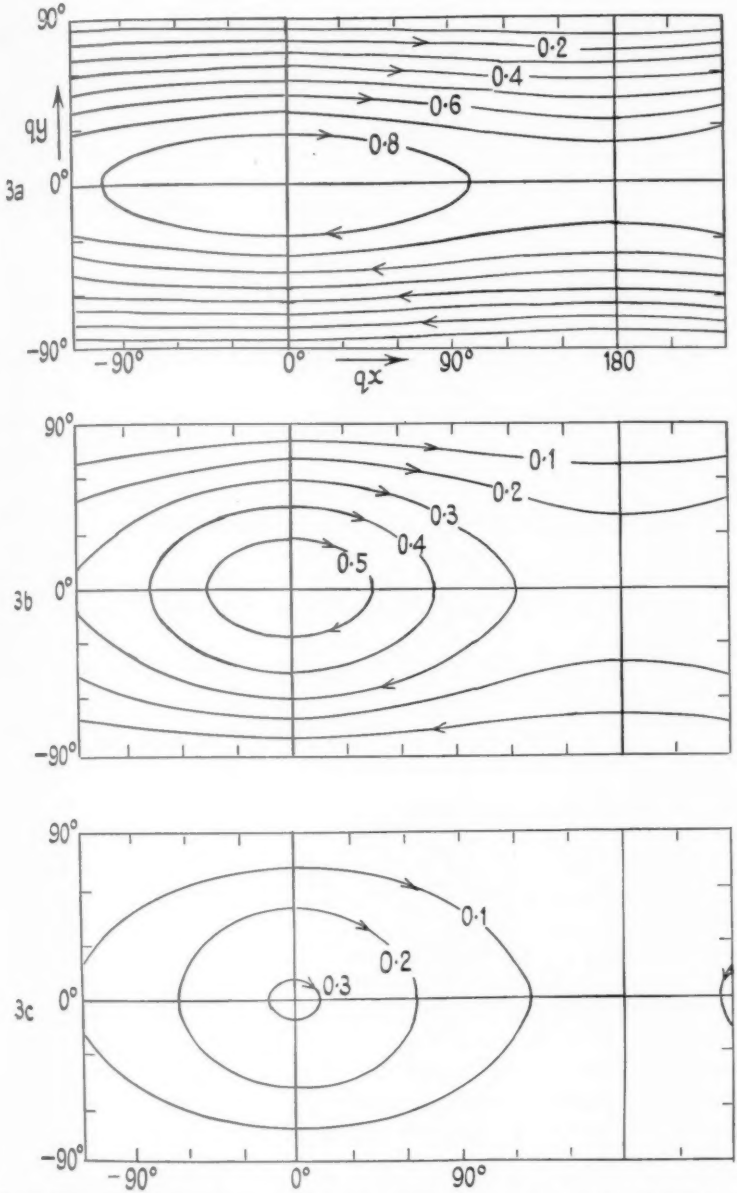

FIG. 3. The freely decaying current-system produced initially by a sudden change in the inducing field. The current lines are drawn for the three epochs (*a*) $\sigma qt = 0{\cdot}2$, (*b*) $\sigma qt = 1{\cdot}0$, (*c*) $\sigma qt = 2{\cdot}0$.

complex numbers, their real and imaginary parts being known functions of the time. The real part of the expression (56) can be made, by suitable choice of E_n^m and I_n^m, to represent the potential of any given inducing field. The E_n^m terms correspond to the part of the inducing field arising from sources external to the sphere of radius r, while the I_n^m terms correspond to the part of internal origin. We shall assume that the field originates outside the shell so that near $r = a$ the I_n^m's will all be identically zero.

In the same way, since the potential $\Omega^{(i)}$ of the induced magnetic field satisfies Laplace's equation, and originates from currents in the shell, it can be expressed in the forms

$$\Omega^{(i)} = a \sum_{m,n} i_n^m \zeta^{-n-1} e^{im\lambda} P_n^m(\cos\theta) \quad (r > a), \tag{57}$$

$$\Omega^{(i)} = a \sum_{m,n} e_n^m \zeta^n e^{im\lambda} P_n^m(\cos\theta) \qquad (r < a). \tag{58}$$

The coefficients i_n^m and e_n^m, which occur in these expressions, are complex functions of the time, and the problem is to determine them in terms of the known time-functions E_n^m.

Since the normal component $(-\partial\Omega^{(i)}/\partial r)$ of the induced field is continuous at $r = a$, we have that

$$\sum_{m,n} (n+1) i_n^m e^{im\lambda} P_n^m(\cos\theta) = -\sum_{m,n} n e_n^m e^{im\lambda} P_n^m(\cos\theta), \tag{59}$$

and, since this is true over the whole sphere, we may equate the coefficients of the separate harmonics, giving

$$(n+1) i_n^m = -n e_n^m. \tag{60}$$

Hence, from (57) and (60) we have that

$$\Omega^{(i)} = -a \sum_{m,n} \frac{n}{n+1} e_n^m \zeta^{-n-1} e^{im\lambda} P_n^m(\cos\theta) \quad \text{for} \quad r > a, \tag{61}$$

which gives the induced field outside the shell in terms of the induced field (58) inside the shell.

Substituting from equations (56), (58), and (61) into (55) we obtain

$$\left\{\frac{\partial\rho}{\partial\theta}\frac{\partial}{\partial\theta} + \frac{1}{\sin^2\theta}\frac{\partial\rho}{\partial\lambda}\frac{\partial}{\partial\lambda} + \frac{\rho}{\sin\theta}\frac{\partial}{\partial\theta}\left(\sin\theta\frac{\partial}{\partial\theta}\right) + \right.$$

$$\left. + \frac{\rho}{\sin^2\theta}\frac{\partial^2}{\partial\lambda^2}\right\} \sum_{m,n} \frac{2n+1}{n+1} e_n^m e^{im\lambda} P_n^m(\cos\theta)$$

$$= 4\pi a \sum_{m,n} n\left(\frac{dE_n^m}{dt} + \frac{de_n^m}{dt}\right) e^{im\lambda} P_n^m(\cos\theta). \tag{62}$$

This equation may be simplified by using the relation

$$\frac{1}{\sin\theta}\frac{\partial}{\partial\theta}\left(\sin\theta\frac{\partial S_n}{\partial\theta}\right) + \frac{1}{\sin^2\theta}\frac{\partial^2 S_n}{\partial\lambda^2} + n(n+1)S_n = 0, \tag{63}$$

which is satisfied by any surface harmonic of degree n. The equation (62) is thereby reduced to the form

$$\sum_{m,n} e_n^m \nabla_n \{e^{im\lambda} P_n^m(\cos\theta)\} = 4\pi a \sum_{m,n} \left(\frac{d}{dt} E_n^m + \frac{d}{dt} e_n^m\right) n e^{im\lambda} P_n^m(\cos\theta), \qquad (64)$$

where ∇_n is the operator defined by

$$\nabla_n = \frac{2n+1}{n+1}\left\{\frac{\partial\rho}{\partial\theta}\frac{\partial}{\partial\theta} + \frac{1}{\sin^2\theta}\frac{\partial\rho}{\partial\lambda}\frac{\partial}{\partial\theta} - n(n+1)\rho\right\}. \qquad (65)$$

This operator depends on the distribution of conductivity in the shell; it reduces to a constant when the distribution is uniform.

The equation (64) is satisfied over the whole surface of the sphere. Hence, multiplying by $e^{-iM\lambda} P_N^M(\cos\theta)$, and integrating over the surface of the sphere, we obtain

$$\sum_{m,n} e_n^m \int_0^{2\pi}\int_0^{\pi} e^{-iM\lambda} P_N^M(\cos\theta) \nabla_n \{e^{im\lambda} P_n^m(\cos\theta)\} \sin\theta \, d\theta d\lambda$$

$$= 4\pi a \sum_{m,n} n\left(\frac{d}{dt} E_n^m + \frac{d}{dt} e_n^m\right) \int_0^{2\pi}\int_0^{\pi} e^{i(m-M)\lambda} P_n^m(\cos\theta) P_N^M(\cos\theta) \sin\theta \, d\theta d\lambda$$

$$= 4\pi a N \left(\frac{d}{dt} E_N^M + \frac{d}{dt} e_N^M\right) \frac{(N+M)!}{(N-M)!} \frac{4\pi}{2N+1}, \qquad (66)$$

by the orthogonal properties of tesseral and zonal harmonics.

The coefficients of e_n^m in the expansion on the left of equation (66) are constants which can be determined if the function ρ is given. Hence equation (66) is a linear differential equation in t with constant coefficients. There will be an equation of this form corresponding to each pair of positive integers (M, N) where $N \geqslant M \geqslant 0$. The required time functions e_n^m are therefore determined by a doubly infinite set of simultaneous linear differential equations (66).

It will be seen that, if ρ is a function of θ only, the coefficient of e_n^m in the expansion on the left of equation (66) will be zero unless $m = M$. Hence the functions e_n^m which have different values of m will be independent; this corresponds to the fact that the harmonics of different rank in the potential of the induced magnetic field will be independent. In this case we obtain a singly infinite system of equations to determine each set of coefficients corresponding to a given value of m.

The solution of these equations will now be considered for a particular case of the function ρ.

10. Spherical shell with resistance $\rho = \rho_0(1+\epsilon\cos\theta)$

Taking the simple distribution of resistance

$$\rho = \rho_0(1+\epsilon\cos\theta), \tag{67}$$

the operator ∇_n becomes

$$\nabla_n = -\frac{2n+1}{n+1}\rho_0\epsilon\sin\theta\frac{\partial}{\partial\theta} - n(2n+1)\rho_0(1+\epsilon\cos\theta). \tag{68}$$

Hence, using the relations

$$(2n+1)\sin\theta\frac{d}{d\theta}P_n^m = n(n-m+1)P_{n+1}^m - (n+1)(m+n)P_{n-1}^m, \tag{69}$$

$$(2n+1)\cos\theta\,P_n^m = (n-m+1)P_{n+1}^m + (m+n)P_{n-1}^m, \tag{70}$$

which are satisfied by the associated Legendre functions, we find that

$$\nabla_n P_n^m = -\frac{n+2}{n+1}\rho_0\epsilon n(n-m+1)P_{n+1}^m - (2n+1)n\rho_0 P_n^m - \\ -(n-1)(n+m)\rho_0\epsilon P_{n-1}^m. \tag{71}$$

Instead of using the general result (66), it is simpler in this case to substitute directly into equation (64). This gives

$$-\sum_{m,n} e_n^m e^{im\lambda}\left\{\frac{n+2}{n+1}\rho_0\epsilon n(n-m+1)P_{n+1}^m + \right. \\ \left. +(2n+1)n\rho_0 P_n^m + (n-1)(n+m)\rho_0\epsilon P_{n-1}^m\right\} \\ = 4\pi a\sum_{m,n}\left(\frac{d}{dt}E_n^m + \frac{d}{dt}e_n^m\right)ne^{im\lambda}P_n^m. \tag{72}$$

Since each side of this equation is an expansion in tesseral (or zonal) harmonics of rank m, and the equation is satisfied over the whole surface of the sphere, we may equate the coefficients of harmonics of the same degree. Thus, picking out the coefficient of $e^{im\lambda}P_n^m$, we find

$$\rho_0\epsilon(n^2-1)(n-m)e_{n-1}^m + \left\{\rho_0 n^2(2n+1) + 4\pi a n^2\frac{d}{dt}\right\}e_n^m + \\ +\rho_0\epsilon n^2(n+m+1)e_{n+1}^m = -4\pi a n^2\frac{d}{dt}E_n^m. \tag{73}$$

Corresponding to each integer $m \geqslant 0$, there is an infinite set of these equations extending from $n = m$ to $n = \infty$. It will be seen that the correct equation is obtained in the special case $n = m$, since the first term on the left of the equation then becomes zero.

If the inducing field contains only the single term E_m^m, the above equations can be solved by methods exactly similar to those used in §§ 6 to 8, the expression for e_m^m reducing to a continued fraction similar to (37).

In the general case when all the E_n^m's are present, the equations beginning at $n = m$ may be written in the form

$$e_{m+1}^m = a_0 \epsilon^{-1} e_m^m + k_0 \epsilon^{-1} E_m^m,$$

$$e_{m+s}^m = a_{s-1} \epsilon^{-1} e_{m+s-1}^m + b_{s-1} e_{m+s-2}^m + k_{s-1} \epsilon^{-1} E_{m+s-1}^m \quad (s > 1), \qquad (74)$$

where the coefficients a_0, k_0, a_{s-1},..., are linear functions of the operator $D \equiv d/dt$, which are easily determined by comparison with (73). By elimination of the intermediate coefficients from (74) it is possible to express e_{m+s}^m in terms of e_m^m and the known functions E_{m+r}^m for $r = 0$ to $s-1$. Writing

$$e_{m+s}^m = q_s e_m^m + \sum_{r=0}^{s-1} p_{r,s} k_r E_{m+r}^m, \qquad (75)$$

we find that q_s and $p_{r,s}$ satisfy the recurrence relations

$$q_s = a_{s-1} \epsilon^{-1} q_{s-1} + b_{s-1} q_{s-2}, \qquad q_1 = a_0 \epsilon^{-1}, \qquad q_0 = 1, \qquad (76)$$

$$p_{r,s} = a_{s-1} \epsilon^{-1} p_{r,s-1} + b_{s-1} p_{r,s-2}, \qquad p_{r,r+1} = 1, \qquad p_{r,r} = 0. \qquad (77)$$

The coefficients q_s and $p_{r,s}$ may also be expressed as continuants in the form

$$q_s = K_{0,s-1}(\epsilon), \qquad p_{r,s} = K_{r+1,s-1}(\epsilon), \qquad (78)$$

where

$$K_{r,s}(\epsilon) = \begin{vmatrix} a_r \epsilon^{-1} & -1 & 0 & . & . & 0 \\ b_{r+1} & a_{r+1} \epsilon^{-1} & -1 & . & . & 0 \\ 0 & b_{r+2} & a_{r+2} \epsilon^{-1} & . & . & . \\ . & . & . & . & a_{s-1} \epsilon^{-1} & -1 \\ 0 & 0 & 0 & . & b_s & a_s \epsilon^{-1} \end{vmatrix}. \qquad (79)$$

This shows that q_s is a polynomial of degree s in the operator D, and $p_{r,s}$ is a polynomial of degree $s-r-1$ in D, so that (75) is a linear differential equation of order s connecting e_{m+s}^m and e_m^m.

Since the expression (58) for $\Omega^{(i)}$ represents a function which is finite and continuous over the sphere $r = a$, it follows that $e_{m+s}^m \to 0$ as $s \to \infty$. Hence from (75), e_m^m must satisfy the limiting form of the differential equation

$$q_s(D) e_m^m + \sum_{r=0}^{s-1} p_{r,s}(D) k_r \epsilon^{-1} E_{m+r}^m = 0 \qquad (80)$$

as $s \to \infty$. We therefore write

$$e_m^m = -\lim_{s \to \infty} \frac{1}{q_s} \sum_{r=0}^{s-1} p_{r,s} k_r \epsilon^{-1} E_{m+r}^m, \qquad (81)$$

and obtain successive convergents to e_m^m by using (76) and (77). When the field is periodic with period $2\pi/\alpha$ we may replace D by $i\alpha$ and follow the same procedure as in § 7. When the field is aperiodic, the successive

convergents to (81) may be evaluated by using Heaviside's partial fraction rule, in a way similar to that adopted in § 8.

When e_m^m has been found, the remaining coefficients e_{m+1}^m, e_{m+2}^m,..., may be obtained in succession by using equations (74).

Some numerical calculations of this solution for the particular case when the inducing field is of the form

$$\Omega^{(e)} = a\zeta E(t)\cos\lambda\sin\theta \tag{82}$$

have been made by A. A. Ashour and the writer (**4**, 1948) and have been used to discuss some effects of the non-uniform distribution of conductivity in the ionosphere.

11. Solution in ascending powers of ϵ

Instead of finding successive convergents to the limiting expression (81) for e_m^m in the manner indicated above, it is also possible to express e_m^m as a power series in ascending powers of ϵ^2. To do this we first obtain the 'corresponding' series for the limiting ratio $K_{r,s}(\epsilon)/K_{0,s}(\epsilon)$ as $s \to \infty$, where $K_{r,s}(\epsilon)$ is the continuant defined in (79).

Expanding $K_{r,s}(\epsilon)$ by Sylvester's rule, we find that

$$K_{r,s}(\epsilon) = \epsilon^{r-s-1} a_r a_{r+1} \ldots a_s (1 + \sum A_{n,r} \epsilon^{2n}), \tag{83}$$

where
$$A_{n,r} = 0 \quad \text{for} \quad 2n > s-r+1, \tag{84}$$

and
$$A_{n,r} = \sum_{t_1=r+1}^{s-2n+2} \sum_{t_2=t_1+2}^{s-2n+4} \cdots \sum_{t_n=t_{n-1}+2}^{s} \beta_{t_1}\beta_{t_2}\ldots\beta_{t_n} \quad \text{for} \quad 2n \leqslant s-r+1, \tag{85}$$

where
$$\beta_t = b_t/a_{t-1}a_t. \tag{86}$$

Hence,
$$\frac{K_{r,s}(\epsilon)}{K_{0,s}(\epsilon)} = \frac{\epsilon^r}{a_0 a_1 \ldots a_{r-1}} \frac{1 + \sum A_{n,r}\epsilon^{2n}}{1 + \sum A_{n,0}\epsilon^{2n}}, \tag{87}$$

and provided all the a's and b's have finite non-zero values, this ratio is an analytic function of ϵ (regarded as a complex variable) near the origin. We may therefore expand it by Taylor's theorem in the form

$$\frac{K_{r,s}(\epsilon)}{K_{0,s}(\epsilon)} = \frac{\epsilon^r}{a_0 a_1 \ldots a_{r-1}} \Big(1 + \sum_{n=1}^{\infty} c_n \epsilon^{2n}\Big), \tag{88}$$

where
$$(1 + \sum c_n \epsilon^{2n})(1 + \sum A_{n,0}\epsilon^{2n}) = 1 + \sum A_{n,r}\epsilon^{2n}. \tag{89}$$

Equating coefficients of like powers of ϵ^2 on the two sides of the identity (89), we have that

$$c_p + c_{p-1}A_{1,0} + c_{p-2}A_{2,0} + \ldots + A_{p,0} = A_{p,r} \tag{90}$$

for all positive integral values of p. Taking $p = 1$ and using (85) we find that

$$c_1 = A_{1,r} - A_{1,0} = \sum_{t=r+1}^{s} \beta_t - \sum_{t=1}^{s} \beta_t = -\sum_{t=1}^{r} \beta_t. \tag{91}$$

Taking $p = 2$ we have similarly that

$$\begin{aligned} c_2 &= A_{2,r} - A_{2,0} - c_1 A_{1,0} \\ &= \sum_{t_1=r+1}^{s-2} \sum_{t_2=t_1+2}^{s} \beta_{t_1}\beta_{t_2} - \sum_{t_1=1}^{s-2} \sum_{t_2=t_1+2}^{s} \beta_{t_1}\beta_{t_2} + \sum_{t_1=1}^{r} \beta_{t_1} \sum_{t_2=1}^{s} \beta_{t_2} \\ &= -\sum_{t_1=1}^{r} \sum_{t_2=t_1+2}^{s} \beta_{t_1}\beta_{t_2} + \sum_{t_1=1}^{r} \sum_{t_2=1}^{s} \beta_{t_1}\beta_{t_2} = \sum_{t_1=1}^{r} \sum_{t_2=1}^{t_1+1} \beta_{t_1}\beta_{t_2}. \end{aligned} \tag{92}$$

It is now easy to prove by induction that, for all integral values of $n \leqslant \frac{1}{2}(s-r+1)$,

$$c_n = (-1)^n \sum_{t_1=1}^{r} \sum_{t_2=1}^{t_1+1} \cdots \sum_{t_n=1}^{t_{n-1}+1} \beta_{t_1}\beta_{t_2}\ldots\beta_{t_n}. \tag{93}$$

For values of $n > \frac{1}{2}(s-r+1)$ the coefficients c_n will depend on s, but (93) shows that *for* $n \leqslant \frac{1}{2}(s-r+1)$ *the coefficients* c_n *are independent of* s. Hence, if we make $s \to \infty$ the series on the right of (88) defines a power series which has the property that its terms as far as ϵ^{2n+r} for any positive integer n, are identical with those of the Taylor expansion of $K_{r,s}(\epsilon)/K_{0,s}(\epsilon)$ for every $s \geqslant 2n+r-1$.

In the special case $r = 1$, the ratio $K_{1,s}(\epsilon)/K_{0,s}(\epsilon)$ is the $(s+1)$th convergent of the infinite continued fraction

$$\frac{1}{a_0\epsilon^{-1}+}\frac{b_1}{a_1\epsilon^{-1}+}\frac{b_2}{a_2\epsilon^{-1}+}\cdots \equiv \frac{\epsilon}{a_0+}\frac{b_1\epsilon^2}{a_1+}\frac{b_2\epsilon^2}{a_2+}\cdots, \tag{94}$$

and the existence of a series having the above property is well known (Perron, **6**, 1912). It is called the 'corresponding' series of the fraction, and the relation between the fraction and the series is indicated by

$$\frac{\epsilon}{a_0+}\frac{b_1\epsilon^2}{a_1+}\frac{b_2\epsilon^2}{a_2+}\cdots \sim \frac{\epsilon}{a_0}\Big(1 + \sum_{n=1}^{\infty} c_n \epsilon^{2n}\Big). \tag{95}$$

Adopting the same notation for the general case (i.e. for any positive integral value of r), we write

$$\lim_{s\to\infty} \frac{K_{r,s}(\epsilon)}{K_{0,s}(\epsilon)} \sim \frac{\epsilon^r}{a_0 a_1 \ldots a_{r-1}}\Big(1 + \sum_{n=1}^{\infty} c_n \epsilon^{2n}\Big), \tag{96}$$

where c_n is now given by the formula (93) for *all* values of n.

As far as the writer knows, the explicit formula (93) for the coefficient c_n of the corresponding series, either for the special case of the continued fraction or for the more general case of the ratio of two continuants, has not previously been obtained, although, in the case of the continued fraction, both Stieltjes (**7**, 1889) and E. T. Whittaker (**8**, 1915) have indicated general processes whereby any particular term may be calculated. Thus Whittaker has shown in effect that the coefficient c_n is equal to the leading element of the $2n$th power of a certain matrix.

The sign $\sim$ cannot in general be replaced by the sign of equality, since the process of deriving the 'corresponding' series involves changing the order of a double limit, but if the expression on the left of (96) converges uniformly to the limit $L(\epsilon)$ in a closed domain D containing the origin, then the series on the right of (96) is convergent inside any circle $\epsilon = \epsilon_0$ within D, and its sum is $L(\epsilon)$. This may be proved by a simple extension of the corresponding theorem given by Perron (**6**, chap. 8, theorem 20) for infinite continued fractions. The uniform convergence of the expression on the left of (96) follows in the present case from the fact that a_s and b_s tend to finite limits (namely -2 and -1) as $s \to \infty$, and we are therefore justified in equating the two sides of (96).

We can now use (96) together with (78) to express the limiting value of $p_{r,s}/q_s$ as $s \to \infty$ in the form of a power series in ϵ^2, explicit formulae for the coefficients of this power series being obtained from (93). On substituting in (81) we get a corresponding expression for e_m^m as a power series in ϵ^2. The coefficients of this power series will be rational functions of the operator D, and the evaluation of e_m^m as an explicit function of the time for both periodic and aperiodic fields can be effected by methods similar to those of the previous sections.

In practice it has been found that the method of solution described in § 10 is generally more convenient than the one just described, but the latter has the advantage that one calculation serves for all values of ϵ, the series obtained being fairly rapidly convergent if $\epsilon < 1/3$.

12. Applicability of 'relaxation' methods to the problem

The analytic methods described in the above §§ 4–11 for obtaining solutions of the fundamental equations of § 3 lead to manageable calculations only when the distribution of conductivity is of a fairly simple form. In some geophysical problems it is desirable to estimate the effects of irregular distributions of conductivity, given as empirical functions over the surface of the earth (for example the integrated conductivity of the oceans), and to deal with these cases other methods for approximating to the solution must be found.

The possibility of using 'relaxation' methods for this purpose is first considered. The present problem involves the determination of a potential function $\Omega^{(i)}$ which satisfies Laplace's equation, with appropriate conditions at infinity, and the boundary condition expressed by equation (11) of § 3 at the conducting surface. The latter boundary condition involves the time-variable, but in the case of periodic fields (to which we shall now confine our discussion) this variable can be eliminated if $\Omega^{(i)}$ is treated as complex, as in § 7. The required function $\Omega^{(i)}$ is then, in general, a complex

function of three space-variables. The familiar relaxation methods for solving Laplace's equation can be used to determine $\Omega^{(i)}$ provided the number of space-variables can be reduced to two, but this is only possible when the distribution of conductivity is expressible in terms of only *one* variable. For example, in the case of the spherical shell, if the conductivity is a function of θ only, the inducing field $\Omega^{(e)}$ may be analysed into spherical harmonics of the form $E_n^m P_n^m(\cos\theta)\cos(m\lambda+\epsilon_m)$, and the harmonics of different rank (m) treated separately, as shown in § 10. The term in $\Omega^{(i)}$ corresponding to the harmonic of rank m will then be of the form

$$\Omega_m^{(i)}\cos(m\lambda+\epsilon_m),$$

where $\Omega_m^{(i)}$ is a (complex) function of the two variables (r, θ), which can be found by relaxation methods.

The above shows that the straightforward application of relaxation methods makes it possible to extend the solution obtained in § 10 (for which numerical calculations have been made by Ashour and Price) to the case where ρ is any function of θ. Relaxation methods alone will not, however, enable us to deal with the case where ρ is a function of both θ and λ, unless such methods are extended to three dimensions. This, of course, would be theoretically possible, but does not seem likely to lead to a convenient method for dealing with the present problem. What is really required is some way of analysing the mathematical problem into a number of simpler ones, each of which involves a manageable set of calculations. Two possible ways of doing this, suggested by physical considerations, are described in the next section.

13. Alternative methods of approximating to the solution

If the equation (11) is written in the form

$$\rho\,\mathrm{div}\,\mathrm{grad}\,\Psi+\mathrm{grad}\,\rho\,.\,\mathrm{grad}\,\Psi=-\frac{\partial^2\Omega^{(e)}}{\partial t\partial n}-\frac{\partial^2\Omega^{(i)}}{\partial t\partial n}, \tag{97}$$

where Ψ is the current function given by (8), it will be seen that Ψ can be divided into two parts $\Psi^{(e)}$ and $\Psi^{(i)}$, which respectively satisfy the equations

$$\rho\,\mathrm{div}\,\mathrm{grad}\,\Psi^{(e)}+\mathrm{grad}\,\rho\,.\,\mathrm{grad}\,\Psi^{(e)}=-\frac{\partial^2\Omega^{(e)}}{\partial t\partial n}, \tag{98}$$

$$\rho\,\mathrm{div}\,\mathrm{grad}\,\Psi^{(i)}+\mathrm{grad}\,\rho\,.\,\mathrm{grad}\,\Psi^{(i)}=-\frac{\partial^2\Omega^{(i)}}{\partial t\partial n}. \tag{99}$$

The first part $\Psi^{(e)}$ corresponds to the current system which would be obtained if self-induction were ignored. This part can be calculated directly from (98) since $\Omega^{(e)}$ is a given function, the calculation being made by relaxation or other numerical methods, if analytic methods are not convenient.

The second part $\Psi^{(i)}$ represents the effect of self-induction. It cannot, of course, be calculated directly from (99) because $\Omega^{(i)}$ is unknown. But under certain circumstances (which are examined below) a first approximation Ω_1 to $\Omega^{(i)}$ can be obtained by calculating the magnetic potential of the current system $\Psi^{(e)}$. In the case of the plane sheet or spherical shell this can be done by known methods. If we now substitute Ω_1 for $\Omega^{(i)}$ on the right of (97), and solve the resulting equation by 'relaxation' or other methods, we get a corresponding approximation Ψ_1' to Ψ'.

A second approximation Ψ_2' can now be obtained by calculating the potential Ω_2 of the field due to Ψ_1', substituting Ω_2 for $\Omega^{(i)}$ in (97), and again solving this equation.

This process can evidently be continued and, if convergent, will lead to the required function Ψ' and the corresponding potential $\Omega^{(i)}$. In practice it is slightly more convenient to use (99) instead of (97) in the iteration process; this leads to the sequence of correction terms $\Psi_1'-\Psi^{(e)}, \Psi_2'-\Psi_1', \ldots$, which must, of course, tend to zero.

To determine the conditions under which this process will lead to a solution, it is sufficient to consider a trivial case for which the analytic solution is known. We consider the case of a plane uniform sheet, so that equation (11) reduces to

$$\rho\left(\frac{\partial^2\Psi'}{\partial x^2}+\frac{\partial^2\Psi'}{\partial y^2}\right)=-\frac{\partial^2\Omega^{(e)}}{\partial t\partial z}-\frac{\partial^2\Omega^{(i)}}{\partial t\partial z} \quad \text{at} \quad z=0, \tag{100}$$

and the relation between Ψ' and $\Omega^{(i)}$ is given by (14). If the inducing field is given by

$$\Omega^{(e)}=e^{\lambda z}\cos\lambda x\, e^{i\alpha t}, \tag{101}$$

the analytic solution for the induced field (cf. (16) and (17)) is given by

$$\Omega^{(i)}=\frac{\beta}{1+\beta}e^{-\lambda z}\cos\lambda x\, e^{i\alpha t}, \tag{102}$$

where

$$\beta=2\pi i\alpha/\lambda\rho. \tag{103}$$

Now applying the method described above, we find that

$$\Psi^{(e)}=\frac{i\alpha}{\lambda\rho}\cos\lambda x\, e^{i\alpha t},$$

whence

$$(\Omega_1)_{z=0}=2\pi\Psi^{(e)}=\beta\cos\lambda x\, e^{i\alpha t}, \tag{104}$$

and therefore

$$\Omega_1=\beta e^{-\lambda z}\cos\lambda x\, e^{i\alpha t}. \tag{105}$$

In the next step the equations are of exactly the same form as before, except that Ω_1 replaces $\Omega^{(e)}$; it easily follows that

$$\Omega_2-\Omega_1=-\beta^2 e^{-\lambda z}\cos\lambda x\, e^{i\alpha t},$$

and continuing the process, we evidently get

$$\Omega_n=\beta\{1-\beta+\beta^2-\ldots+(-\beta)^{n-1}\}e^{-\lambda z}\cos\lambda x\, e^{i\alpha t}. \tag{106}$$

Hence this process converges to the correct solution (102), provided that

$$|\beta| = \frac{2\pi\alpha}{\lambda\rho} \leqslant 1. \tag{107}$$

It will be observed that β depends on the conductivity $(1/\rho)$ of the sheet, and on the period $(2\pi/\alpha)$ and spatial distribution (wave-length $2\pi/\lambda$) of the inducing field.

The above indicates that this method will in general work best for the case of low conductivities, slow oscillations, and high (spatial) harmonics in the total field. The influence of the spatial distribution of the field is particularly important in the case of non-uniform distributions, for reasons indicated below.

The method just described is based on the possibility of obtaining a satisfactory first approximation by neglecting self-induction. This method is not satisfactory if the conductivity is too high, but physical considerations suggest that in this case a suitable first approximation may be obtained by neglecting the resistance. Thus, putting $\rho = 0$ in (97), and denoting the resulting approximation to $\Omega^{(i)}$ by $\Omega^{(1)}$ we obtain

$$\frac{\partial\Omega^{(1)}}{\partial n} = -\frac{\partial\Omega^{(e)}}{\partial n}, \tag{108}$$

from which $\Omega^{(1)}$ may be determined since $\Omega^{(e)}$ is known. In the cases of the plane sheet and spherical shell the formulae required for this determination are well known.

Corresponding to this value of $\Omega^{(1)}$ a current function $\Psi^{(1)}$ can be found, and substituting $\Psi^{(1)}$ in (97) a second approximation $\Omega^{(2)}$ to $\Omega^{(i)}$ is obtained. If this procedure is repeated, a third approximation $\Omega^{(3)}$ can be obtained, and so on.

Applying this method to the simple case already treated by the first method, we easily find

$$\Omega^{(n)} = \left(1 - \frac{1}{\beta} + \frac{1}{\beta^2} - \ldots + \left(-\frac{1}{\beta}\right)^{n-1}\right) e^{-\lambda z}\cos\lambda x\, e^{i\alpha t}, \tag{109}$$

which tends to the correct limit (102), provided

$$|\beta| = \frac{2\pi\alpha}{\lambda\rho} \geqslant 1. \tag{110}$$

Hence comparing (110) with (107) we see that the two methods are complementary, in the sense that when one does not converge the other does. We can therefore expect one or other of these methods to be applicable in all cases.

A point arises in connexion with the application of the second method to non-uniform distributions, which is not brought out by the above

example. This relates to the spatial distribution of the computed field $\Omega^{(n)}$. This distribution remains constant in the above example, but in the general case it will change at each step in the approximation. Now, the inequality (110) shows that for the second method to be convergent the field must not contain spatial harmonics of excessively high order. For example, in the case of the plane sheet the wave-length $2\pi/\lambda$ must not be too small, and, correspondingly, in the case of the spherical shell, the spherical harmonics in the field must not be too high. While this condition may be fulfilled by the inducing field itself, and possibly by the first few approximations $\Omega^{(1)}$, $\Omega^{(2)}$,..., to $\Omega^{(i)}$ there may come a stage when $\Omega^{(n)}$ contains harmonics of such high order that the method is not convergent. If this occurs, however, it is always possible to separate the part of the field containing the high harmonics, and deal with this part by the first method. Hence for some problems a combination of the two methods will be required. It will be evident that physical considerations can be of great assistance in guiding the work and reducing the labour of computing such problems.

The two methods described above have been tested by J. M. de Wet (**9**, 1948) against the analytic solution for the particular non-uniform spherical shell problem treated by Ashour and Price (**4**, 1948), and are found to work well when proper precautions, such as those noted above, are taken to ensure the convergence of the method. It seems likely that these methods will prove useful in considering the effects of the oceans on geomagnetic variations.

REFERENCES

1. S. Chapman and A. T. Price, *Phil. Trans. Roy. Soc.* A, **229** (1930), 427.
2. B. N. Lahiri and A. T. Price, ibid. **237** (1939), 509.
3. N. F. Barber, *Mon. Not. Roy. Astron. Soc. Geophys. Supp.* **5** (1948), 258.
4. A. A. Ashour and A. T. Price, *Proc. Roy. Soc.* A, **195** (1948), 198.
5. Clerk Maxwell, *Electricity and Magnetism*, 3rd ed. (1904), 299.
6. O. Perron, *Kettenbrüchen* (1912), ch. 8.
7. T. J. Stieltjes, *Annal. de Toulouse*, **3** (1889), mém. no. 8.
8. E. T. Whittaker, *Proc. Roy. Soc. Edin.* **36** (1915), 243.
9. J. M. de Wet, Thesis in preparation.

ON WEBER'S FUNCTION

By C. G. DARWIN (*National Physical Laboratory, Teddington, Middlesex*)

[Received 2 November 1948]

SUMMARY

The equation $\frac{d^2u}{dx^2}+(\frac{1}{4}x^2-a)u = 0$ occurs in a number of wave problems, and tables of its real solutions are in course of preparation. The solutions are specializations of the $W_{k,m}$ function of Whittaker, but the present work proceeds from first principles so as to avoid this over-generalization. The appropriate solutions are mirror images in $x = 0$. For positive a the first of them resembles an exponential near the origin, rises to a large value near $2\sqrt{a}$, and then oscillates with slowly decreasing amplitude and wave-length. The second resembles an exponential with negative argument and after $2\sqrt{a}$ also oscillates. Near infinity the two curves are 90° out of phase. For negative a there is a similar pair of solutions, but the oscillations start at zero, and are roughly of equal amplitude; near infinity they are 90° out of phase.

Convergent power series are given for the two solutions, and also the associated asymptotic series for large x. Neither of these types of series would be much use when a is large, whether positive or negative, and another set of series is developed applicable for large a. For positive a there are two such series, one applicable for values of x from infinity down to somewhere not far above $2\sqrt{a}$, and the other for values of a from zero to a point somewhat below $2\sqrt{a}$. For large negative a the similar series appears to converge for all values of x.

1. THE purpose of the present note is to discuss the various solutions of the differential equation

$$\frac{d^2u}{dx^2}+(\tfrac{1}{4}x^2-a)u = 0. \tag{1.1}$$

The equation has occurred in various problems of vibration, and in particular in connexion with the propagation of electro-magnetic waves in the ionosphere. Tables are in course of preparation for its solutions; they are being prepared by Scientific Computing Service Ltd., on behalf of the National Physical Laboratory, and it was this that stimulated the undertaking of the present work.

The equation is discussed at some length in Whittaker and Watson's *Modern Analysis* (§ 16.5), but with the difference that the term in x^2 is negative, signifying that the real axis is 45° different from that taken here. This, of course, makes no difference to its character in the complex plane, but makes a very considerable difference when the question of real solutions with real a is considered; for example, the scales of relation, so valuable when x^2 has negative sign, are no longer serviceable. The approach in Whittaker and Watson is by specializing a more general function, and it

does not fully consider which among the various solutions are practically most convenient. This approach from the general Whittaker function was also used by J. C. P. Miller and C. W. Jones in the preliminary work for the forthcoming tables, but it of course entails mastering the properties of more general forms than those actually required. The present work has therefore started from first principles, though broadly following similar lines. At the end, however, certain asymptotic solutions are developed which are not to be found in Whittaker and Watson.

The accepted form of the equation contains the term $\frac{1}{4}x^2$, but it is by no means clear why the $\frac{1}{4}$ was introduced. It complicates the algebra of all the solutions and disfigures nearly every formula by an unnecessary factor $\sqrt{2}$, which would not have occurred if the term had been taken simply as x^2. In fact most of the present work was done without the factor $\frac{1}{4}$, but I have concluded with some reluctance to restore it so as to agree with the form which is to be used in the tables, where, after due consideration, it was decided to retain it. If the function were to have the same sort of widespread use as the Bessel functions it would certainly be best to alter it, but with its more restricted importance, and with numerical tables which are to appear in this form, it seemed that the inconvenience of changing over would outweigh the inconvenience of the accepted form.

The general geometrical character of the solutions is easily seen. First take the more interesting case of $a > 0$. From (1.1) it appears that if $|x| < 2\sqrt{a}$, the curve is convex to the x-axis, while if $|x| > 2\sqrt{a}$ it is concave. It is clear that there are two solutions, one an even function, and the other odd, and these make a convenient starting-point. Near the origin the even function, say u_0, is like a hyperbolic cosine. It gradually drops below the curve $\cosh x\sqrt{a}$, but rises to a rather large value at $2\sqrt{a}$, which is a point of inflexion. It then turns gradually towards the axis, crosses it and executes oscillations, slowly diminishing in amplitude and wave-length. The odd function u_1 starts like a hyperbolic sine and then behaves in the same way, bending back and oscillating after $2\sqrt{a}$. For large positive values of x the two solutions become nearly proportional to one another, while for large negative values they are nearly proportional but of opposite sign. This implies that these two solutions are not the best to take, but that instead one solution should be a combination which cancels out the main asymptotic expression; in fact they should correspond to the exponential functions instead of the hyperbolic. From the form of the differential equation it is evidently possible to take the two solutions as mirror images of one another in $x = 0$, so that $u_{\mathrm{II}}(x) = u_{\mathrm{I}}(-x)$, and this has the advantage that such a pair need only be tabulated for positive values of x. For use in problems of wave propagation the right

choice of the pair is that near infinity their oscillations should be 90° out of phase with one another. As will appear, these conditions imply that the amplitudes of either curve at its two ends are as different as possible, one large and the other small, and that near zero they have the character of the exponential function.

For negative a the curves u_0 and u_1 are always concave to the x-axis, and so resemble roughly cosine and sine functions. Nevertheless, to adopt the even and odd functions is again not convenient, since their asymptotic values again tend towards the same form. Instead it is again best to adopt the principle that the two asymptotic solutions near infinity should be those with phases 90° apart.

2. By routine methods the even and odd solutions may be found in absolutely convergent series. They are normalized respectively to values 1 and x, and are:

$$u_0 = \frac{e^{ix^2/4}}{\Gamma_1} \sum_{\substack{0 \\ n \text{ even}}}^{\infty} \frac{\Gamma(\frac{1}{2}n+\frac{1}{4}+\frac{1}{2}ia)}{n!}(\sqrt{2}xe^{-i\pi/4})^n, \tag{2.1}$$

$$u_1 = \frac{e^{ix^2/4}}{\sqrt{2}e^{-i\pi/4}\Gamma_3} \sum_{\substack{1 \\ n \text{ odd}}}^{\infty} \frac{\Gamma(\frac{1}{2}n+\frac{1}{4}+\frac{1}{2}ia)}{n!}(\sqrt{2}xe^{-i\pi/4})^n, \tag{2.2}$$

where
$$\Gamma_1 = \Gamma(\tfrac{1}{4}+\tfrac{1}{2}ia), \qquad \Gamma_3 = \Gamma(\tfrac{3}{4}+\tfrac{1}{2}ia). \tag{2.3}$$

In spite of their complex forms both these solutions are real, as is evident from the fact that the imaginary part of (2.1) must be a solution, but, unlike the real part, could only start at the term in x^2 and there is only room for one even solution.

Expanded for the first few terms, the solutions give

$$u_0 = 1+a\frac{x^2}{2!}+(a^2-\tfrac{1}{2})\frac{x^4}{4!}+(a^3-\tfrac{7}{2}a)\frac{x^6}{6!}+\ldots, \tag{2.4}$$

$$u_1 = x+a\frac{x^3}{3!}+(a^2-\tfrac{3}{2})\frac{x^5}{5!}+(a^3-\tfrac{13}{2}a)\frac{x^7}{7!}+\ldots. \tag{2.5}$$

3. The expressions Γ_1, Γ_3 of (2.3) play a great part in the solution.

Write
$$\Gamma_1 = G_1 e^{i\gamma_1}, \qquad \Gamma_3 = G_3 e^{i\gamma_3}. \tag{3.1}$$

Also let
$$\tan\beta = e^{-\pi a}. \tag{3.2}$$

Then the following relations follow from the properties of gamma functions:

$$G_1 G_3 = 2\pi\cos\beta\, e^{-\pi a/2} \tag{3.3}$$

$$\gamma_1-\gamma_3 = \beta-\tfrac{1}{4}\pi. \tag{3.4}$$

Asymptotic expansions are also required. For large positive a they are:

$$\ln G_1 = -\frac{\pi a}{4} - \tfrac{1}{4}\ln \tfrac{1}{2}a + \tfrac{1}{2}\ln 2\pi + \frac{1}{32a^2} + \frac{5}{256a^4} + \frac{61}{1536a^6}, \tag{3.5}$$

$$\ln G_3 = -\frac{\pi a}{4} + \tfrac{1}{4}\ln \tfrac{1}{2}a + \tfrac{1}{2}\ln 2\pi - \frac{1}{32a^2} - \frac{5}{256a^4} - \frac{61}{1536a^6}, \tag{3.6}$$

$$\gamma_1 + \frac{\pi}{8} = \gamma_3 - \frac{\pi}{8} = \tfrac{1}{2}a\ln \tfrac{1}{2}a - \tfrac{1}{2}a + \frac{1}{48a} + \frac{7}{5760a^3} + \frac{31}{80640a^5}. \tag{3.7}$$

For large negative a, write $-a$ for a in (3.5) and (3.6); in (3.7) change the sign of $\frac{1}{8}\pi$ and replace the first term by $\frac{1}{2}a\ln(-\frac{1}{2}a)$, leaving the rest unaltered.

Another relation that will be used is:

$$\Gamma(\tfrac{1}{2}+ia) = \sqrt{(2\pi)}\cos\beta\, e^{-\pi a/2} 2^{ia} e^{i(\gamma_1+\gamma_3)}. \tag{3.8}$$

4. The expressions (2.1) and (2.2) combine very obviously into the solutions:

$$u_2 = \Gamma_1 u_0 + \sqrt{2}e^{-i\pi/4}\Gamma_3 u_1 = e^{ix^2/4}\sum_0^\infty \Gamma(\tfrac{1}{2}n+\tfrac{1}{4}+\tfrac{1}{2}ia)(\sqrt{2}xe^{-i\pi/4})^n/n! \tag{4.1}$$

$$u_3 = \Gamma_1 u_0 - \sqrt{2}e^{-i\pi/4}\Gamma_3 u_1 = e^{ix^2/4}\sum_0^\infty (-)^n\Gamma(\tfrac{1}{2}n+\tfrac{1}{4}+\tfrac{1}{2}ia)(\sqrt{2}xe^{-i\pi/4})^n/n!. \tag{4.2}$$

These have the relation $u_3(x) = u_2(-x)$ that is wanted, but they are complex. They, however, give the easiest approach for the asymptotic series, which can be best made by Barnes's method. The appropriate integral is

$$\int_{-i\infty}^{i\infty} \Gamma(s)\Gamma(b-2s)(\sqrt{2}xe^{i\lambda})^{2s}\, ds, \tag{4.3}$$

taken so as to leave all the poles of the first factor on the left and of the second on the right. For convergence $|\lambda| < \frac{3}{4}\pi$. By extending the integral round an infinite positive semicircle, over which it vanishes, it is easy to choose b and λ so as to get a series of the form of (4.2). The result is thus:

$$u_3 = \frac{e^{ix^2/4}}{\pi i}\int_{-i\infty}^{i\infty} \Gamma(s)\Gamma(\tfrac{1}{2}+ia-2s)(\sqrt{2}xe^{-i\pi/4})^{2s-\frac{1}{2}-ia}\, ds. \tag{4.4}$$

For the asymptotic series the Barnes contour is transferred to the left over a number of the poles of $\Gamma(s)$. The result, using (3.8), is:

$$u_3 = 2\sqrt{\pi}\cos\beta\, e^{-3\pi a/4} e^{i(\gamma_1+\gamma_3+\pi/8)} u_a, \tag{4.5}$$

where

$$u_a \sim \frac{e^{ix^2/4}}{(x/\sqrt{2})^{\frac{1}{2}+ia}}\left\{1 + \frac{(\frac{1}{2}+ia)(\frac{3}{2}+ia)}{1!\,(2ix^2)} + \frac{(\frac{1}{2}+ia)(\frac{3}{2}+ia)(\frac{5}{2}+ia)(\frac{7}{2}+ia)}{2!\,(2ix^2)^2} + \ldots\right\}. \tag{4.6}$$

5. This method cannot be applied so as to yield an asymptotic series for u_2 because λ in (4.3) would have to be $\frac{3}{4}\pi$, which is not admissible. But we have as a second solution of (1.1) the conjugate complex of (4.5), and u_2 can be expressed as a linear combination of these two solutions. To do this, u_0 and u_1 (which are real) are expressed in terms of u_3 and u_3^*, and u_2 is given by (4.1). The result is

$$u_2 = -iu_3 \cot\beta + u_3^* \operatorname{cosec}\beta\, e^{i(\gamma_1+\gamma_3+\pi/4)}, \tag{5.1}$$

and, using (4.5) and (3.2),

$$u_2 = 2\sqrt{\pi}e^{\pi a/4}\{\cos\beta\, e^{i(\gamma_1+\gamma_3-3\pi/8)}u_a + e^{i\pi/8}u_a^*\}. \tag{5.2}$$

6. From these solutions real ones must now be constructed. They should have the following characters: (1) One should be the reflection of the other in $x = 0$; this implies that if one is $u_{\mathrm{I}} = Au_2 + A^*u_2^*$, the other must be $u_{\mathrm{II}} = Au_3 + A^*u_3^*$; (2) the oscillations near infinity should be 90° out of phase; (3) since the amplitude of u_2 towards infinity is much larger than that of u_3, they are fittingly chosen so that the product of these amplitudes is of order unity. These three conditions define most of the factors in A, but any other real factor of order unity may be introduced. The normalization to be used in the tables will be that the two solutions should conform to the equation

$$u_{\mathrm{II}}\frac{du_{\mathrm{I}}}{dx} - u_{\mathrm{I}}\frac{du_{\mathrm{II}}}{dx} = 1, \tag{6.1}$$

and this will be adopted here as being best, in spite of a slight loss of formal elegance, since normalizations depending on squares or products usually, as here, introduce unwanted square roots into the formulae.

Take $$A = \frac{2^{-\frac{1}{4}}}{4\sqrt{\pi}} \sec\tfrac{1}{2}\beta \sqrt{(\sec\beta)} e^{\pi a/4} e^{-i\{\frac{1}{2}(\gamma_1+\gamma_3)-\frac{1}{4}\pi\}}.$$

The asymptotic series then are:

$$u_{\mathrm{I}} = 2^{-\frac{1}{4}}e^{\pi a/2}\cos\tfrac{1}{2}\beta\sqrt{(\sec\beta)}\{u_a\, e^{i\{\frac{1}{2}(\gamma_1+\gamma_3)-\frac{1}{4}\pi\}} + u_a^* e^{-i\{\frac{1}{2}(\gamma_1+\gamma_3)-\frac{1}{4}\pi\}}\} \tag{6.2}$$

$$u_{\mathrm{II}} = 2^{-\frac{1}{4}}e^{-\pi a/2}\sec\tfrac{1}{2}\beta\sqrt{(\cos\beta)}\{u_a\, e^{i\{\frac{1}{2}(\gamma_1+\gamma_3)+\frac{1}{4}\pi\}} + u_a^* e^{-i\{\frac{1}{2}(\gamma_1+\gamma_3)+\frac{1}{4}\pi\}}\}. \tag{6.3}$$

Again substituting back into (4.1), (4.2),

$$u_{\mathrm{I}} = 2^{-\frac{1}{4}}\pi^{-\frac{1}{2}}e^{\pi a/4}\sqrt{(\sec\beta)}\{G_1 u_0 + \sqrt{2}G_3 u_1\} \tag{6.4}$$

$$u_{\mathrm{II}} = 2^{-\frac{1}{4}}\pi^{-\frac{1}{2}}e^{\pi a/4}\sqrt{(\sec\beta)}\{G_1 u_0 - \sqrt{2}G_3 u_1\}. \tag{6.5}$$

These formulae suffice to give the solutions for any value of x, provided a is not too large. They are valid whether a is positive or negative, but it should be noticed that whereas, when a is large positive, $\cos\beta$ and $\cos\frac{1}{2}\beta$ are near 1, so that (6.2) has amplitude very much greater than (6.3), when

a is large negative $\cos\beta$ tends to zero like $e^{\pi a}$, and the two asymptotic expressions have amplitudes of the same order.

In the neighbourhood of the origin, the leading terms are found from (3.5), (3.6) to be

$$u_{\mathrm{I}} = 2^{-\frac{1}{3}}|a|^{-\frac{1}{4}}(1+x\sqrt{|a|}) \tag{6.6}$$

$$u_{\mathrm{II}} = 2^{-\frac{1}{3}}|a|^{-\frac{1}{4}}(1-x\sqrt{|a|}) \tag{6.7}$$

for large a whether positive or negative.

7. When a is large (6.2–5) are of little use. Take the case of a positive. The convergent series (6.4), (6.5) will require a very large number of terms even for small values of x, and the asymptotic series (4.6) will not be useful until x is considerably greater than a, whereas the curve starts oscillating shortly after $x = 2\sqrt{a}$. There is clearly need of series in which x and a are both large, and these are provided by the well-known solution which starts

$$e^{i\int\sqrt{(\frac{1}{4}x^2-a)}\,dx}/(\tfrac{1}{4}x^2-a)^{\frac{1}{4}}.$$

I have not succeeded in formally converting the general solution into one of this type, but have obtained the result by solving the differential equation in this form, and then matching the result with the appropriate series in (6.2), etc. This method has, of course, the weakness that there is no obvious remainder theorem, as there is for (4.6).

An interesting point in the solution is that the work is made very much easier by taking the whole solution as an exponential rather than as in (4.6) as a power series. (This form is also much the best for the expression of the Bessel function $J_n(x)$ when both x and n are large.)

Let

$$\sqrt{(x^2-4a)} = X \tag{7.1}$$

and let

$$\phi = \tfrac{1}{2}\int_{2\sqrt{a}}^{x} X\,dx = \tfrac{1}{4}xX - a\ln\frac{x+X}{2\sqrt{a}}; \tag{7.2}$$

then the solution is of the form

$$\ln u_b = i\phi - \tfrac{1}{2}\ln X + \frac{ig}{X^3} + \frac{h}{X^6} + \frac{il}{X^9} + \frac{m}{X^{12}} + \frac{in}{X^{15}} + \frac{p}{X^{18}}, \tag{7.3}$$

where g, h, l,... are to be determined as functions of x.

On substituting in (1.1) a sequence of equations is given, from which

$$X^2\frac{dg}{dx} - 3xg, \qquad X^2\frac{dh}{dx} - 6xh, \qquad X^2\frac{dl}{dx} - 9xl,...$$

can in turn be evaluated as polynomials in x and a. Each of these can now be integrated, and in doing so the complementary functions may be

omitted, since they are proportional to X^3, X^6,..., etc., and so only yield an over-all arbitrary constant. The results are:

$$g = \frac{1}{a}\left(\frac{x^3}{48} - \frac{ax}{2}\right) \tag{7.4}$$

$$h = -(\tfrac{3}{4}x^2 + 2a) \tag{7.5}$$

$$l = \frac{1}{a^3}\left(\frac{7}{5760}x^9 - \frac{7}{320}ax^7 + \frac{49}{320}a^2x^5 + \frac{31}{12}a^3x^3 + 19a^4x\right) \tag{7.6}$$

$$m = \frac{153}{8}x^4 + 186ax^2 + 80a^2 \tag{7.7}$$

$$n = \frac{1}{a^5}\left(\frac{31}{80640}x^{15} - \frac{31}{2688}ax^{13} + \frac{403}{2688}a^2x^{11} - \frac{4433}{4032}a^3x^9 + \right.$$
$$\left. + \frac{4433}{896}a^4x^7 - \frac{13643}{80}a^5x^5 - \frac{13049}{6}a^6x^3 - 2524a^7x\right) \tag{7.8}$$

$$p = -\left(\frac{6381}{4}x^6 + 29862ax^4 + 62292a^2x^2 + \frac{31232}{3}a^3\right). \tag{7.9}$$

The solution is then

$$u_b \sim X^{-\frac{1}{2}}\exp\left\{i\left(\phi + \frac{g}{X^3} + \frac{l}{X^9} + \frac{n}{X^{15}}\right) + \left(\frac{h}{X^6} + \frac{m}{X^{12}} + \frac{p}{X^{18}}\right)\right\}. \tag{7.10}$$

There is, of course, a second solution conjugate to this.

8. The terms in g, h,... decrease in the asymptotic manner provided $x > 2\sqrt{a}$, and though there is no evident remainder theorem, as there is for (4.6), it may be presumed they give a good approximation. If now x is taken much greater than a, the series should become proportional to (4.6), though the constant of proportionality might be a function of a.

Neglecting $\frac{\sqrt{a}}{x}$ in (7.2) ϕ becomes

$$\tfrac{1}{4}x^2 - a\ln x + \frac{a}{2}\ln a - \frac{a}{2}, \tag{8.1}$$

and of the contributions from (7.4–9) only the first terms of g, l, n survive, so

$$u_b \to x^{-\frac{1}{2}-ia}\exp i\left\{\frac{x^2}{4} + \frac{a}{2}\ln a - \frac{a}{2} + \frac{1}{48a} + \frac{7}{5760a^3} + \frac{31}{80640a^5}\right\}$$
$$= 2^{ia/2}x^{-\frac{1}{2}-ia}e^{i\{\frac{1}{4}x^2 + \frac{1}{2}(\gamma_1+\gamma_2)\}} \tag{8.2}$$

by the use of (3.7).

In the same approximation

$$u_a \to (x/\sqrt{2})^{-\frac{1}{2}-ia}e^{\frac{1}{4}ix^2}, \tag{8.3}$$

so that as far as concerns the leading terms

$$u_b = 2^{-\frac{1}{4}} u_a e^{\frac{1}{2}i(\gamma_1+\gamma_3)}. \tag{8.4}$$

It is a remarkable fact that the asymptotic series in a on the two sides of (8.4) should coincide so exactly, but the algebraic intricacies of the Bernoulli numbers, and the complication of the solutions of the equations (7.4–9) are so great that a general proof of their identity for further terms would be difficult. If the series for u_b is expanded beyond the leading term in inverse powers of x, it may be verified directly that there is the same correspondence with u_a for the later terms, but this is unnecessary since both expansions satisfy the differential equation.

For large positive a, β becomes nearly zero, and $\cos\beta$, $\cos\frac{1}{2}\beta$ become unity to an approximation depending on $e^{-\pi a}$ which is negligible. Then substituting for (8.4) in (6.2) and (6.3) we have

$$u_{\mathrm{I}} \sim 2X^{-\frac{1}{4}}\exp\left(\frac{\pi a}{2}+\frac{h}{X^6}+\frac{m}{X^{12}}+\frac{p}{X^{18}}\right)\cos\left(-\frac{\pi}{4}+\phi+\frac{g}{X^3}+\frac{l}{X^9}+\frac{n}{X^{15}}\right) \tag{8.5}$$

$$u_{\mathrm{II}} \sim X^{-\frac{1}{4}}\exp\left(-\frac{\pi a}{2}+\frac{h}{X^6}+\frac{m}{X^{12}}+\frac{p}{X^{18}}\right)\cos\left(\frac{\pi}{4}+\phi+\frac{g}{X^3}+\frac{l}{X^9}+\frac{n}{X^{15}}\right). \tag{8.6}$$

9. It is easy to use the work of § 7 to give series for small x. It is only necessary to write

$$Y = \sqrt{(4a-x^2)} = iX \tag{9.1}$$

and to replace $i\phi$ by

$$\psi = \tfrac{1}{2}\int_0^x Y\,dx = \tfrac{1}{4}xY + a\sin^{-1}\frac{x}{2\sqrt{a}}. \tag{9.2}$$

Then

$$u_c = Y^{-\frac{1}{4}}\exp\left(\psi+\frac{g}{Y^3}-\frac{h}{Y^6}-\frac{l}{Y^9}+\frac{m}{Y^{12}}+\frac{n}{Y^{15}}-\frac{p}{Y^{18}}\right), \tag{9.3}$$

and there is a second solution, say u_c', in which the sign of x is changed; this changes the signs of ψ, g, l, n and leaves the rest unaltered.

Some combination of these two solutions must be fitted so as to match with (6.4) near the origin. It will suffice to compare the first two terms, the constant term and that in x, since the satisfying of the differential equation will then ensure the equality of the rest. This time it will be the last terms in (7.4–9) that will survive, instead of the first.

Then

$$u_c \to 2^{-\frac{1}{4}}a^{-\frac{1}{4}}\exp\left(\tfrac{1}{4}x(2\sqrt{a})+\frac{ax}{2\sqrt{a}}-\frac{x}{2(4a)^{3/2}}+\frac{2a}{(4a)^3}-\right.$$
$$\left.-\frac{19ax}{(4a)^{9/2}}+\frac{80a^2}{(4a)^6}-\frac{2524a^2x}{(4a)^{15/2}}+\frac{31232a^3}{3(4a)^9}\right), \tag{9.4}$$

which can be reduced to

$$2^{-\frac{1}{2}}a^{-\frac{1}{4}}\exp\left(\frac{1}{32a^2}+\frac{5}{256a^4}+\frac{61}{1536a^6}\right)+2^{-\frac{1}{2}}a^{\frac{1}{4}}x\exp\left(-\frac{1}{32a^2}-\frac{5}{256a^4}-\frac{61}{1536a^6}\right)$$
$$=2^{-\frac{3}{4}}\pi^{-\frac{1}{2}}e^{\pi a/4}\{G_1+x\sqrt{2}G_3\} \qquad (9.5)$$

by the use of (3.5), (3.6). Hence comparing with (6.4) and taking $\cos\beta = 1$ we have

$$u_c = u_{\mathrm{I}}, \qquad (9.6)$$

and there is no need to take any term in u_c'. Once again it is remarkable how exactly the two series match one another.

10. In the case of negative a, as has been pointed out, the solutions of § 6 stand unchanged, but when $-a$ becomes large the approximate expressions are altered. The important change is that β approaches 90° instead of zero, so that $\cos\beta = e^{\pi a}$, $\cos\frac{1}{2}\beta = 1/\sqrt{2}$ to the correct approximation. The changes in the asymptotic expansions of G_1, etc., have been indicated in § 3. X is now greater than x, and ϕ must be replaced by

$$\chi = \tfrac{1}{2}\int_0^x X\,dx = \tfrac{1}{4}xX - a\ln\frac{x+X}{2\sqrt{(-a)}}. \qquad (10.1)$$

All the expressions (7.4–9) stand unchanged, and u_b is the same as (7.10) with χ replacing ϕ. Allowing for the changed values of γ_1 and γ_3 the equation

$$u_b = 2^{-\frac{1}{2}}u_a e^{\frac{1}{2}i(\gamma_1+\gamma_3)} \qquad (10.2)$$

still holds. Introducing the changed values of $\cos\beta$ and $\cos\frac{1}{2}\beta$ the results are:

$$u_{\mathrm{I}} \sim \frac{\sqrt{2}}{X^{\frac{1}{2}}}\exp\left(\frac{h}{X^6}+\frac{m}{X^{12}}+\frac{p}{X^{18}}\right)\cos\left(-\frac{\pi}{4}+\chi+\frac{g}{X^3}+\frac{l}{X^9}+\frac{n}{X^{15}}\right) \qquad (10.3)$$

$$u_{\mathrm{II}} \sim \frac{\sqrt{2}}{X^{\frac{1}{2}}}\exp\left(\frac{h}{X^6}+\frac{m}{X^{12}}+\frac{p}{X^{18}}\right)\cos\left(\frac{\pi}{4}+\chi+\frac{g}{X^3}+\frac{l}{X^9}+\frac{n}{X^{15}}\right). \qquad (10.4)$$

When x is small, but a still large negative, a calculation may be made with these expressions similar to that of § 9, and it is found that the series correspond again exactly to (6.4) and (6.5). Moreover the expression (10.3) is also applicable for negative x, since on changing the sign of x it passes over into (10.4), so that it appears to be valid for all values of x.

It would seem that the series (10.3) may merit study by an expert analyst, for an asymptotic solution that is valid for both large and small, positive and negative values of the argument, and so also presumably for intermediate, is certainly remarkable. Indeed it does not fall into the category of asymptotic series as ordinarily defined and may well be convergent. The discussion would, however, be difficult because there

seems little likelihood of finding a general form for the terms g, h,... of the series. That it is asymptotic with regard to a must be remembered, since terms in $e^{\pi a}$ have been neglected.†

Conclusion

The two standard solutions u_{I} and u_{II} adopted for equation (1.1) have the properties of being mirror images in $x = 0$. For positive a, u_{I} resembles an exponential function near the origin; at $\pm 2\sqrt{a}$ it turns and becomes oscillatory, decreasing towards $\pm\infty$. The amplitude is large at the positive end and small at the negative, and the phases of the oscillations are 90° apart. For negative a the curve is oscillatory throughout, and has amplitudes of equal order at the two ends. The solutions are normalized according to (6.1).

The general solutions are given in (6.2–5), in which the symbols are defined in §§ 2, 3, and in (4.6).

These solutions are of little value for large a whether positive or negative. For positive a asymptotic series for large x are given in (8.5), (8.6), where the symbols are defined in § 7. A series for small x is given in (9.3) using symbols defined in §§ 9 and 7.

For large negative a the solutions are given in (10.3), (10.4) using symbols defined in §§ 10 and 7. These solutions are valid for both large and small values of x.

† The numerical convergence has been tested for $a = -10$, and (10.3) is valid to seven places of decimals for any x. For $a = +10$, with critical point at about 6, there is a gap in which neither (8.5) nor (9.3) can be used; this is from about 4 to 8 for three-place accuracy, and from 3 to 9 for four-place accuracy.

FURTHER NOTES ON THE SOLUTION OF ALGEBRAIC LINEAR SIMULTANEOUS EQUATIONS

By A. N. BLACK (*Engineering Department, The University, Oxford*)

[Received 28 September 1948]

SUMMARY

In a recent paper several methods of solving simultaneous equations and inverting matrices have been described. This note describes an alternative method believed to be more convenient than any given there.

1. Introduction

Fox *et al.* (**1**) have described several methods for solving simultaneous equations, but have omitted the abbreviated Doolittle method (**2, 3**), which is shorter and more convenient than any which they give. It is slightly less accurate than the Choleski method, but, as will be shown later, this is a trifling matter. The layout given here is believed to be original.

2. Method of solution

The method used is elimination, deducing a triangular matrix from the given square matrix, and solving by back-substitution. But instead of using the largest term as pivot, as in pivotal elimination, the terms on the main diagonal are used as pivots in order. This sacrifices the accuracy gained by using the largest term as pivot, but gains accuracy by greatly reducing the number of rounding-offs.

Since the convenience of the method lies largely in the details of layout, the method must be described minutely. Three matrices are written down. **A** is the given matrix, of which the terms below the diagonal need not be written. For solution of equations the column **b** of absolute terms must be written after **A**. For matrix inversion no such column is needed. There will also be the usual sum column for checking. **C** is the deduced triangular matrix, with **b** and sum columns added, as for **A**. **D** is a triangular matrix derived from **C** by the rule

$$d_{rs} = -c_{rs}/c_{rr}, \quad \text{for } s > r,$$

d_{rr} is not required. **D** has no columns for **b** or sum, and it must be written on a separate sheet, which can be folded along the lines dividing the columns.

Row 1 of **C** is the same as row 1 of **A**. The formation of the remaining rows proceeds cyclically as follows. Assume that $r-1$ rows of **C** and **D**

[Quart. Journ. Mech. and Applied Maths., Vol. II, Pt. 3 (1949)]
5092.7

have been formed. Fold sheet **D** so that the rth column appears on the right-hand margin. Set it beside the rth and subsequent columns of **C** forming successively

$$c_{rs} = a_{rs} + \sum_{t=1}^{r-1} c_{ts} d_{tr}, \quad \text{for } s > r.$$

Check the row sum. Form row r of **D** and repeat the cycle.

When **C** is complete the equations can be solved by back-substitution.

It is convenient to write **x** as formed on a horizontal strip of paper, which should have -1 written in the **b** column. Check that the scalar product of **x** with the column sums equals the sum of the **b** column in the **A** matrix. In the case of matrix inversion the required **b** in the **C** matrix are known, for $b_{rr} = 1$, and $b_{rs} = 0$, for $s > r$. The terms b_{rs} for $s < r$ may be non-zero, but are not required in the back-substitution. Check that the scalar product of each row of the inverse matrix with the row sums of **A** is equal to 1.

3. Convenience

The advantage of this layout is that all quantities whose product is required appear adjacent. The position where the answer is to be written can be marked by an arrow on the moving sheet. Instead of folding sheet **D**, each column in turn can be cut off as it is wanted. The single column is more easily slid into exact register, and the disadvantages of cutting up the sheet are small, as each stage is completely checked.

The method can be readily extended to asymmetric equations, and in either case products are always written on the computing sheet opposite an arrow on the moving sheet, and dividends on the moving sheet opposite the divisor on the computing sheet. The sign is always that indicated by the calculating machine. There is therefore little chance of error.

An attempt has been made to compare the number of machine operations in this method with that of Choleski, for the case of six equations. Such comparisons cannot be definite, for they depend in part on the machine used and the user's technique; for instance on whether successive divisions by the same divisor are done by direct division or multiplication by the reciprocal, and in the latter case whether the reciprocal is formed by break-down or build-up division.

The table below shows the comparison between the two methods, both for solution of equations and for inversion. Setting means setting a number on keys or levers, for summing, multiplication, or division. Summing is the operation of turning a number, already set, once into the product register. Square rooting means the complete operation of obtaining a

square root; this has not been broken down into its elements as the process depends on the number of figures needed.

Operation	*One set of equations*		*Matrix inversion*	
	Choleski	*Doolittle*	*Choleski*	*Doolittle*
Set	216	218	329	279
Sum	100	111	108	87
Multiply . . .	98	86	189	156
Divide . . .	28	21	37	36
Square root . .	6	0	6	0

It will be seen that the balance of advantage lies slightly but definitely with the Doolittle method for solution of one set of equations. This advantage is greater if the complete inversion is required.

4. Accuracy

The solution by this method of the set of equations treated by Fox *et al.* (1) is given below. The errors in the fifth decimal of x (cf. p. 162) are 28, 15, 51, 27, 29, 15, so that the accuracy is superior to their elimination process, equal to that of Morris, and inferior to the other methods, Choleski in particular. However, these errors correspond to an error in the calculated coefficients of 2 to 3 units of the last decimal carried in the working. They are therefore fully covered by the retention of one place of decimals as guarding figure, which would be required in any case. Any labour expended in attempting greater accuracy is wasted for the reasons stated in the paper under discussion.

A

x_1	x_2	x_3	x_4	x_5	x_6	b	Σ
+ 53999900	+ 52328600	+ 43578500	+ 36224200	+ 27647200	+ 18469100	+ 12367900	+ 244615400
	+ 78719000	+ 36224200	+ 52565100	+ 18469100	+ 28026900	+ 4844800	+ 271177700
		+ 38814100	+ 29730400	+ 26397400	+ 16793600	+ 12495000	+ 204033200
			+ 43767700	+ 16793600	+ 26324600	+ 4730400	+ 210136000
				+ 20157800	+ 11492100	+ 10647000	+ 131604200
					+ 19406500	+ 3783100	+ 124295900
+232247500	+266332900	+ 191538200	+205405600	+120957200	+120512800	+ 48868200	

C

+ 53999900	+ 52328600	+ 43578500	+ 36224200	+ 27647200	+ 18469100	+ 12367900	+244615400
	+ 28009973	− 6005543	+ 17462041	− 8322418	+ 10129420	− 7140313	+ 34133161
		+ 2358150	+ 4241070	+ 2301425	+ 4060659	+ 983036	+ 13944342
			+ 954114	− 703359	+ 317270	− 882766	− 314745
				+ 765461	+ 1316771	+ 583101	+ 2665330
					+ 63536	− 267067	− 203528

D

	− 96904994	− 80701075	− 67081976	− 51198613	− 34202100
		+ 21440731	− 62342227	+ 29712339	− 36163619
			−179847338	− 97594513	−172196807
				+ 73718549	− 33252840
					−172023264

x

+538597826	−281320379	−1159180697	+636454527	+799258435	−420339650	−100000000

Although it does not arise with this set of equations, it should be emphasized that accuracy cannot be obtained unless all the terms on the principal diagonal and the largest term in each **b** column are brought to the same order of size by suitable changes in the roots of the equations.

REFERENCES

1. L. Fox, H. D. Huskey, and J. H. Wilkinson, 'Notes on the solution of algebraic linear simultaneous equations': *Quart. J. Mech. and Applied Math.* **1** (1948), 149.
2. P. S. Dwyer, 'The Doolittle technique': *Ann. Math. Stat.* **12** (1941), 449.
3. Prescott D. Crout, 'A short method for evaluating determinants and solving systems of linear equations with real or complex coefficients': *Trans. Amer. Inst. Elect. Eng.* **60** (1941), 1235.

THE WAVE RESISTANCE OF A CYLINDER STARTED FROM REST

By T. H. HAVELOCK (*King's College, Newcastle-on-Tyne*)

[Received 13 August 1948]

SUMMARY

A method of obtaining expressions for wave resistance in accelerated motion is given, but the particular problem examined is the motion due to a circular cylinder submerged at a given depth below the free surface, the cylinder being suddenly started from rest and made to move with uniform velocity. The surface elevation at any time is discussed, and expressions obtained for the finite wave resistance at any time after the start. Numerical calculations have been made for three different speeds, and curves are given showing how the resistance rises initially and oscillates about the steady value for each speed.

1. Introduction

CALCULATIONS of wave resistance have hitherto been made only for a body moving with constant velocity, the problem being treated directly as one of a steady state when referred to axes moving with the body. The case of non-uniform motion is of interest in itself, and also has possible applications. For instance, in measuring the resistance of ship models, the question arises how long it is before the effect of the starting conditions becomes inappreciable. As a matter of fact, measured resistance curves always show oscillations about the steady value for a given speed, but these are no doubt mainly due to the natural period of the measuring apparatus; however, it would be of interest to have some examination of the approach to the steady resistance after the initial stage of accelerated motion.

Expressions for wave resistance in accelerated motion have been given by Sretensky (**1**), who obtained them by transforming the hydrodynamical equations to a form suitable for axes moving with acceleration, but the formulae are too complicated for numerical calculations in general; Sretensky has, it is understood, made some calculations more recently for a particular law of acceleration, but the results are not available.

In some early work (**2**), instead of assuming the steady state as established, I used an alternative method for uniform motion. This may be described as finding the disturbance due to an infinitesimal step in the motion of the body and then integrating. It was pointed out at the time that the method could be applied to motion with variable velocity. It is shown now that this method leads directly to expressions equivalent to those obtained otherwise by Sretensky. However, the present note deals mainly with one particular problem, namely, a circular cylinder submerged

in water at a given depth, suddenly started from rest with a given velocity and maintained at that speed. It has been found possible to make numerical calculations in this case, and the results illustrate various points of interest.

2. Circular cylinder

Take the origin O at the centre of the circular section, of radius a, at a depth f below the free surface, with Ox horizontal and Oy vertically upwards. If the cylinder is given a small horizontal displacement $c\,\delta\tau$, from rest to rest, the velocity potential of the subsequent fluid motion is given by

$$\phi = 2ca^2g^{\frac{1}{2}}\,\delta\tau \int_0^\infty e^{-\kappa(2f-y)}\sin(\kappa x)\sin(g^{\frac{1}{2}}t\kappa^{\frac{1}{2}})\kappa^{\frac{1}{2}}\,d\kappa. \tag{1}$$

This is equation (12) of the paper already quoted (**2**), obtained there by a Fourier integral method; it can also be derived in the manner given later by Lamb (**3**) for the three-dimensional case.

The velocity potential for continuous motion with variable velocity can be found by a direct integration. We consider first the simple case when the cylinder is suddenly started at time $t = 0$ and made to move with uniform velocity c. We obtain, noting that the origin is at the centre of the moving cylinder,

$$\phi = \frac{ca^2x}{x^2+y^2} - \frac{ca^2x}{x^2+(2f-y)^2} + \\ + 2ca^2g^{\frac{1}{2}} \int_0^t d\tau \int_0^\infty e^{-\kappa(2f-y)}\sin\{\kappa(x+ct-c\tau)\}\sin\{g^{\frac{1}{2}}\kappa^{\frac{1}{2}}(t-\tau)\}\kappa^{\frac{1}{2}}\,d\kappa. \tag{2}$$

Deriving the surface elevation η from the relation

$$\frac{\partial\eta}{\partial t} = -\frac{\partial\phi}{\partial y} \quad (y = f), \tag{3}$$

we obtain

$$\eta = 2ca^2 \int_0^t d\tau \int_0^\infty e^{-\kappa f}\sin\{\kappa(x+ct-c\tau)\}\cos\{g^{\frac{1}{2}}\kappa^{\frac{1}{2}}(t-\tau)\}\kappa\,d\kappa. \tag{4}$$

Hence we have

$$\eta = \frac{2a^2f}{x^2+f^2} + 2\kappa_0 a^2 \int_0^\infty \frac{\cos\kappa x}{\kappa-\kappa_0}e^{-\kappa f}\,d\kappa - \\ - ca^2 \int_0^\infty \left\{\frac{\cos(\kappa x+\kappa ct+g^{\frac{1}{2}}t\kappa^{\frac{1}{2}})}{\kappa c+g^{\frac{1}{2}}\kappa^{\frac{1}{2}}} + \frac{\cos(\kappa x+\kappa ct-g^{\frac{1}{2}}t\kappa^{\frac{1}{2}})}{\kappa c-g^{\frac{1}{2}}\kappa^{\frac{1}{2}}}\right\}\kappa e^{-\kappa f}\,d\kappa, \tag{5}$$

where $\kappa_0 = g/c^2$, and the principal values of the integrals are to be taken.

The first two terms in (5) give

$$\eta_1 = \frac{2a^2 f}{x^2+f^2} - 2\pi\kappa_0 a^2 e^{-\kappa_0 f}\sin\kappa_0 x - \\ - 2\kappa_0 a^2 \int_0^\infty \frac{\kappa_0 \sin\kappa f - \kappa\cos\kappa f}{\kappa^2+\kappa_0^2} e^{-\kappa x}\, d\kappa \quad (x>0),$$

$$\eta_1 = \frac{2a^2 f}{x^2+f^2} + 2\pi\kappa_0 a^2 e^{-\kappa_0 f}\sin\kappa_0 x - \\ - 2\kappa_0 a^2 \int_0^\infty \frac{\kappa_0 \sin\kappa f - \kappa\cos\kappa f}{\kappa^2+\kappa_0^2} e^{\kappa x}\, d\kappa \quad (x<0). \quad (6)$$

The expressions for η_1 represent a steady state relative to the moving cylinder and symmetrical fore and aft of it. With $x+ct = \xi =$ distance from a fixed origin at the starting-point, the last two terms in (5) represent the surface elevation at any time due to an initial displacement and velocity which is the negative of that given by (6); this must be the case in the present problem and it can be directly verified. With a change of variable, and with $u_0^2 = \kappa_0$, the last two terms in (5) are given by the real part of

$$\eta_2 = -2a^2 \int_{-\infty}^{\infty} \frac{e^{i(\xi u^2 - g^{\frac{1}{2}}tu)}}{u-u_0} u^2 e^{-fu^2}\, du - 4a^2 \int_0^\infty \frac{e^{i(\xi u^2 + g^{\frac{1}{2}}tu)}}{u+u_0} u^2 e^{-fu^2}\, du. \quad (7)$$

The limiting value of η_2 as t becomes infinite is derived from the principal value of the first integral in (7); taking the real part, we find that

$$\eta_2 \to 2\pi\kappa_0 a^2 e^{-\kappa_0 f}\sin\kappa_0 x \quad \text{as} \quad t\to+\infty. \quad (8)$$

Turning to (6), we see that ultimately (8) cancels out the regular waves in advance of the cylinder and doubles the amplitude of those in the rear. Without examining the surface elevation in detail, we may specify more closely the part which at any time consists of a regular train of waves accompanying the moving cylinder. It is clear from the form of the integrals in (7) that the only contribution to such a train comes from the first integral, or from

$$-2a^2 u_0^2 \int_{-\infty}^{\infty} \frac{e^{i(\xi u^2 - g^{\frac{1}{2}}tu)}}{u-u_0} e^{-fu^2}\, du, \quad (9)$$

and is due to the pole at $u = u_0$. Regarding u as a complex variable, the path is along the real axis indented at $u = u_0$. There is a saddle-point at $u = g^{\frac{1}{2}}t/2\xi$. First suppose $\xi > 0$. The path of integration may be rotated round the saddle-point to the line of steepest descent, namely, the line $u = g^{\frac{1}{2}}t/2\xi + re^{\frac{1}{4}i\pi}$, the contribution of the circular arcs required to complete the closed contour being zero in the limit. We have also to take account

of the indentation at u_0 according as $u_0 >$ or $< g^{\frac{1}{2}}t/2\xi$, that is, according as $\xi >$ or $< \frac{1}{2}ct$. In this manner, it is found that as far as the regular waves are concerned, (9) gives

$$2\pi\kappa_0 a^2 e^{-\kappa_0 f}\sin\kappa_0 x \quad (\xi > \tfrac{1}{2}ct),$$

$$-2\pi\kappa_0 a^2 e^{-\kappa_0 f}\sin\kappa_0 x \quad (\xi < \tfrac{1}{2}ct). \tag{10}$$

Similarly if $\xi < 0$ the line of steepest descent is the line $u = g^{\frac{1}{2}}t/2\xi + re^{\frac{1}{4}i\pi}$ and the corresponding contribution is $-2\pi\kappa_0 a^2 e^{-\kappa_0 f}\sin\kappa_0 x$.

Summing up this outline of an analysis, the surface elevation at any time is made up of three parts: (i) the local symmetrical disturbance travelling with the cylinder given by the first and third terms in (6); (ii) a regular train of waves $4\pi\kappa_0 a^2 e^{-\kappa_0 f}\sin\kappa_0 x$ behind the cylinder extending from $x = 0$ to $x = -\frac{1}{2}ct$; (iii) the part given by the remaining integrals, representing a disturbance which spreads out in both directions and diminishes in magnitude as time goes on.

The second part agrees with the general description using the idea of group velocity. The third part has not been examined in detail, but an asymptotic expansion suitable for large values of ξ and t may be found from the transformed integrals indicated in the previous discussion. For large positive values of ξ and $(g^{\frac{1}{2}}t/2\xi^{\frac{1}{2}}) - u_0\xi^{\frac{1}{2}}$, the first term in such an expansion is

$$\frac{\pi^{\frac{1}{2}}g^{\frac{1}{2}}at^2}{2\xi^{\frac{3}{2}}(\xi-\frac{1}{2}ct)}\, e^{-gt^2 f/\xi^2}\cos(\tfrac{1}{4}\pi - gt^2/4\xi). \tag{11}$$

For $\xi = ct$, that is, at a point over the centre of the moving cylinder, this reduces to

$$a^2\left(\frac{\pi\kappa_0}{ct}\right)^{\frac{1}{2}} e^{-\frac{1}{2}\kappa_0 f}\cos\tfrac{1}{4}(\pi - \kappa_0 ct), \tag{12}$$

a result which can be obtained directly from the integrals in (7) by using the method of stationary phase. After a sufficient time, (12) gives approximately the departure of the motion over the cylinder from the quasi-steady state consisting of the local symmetrical disturbance and the regular train of waves to the rear. If $\lambda_0\ (= 2\pi/\kappa_0)$ is the wave-length in the regular train, the wave-length of the disturbance near the cylinder is $4\lambda_0$, the wave-length for which c is the group velocity. The usual direct solution for motion with uniform velocity leads to the surface elevation (6) with regular waves in advance as well as to the rear. The so-called practical solution is then obtained by superposing a free infinite wave train cancelling out those in advance and doubling the amplitude to the rear. Another well-known method of obtaining this practical solution directly is to use the frictional coefficient introduced by Rayleigh. In the present analysis we have not used this frictional coefficient, the values of the integrals being interpreted

as principal values wherever necessary. The chief point of the discussion is that there is no ambiguity when the motion starts from rest. The motion which is gradually established as time goes on is the practical solution for the steady state, with regular waves only to the rear of the cylinder; this result is in fact associated with the group velocity being less than the wave velocity.

3. The wave resistance

The wave resistance may now be obtained to the same approximation as for steady motion. From (2), with $z = x+iy$ and $V = (g/\kappa)^{\frac{1}{2}}$, the complex potential function is

$$w = \frac{ca^2}{z} - \frac{ca^2}{z-2if} + ca^2 g^{\frac{1}{2}} \int_0^t d\tau \int_0^\infty \{e^{-i\kappa(c-V)(t-\tau)} - e^{-i\kappa(c+V)(t-\tau)}\} e^{-i\kappa z - 2\kappa f} \kappa^{\frac{1}{2}}\, d\kappa. \tag{13}$$

In this case the resistance is given by the usual form of Blasius's theorem, namely, the real part of

$$-\tfrac{1}{2}\rho i \int \left(\frac{dw}{dz}\right)^2 dz, \tag{14}$$

taken round a small contour enclosing the origin. Expanding (13) in the neighbourhood of the origin, this gives

$$R = 2\pi\rho c^2 g^{\frac{1}{2}} a^4 \int_0^t d\tau \int_0^\infty \{e^{-i\kappa(c-V)(t-\tau)} - e^{-i\kappa(c+V)(t-\tau)}\} \kappa^{\frac{1}{2}} e^{-2\kappa f}\, d\kappa$$

$$= -4\pi g\rho\kappa_0^2 a^4 i \int_0^\infty \left\{\frac{e^{iv(v-1)\kappa_0 ct}}{v-1} - \frac{e^{iv(v+1)\kappa_0 ct}}{v+1}\right\} v^5 e^{+2\kappa_0 f v^2}\, dv, \tag{15}$$

where the real part is to be taken. The value to which R tends as t becomes infinite arises from the first part of the integral; and we find that

$$R \to 4\pi^2 g\rho\kappa_0^2 a^4 e^{-2\kappa_0 f} \quad \text{as} \quad t \to +\infty, \tag{16}$$

which is the resistance for uniform velocity.

With $\alpha = \kappa_0 ct$, $\beta = 2\kappa_0 f$, the form

$$R = 4\pi g\rho\kappa_0^2 a^4 \int_0^\infty \left\{\frac{\sin \alpha v(v-1)}{v-1} - \frac{\sin \alpha v(v+1)}{v+1}\right\} v^5 e^{-\beta v^2}\, dv, \tag{17}$$

is suitable for numerical computation by direct quadrature if α is not too large and β not too small.

For other values of the parameters it is possible to find more suitable

forms by transforming the integrals in (15). We divide the integrals into two parts. Put

$$I_1 = \int_0^\infty \left\{\frac{v^5-1}{v-1}e^{-i\alpha v} - \frac{v^5+1}{v+1}e^{i\alpha v}\right\} e^{i\alpha v^2-\beta v^2}\,dv, \tag{18}$$

and

$$kL = \int_0^\infty e^{i\alpha v^2-\beta v^2}\sin\alpha v\,dv = k\int_0^1 e^{-\frac{1}{4}\alpha^2\mu(1-u^2)}\,du, \tag{19}$$

with $\mu = (\beta+i\alpha)/(\beta^2+\alpha^2)$, and $k = \frac{1}{2}\alpha\mu$.

The second form for L in (19) can be evaluated by quadrature, or from convergent or asymptotic series which can readily be found. It can be shown that

$$I_1 = (i+k)(1-k^2)\frac{k}{\alpha} + (2i+5k)\frac{k^2}{\alpha^2} + \\ + \left\{1-ki-k^2+k^3i+k^4+(1-3ki-6k^2)\frac{k}{\alpha}+3\frac{k^2}{\alpha^2}\right\}kL. \tag{20}$$

The remaining integral from (15) is

$$I_2 = \int_0^\infty \left\{\frac{e^{i\alpha v(v-1)}}{v-1} + \frac{e^{i\alpha v(v+1)}}{v+1}\right\} e^{-\beta v^2}\,dv. \tag{21}$$

Considering v as a complex variable, the path for the first term in (21) is along the real axis indented at the point $v = 1$. We take it now along the real axis from $v = 0$ to $v = \frac{1}{2}$ and then along the line $v = \frac{1}{2}+re^{\frac{1}{4}i\pi}$, with r positive; in the limit, the contribution of the circular arc required to complete the contour is zero. The second term is taken along the real axis from $v = 0$ to $v = -\frac{1}{2}$, and then along the line $v = -\frac{1}{2}+re^{\frac{1}{4}i\pi}$, with r positive. In this way we obtain

$$I_2 = \pi i e^{-\beta} + 2\int_0^{\frac{1}{2}} e^{i\alpha v(v-1)-\beta v^2}\,dv/(v-1) + \\ + e^{\frac{1}{4}i(\pi-\alpha)i}\int_0^\infty \left\{\frac{e^{-\beta(re^{\frac{1}{4}i\pi}+\frac{1}{2})^2}}{re^{\frac{1}{4}i\pi}-\frac{1}{2}} + \frac{e^{-\beta(re^{\frac{1}{4}i\pi}-\frac{1}{2})^2}}{re^{\frac{1}{4}i\pi}+\frac{1}{2}}\right\} e^{-\alpha r^2}\,dr. \tag{22}$$

The integrals in (22) are not too difficult for computation for fairly large values of α and moderate values of β. The resistance R is given by the real part of $-4\pi g\rho\kappa_0^2 a^4 i(I_1+I_2)$.

When α is sufficiently large, the divergence of the resistance from the steady value becomes of the order $\alpha^{-\frac{1}{2}}$; this first term in an asymptotic expansion comes from the first term in (18) and the second term in (22). Applying the method of stationary phase to these integrals leads to the result

$$R \to 4\pi g\rho\kappa_0^2 a^4\{\pi e^{-2\kappa_0 f} - \tfrac{1}{16}(\pi/\kappa_0 ct)^{\frac{1}{2}}e^{-\frac{1}{2}\kappa_0 f}\sin\tfrac{1}{4}(\pi-\kappa_0 ct)\}. \tag{23}$$

The second term in (23) corresponds to the approximate perturbation in the surface elevation given in (12); this can be checked by direct calculation of the extra resistance due to (12).

4. Calculations of the wave resistance

The steady resistance (16) is a maximum at the speed for which $\beta = 2\kappa_0 f = 2$. Calculations have been made for the resistance in the

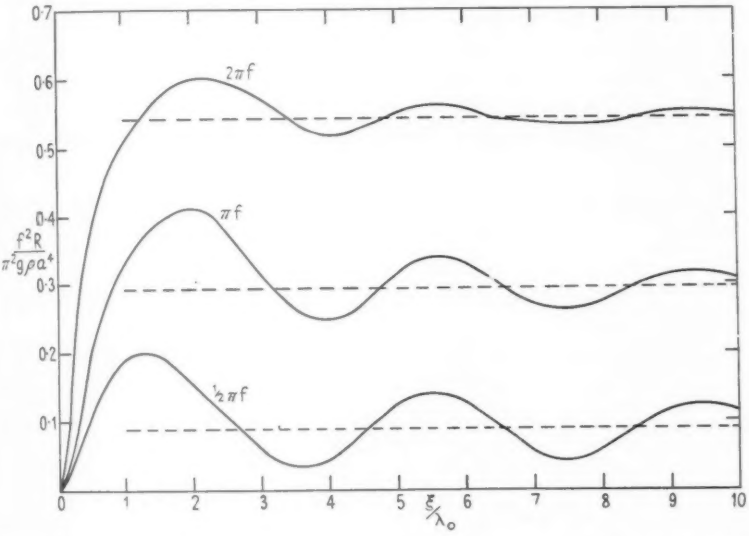

present problem for three different speeds, given by $\beta = 2, 4, 6$. The expression (17) was found suitable for values of α up to about 15, taking an interval of 0·05 for v and not attempting any high degree of accuracy. The forms (20) and (22) were used for higher values; these and (17) being calculated for some values in common for checking purposes. Finally, (23) was found sufficient for very large values of α. About fifteen spots were calculated at each speed, and the results are shown in curves of resistance.

The abscissae are values of ξ/λ_0, where ξ is the distance travelled from the start and λ_0 is the wave-length for the corresponding speed. The ordinates are proportional to the wave-resistance R, the broken straight lines showing the steady resistance at each speed; the wave-lengths for the three speeds are $2\pi f$, πf, and $\frac{1}{2}\pi f$.

The following seem to be the chief points of interest. Considering that the steady resistance is associated with the idea of group velocity and the establishment of a train of waves to the rear, the resistance rises to the neighbourhood of the steady value more rapidly than might have been

expected, especially at the higher speeds. Another point is that the maximum resistance attained is larger relatively at the lower speeds; thus at the highest speed shown the maximum is about 1·11 times the steady value at that speed, while for the lowest speed the maximum is about twice the steady value. After about ten wave-lengths the resistance is given approximately by (23) and the amplitude of the oscillations diminishes slowly with the distance travelled; but even at an earlier stage the period of the oscillations is roughly $4\lambda_0$.

5. Three-dimensional motion

Turning to the general problem, we take the origin O in the free surface, with Oz vertically upwards. Suppose a point source of strength m is suddenly created at the point $(0, 0, -f)$ and maintained for a short time $\delta\tau$. To satisfy the condition at the free surface for the initial motion, we take

$$\phi_0 = \frac{m}{r_1} - \frac{m}{r_2}, \tag{24}$$

with $r_1^2 = x^2+y^2+(z+f)^2$; $r_2^2 = x^2+y^2+(z-f)^2$.

The initial surface velocity found from (24) acting for a time $\delta\tau$ gives a surface elevation which can be put in the form

$$\zeta_0 = \frac{m}{\pi}\delta\tau \int_{-\pi}^{\pi} d\theta \int_0^{\infty} e^{-\kappa f}\cos(\kappa\varpi)\kappa\, d\kappa, \tag{25}$$

with $\varpi = x\cos\theta + y\sin\theta$.

The velocity potential of the fluid motion at any subsequent time t due to this initial displacement without velocity is

$$\phi = \frac{m}{\pi} g^{\frac{1}{2}}\delta\tau \int_{-\pi}^{\pi} d\theta \int_0^{\infty} e^{-\kappa f+\kappa z}\cos(\kappa\varpi)\sin(g^{\frac{1}{2}}t\kappa^{\frac{1}{2}})\kappa^{\frac{1}{2}}\, d\kappa. \tag{26}$$

Consider now a source moving parallel to Ox at constant depth f, the strength m being a function of the time. Let x be measured from a moving origin vertically over the source, ξ from a fixed origin at the starting-point; and let s_t be the ξ-coordinate of the source at any time t. Then we obtain, from (26),

$$\phi = \frac{m(t)}{r_1} - \frac{m(t)}{r_2} + \frac{g^{\frac{1}{2}}}{\pi}\int_0^t m(\tau)\, d\tau \int_{-\pi}^{\pi} d\theta \int_0^{\infty} e^{-\kappa f+\kappa z}\cos(\kappa\varpi')\sin\{g^{\frac{1}{2}}\kappa^{\frac{1}{2}}(t-r)\}\kappa^{\frac{1}{2}}\, d\kappa, \tag{27}$$

with $\varpi' = (\xi - s_\tau)\cos\theta + y\sin\theta$.

We may generalize this result for a solid body moving through the liquid. If the solid moves through an infinite liquid with unit velocity, we may

take the fluid motion to be that due to a certain distribution of sources and sinks over its surface and of amount σ per unit area at each point. We assume this distribution in the present problem in order to obtain the wave motion to the first approximation. Thus in (27) we replace m by $\sigma c(t)$, where c is the velocity at time t; if $(h, k, -f)$ is a point on the surface of the body we also put $x-h$ for x, $y-k$ for y, and

$$\varpi' = (\xi-h-s_\tau)\cos\theta+(y-k)\sin\theta,$$

and the required velocity potential is obtained by integrating over the surface of the body.

We shall not carry the general problem further meantime, but consider the case of a slender ship form. Here the usual approximation is to take $\sigma = -(\partial y/\partial h)/2\pi$, where the surface of the form is given as an equation for y in terms of h and f; further, the source distribution is taken to be in the longitudinal section of the form by the plane $y = 0$. We obtain, in this case,

$$\phi = -\frac{c(t)}{2\pi}\iint\left(\frac{1}{r_1}-\frac{1}{r_2}\right)\frac{\partial y}{\partial h}\,dh\,df- \\ -\frac{g^{\frac{1}{2}}}{2\pi^2}\iint\frac{\partial y}{\partial h}\,dh\,df\int_0^t c(\tau)\,d\tau\int_{-\pi}^{\pi}d\theta\int_0^\infty e^{-\kappa f+\kappa z}\cos(\kappa\varpi')\sin\{g^{\frac{1}{2}}\kappa^{\frac{1}{2}}(t-\tau)\}\kappa^{\frac{1}{2}}\,d\kappa, \tag{28}$$

with $\varpi' = (\xi-h-s_\tau)\cos\theta+y\sin\theta$. This result is equivalent to that obtained by Sretensky by a different method.

The pressure at any point is given by $\rho\,\partial\phi/\partial t$, neglecting the square of the fluid velocity; and the resistance is found from

$$R = -2\iint p(h', 0, -f')\frac{\partial y}{\partial h'}\,dh'df', \tag{29}$$

taken over the longitudinal vertical section. Hence, from (28) and (29), we find

$$R = \frac{\rho\dot{c}}{2\pi}\iint\frac{\partial y}{\partial h'}\,dh'df'\times \\ \times\iint[\{(h'-h)^2+(f'+f)^2\}^{-\frac{1}{2}}-\{(h'-h)^2+(f'+f)^2\}^{\frac{1}{2}}]\frac{dy}{dh}\,dh\,df+ \\ +\frac{g\rho}{\pi^2}\iint\frac{\partial y}{\partial h'}\,dh'df'\iint\frac{\partial y}{\partial h}\,dh\,df\int_0^t c(\tau)\,d\tau\int_{-\pi}^{\pi}d\theta\times \\ \times\int_0^\infty e^{-\kappa(f+f')}\cos(\kappa\varpi')\cos\{g^{\frac{1}{2}}\kappa^{\frac{1}{2}}(t-\tau)\}\kappa\,d\kappa, \tag{30}$$

with $\varpi' = (h'-h+s_t-s_\tau)\cos\theta$.

The coefficient of $\dot{c}$ is an effective mass for this particular problem, taking account of the free surface and assuming no wave formation and noting that the square of the fluid velocity has been neglected.

As a special case, suppose the model to be started from rest with a velocity c which is then maintained constant. The finite resistance at any time after the start is given by the second term of (30), with c a constant and

$$\varpi' = \{h' - h + c(t-\tau)\}\cos\theta.$$

The result can be reduced to the form

$$R = \frac{g\rho c}{\pi^2} \int_0^t d\tau \int_{-\pi}^{\pi} d\theta \int_0^{\infty} (I^2+J^2)\cos\{\kappa c(t-\tau)\cos\theta\}\cos\{g^{\frac{1}{2}}\kappa^{\frac{1}{2}}(t-\tau)\}\kappa\, d\kappa, \tag{31}$$

with

$$I + iJ = \int\int \frac{\partial y}{\partial h}\, e^{-\kappa f + i\kappa h\cos\theta}\, dh df. \tag{32}$$

Integrating with respect to τ, this gives

$$R = \frac{2g\rho c}{\pi^2} \int_0^{\frac{1}{2}\pi} d\theta \int_0^{\infty} (I^2+J^2)\left[\frac{\sin\{(\kappa c\cos\theta - g^{\frac{1}{2}}\kappa^{\frac{1}{2}})t\}}{\kappa c\cos\theta - g^{\frac{1}{2}}\kappa^{\frac{1}{2}}} + \frac{\sin\{(\kappa c\cos\theta + g^{\frac{1}{2}}\kappa^{\frac{1}{2}})t\}}{\kappa c\cos\theta + g^{\frac{1}{2}}\kappa^{\frac{1}{2}}}\right]\kappa\, d\kappa. \tag{33}$$

It can be verified readily that the limiting value to which this tends as t becomes infinite is

$$R = \frac{4\kappa_0 g\rho}{\pi} \int_0^{\frac{1}{2}\pi} (I_0^2 + J_0^2)\sec^3\theta\, d\theta, \tag{34}$$

where $I_0 + iJ_0$ is given by (32) with κ replaced by $\kappa_0\sec^2\theta$.

This result (34) is the known expression for the steady resistance at constant speed.

REFERENCES

1. L. Sretensky, *Joukovsky Cent. Inst. Rep.* **319** (Moscow, 1937).
2. T. H. Havelock, *Proc. Roy. Soc.* A, **93** (1917), 520.
3. H. Lamb, *Proc. Roy. Soc.* A, **111** (1926), 14.

ON THE ROLLING MOTION OF CYLINDERS IN THE SURFACE OF A FLUID†

By F. URSELL (*Department of Mathematics, The University, Manchester*)

[Received 14 October 1948]

SUMMARY

The methods of a previous paper (ref. **1**) are extended to permit the evaluation of the fluid motion when a cylinder of arbitrary symmetrical section performs simple harmonic oscillations of small amplitude about a mean position with its axis of symmetry level with the surface. Special attention is paid to the slow motions, for which a method of successive approximation is developed. Applications are made to the virtual mass in slow heaving, to the determination of the roll axis, and to motion in a sea-way. Finally, the waves generated by the forced rolling motion are studied. It is shown that their amplitude, and thus also the damping decrement, depends critically on the details of the section. A section is calculated whose rolling is undamped to the first order. Experiments are needed.

1. Introduction

In a former paper (ref. **1**) the motion of a fluid was considered when a long circular cylinder executes vertical heaving oscillations about a mean position in the surface. It will be shown that the method of that paper can be extended to discuss the oscillations of a long cylinder of any section, provided that the cylinder is symmetrical about a vertical plane and the principal axes of the section are of the same order of magnitude. The emphasis will be generally on skew-symmetrical (rolling) motions. In these the length of the waves produced by the rolling is usually much greater than the beam of the ship. Application of a method of successive approximation outlined in ref. **1** is therefore permissible.

2. Formulation of the problem

On the assumption that the motion is two-dimensional and simple harmonic of period $2\pi/\sigma$, a velocity potential ϕ and a stream-function ψ exist satisfying

$$\frac{\partial^2\phi}{\partial x^2}+\frac{\partial^2\phi}{\partial y^2}=0, \tag{1}$$

$$\frac{\partial^2\psi}{\partial x^2}+\frac{\partial^2\psi}{\partial y^2}=0, \tag{2}$$

where the origin of coordinates is at the mean position of the centre of the cylinder and y increases with depth, the mean free surface being $y=0$, as in ref. **1**. The stream function is prescribed on the cylinder, or, to a first

† Read to the VIIth International Congress of Applied Mechanics.

approximation, on its mean position. To the same order, the condition for the free surface is

$$K\phi+\frac{\partial\phi}{\partial y}=0 \quad (y=0) \tag{3}$$

where

$$gK=\sigma^2. \tag{4}$$

Introduce dimensionless coordinates ξ,η defined by the isogonal transformation

$$x=c\cosh\xi\sin\eta+c\sum_{r=1}^{\infty}A_{2r+1}e^{-(2r+1)\xi}\sin(2r+1)\eta, \tag{5}$$

$$y=c\sinh\xi\cos\eta-c\sum_{r=1}^{\infty}A_{2r+1}e^{-(2r+1)\xi}\cos(2r+1)\eta. \tag{6}$$

The constants A_{2r+1} are chosen in such a way that the given cylinder becomes the curve $\xi=\xi_0$, and the region occupied by the fluid is mapped isogonally on $-\frac{1}{2}\pi\leqslant\eta\leqslant\frac{1}{2}\pi$, $\xi_0<\xi<\infty$. Equation (1) becomes

$$\frac{\partial^2\phi}{\partial\xi^2}+\frac{\partial^2\phi}{\partial\eta^2}=0 \tag{7}$$

and the surface condition becomes

$$-Kc\Big[\sinh\xi+\sum_{1}^{\infty}(-1)^{r-1}e^{-(2r+1)\xi}A_{2r+1}\Big]\phi\pm\frac{\partial\phi}{\partial\eta}=0 \quad (\eta=\pm\tfrac{1}{2}\pi,\ \xi>\xi_0). \tag{8}$$

3. Skew-symmetric motions

Consider in the first place, motions in which

$$\phi(\xi,\eta)=-\phi(\xi,-\eta), \tag{9}$$

for instance a rolling motion. It is sufficient to consider the region $0\leqslant\eta\leqslant\frac{1}{2}\pi$. Laplace's equation (7) and the surface condition are both satisfied by the skew-symmetric set

$$\begin{aligned}-\phi_{2n+1}(\xi,\eta)&=e^{-(2n+1)\xi}\sin(2n+1)\eta-\\&-Kc\Big[e^{-2n\xi}\frac{\sin 2n\eta}{4n}+e^{-(2n+2)\xi}\frac{\sin(2n+2)\eta}{4n+4}-\\&-\sum_{r=1}^{\infty}A_{2r+1}e^{-(2n+2r+2)\xi}\frac{\sin(2n+2r+2)\eta}{2n+2r+2}\Big]\\&\qquad(n=1,2,3,\ldots).\end{aligned} \tag{10}$$

It will often be convenient to work with the conjugate stream-functions

$$\begin{aligned}\psi_{2n+1}(\xi,\eta)&=e^{-(2n+1)\xi}\cos(2n+1)\eta-\\&-Kc\Big[e^{-2n\xi}\frac{\cos 2n\eta}{4n}+e^{-(2n+2)\xi}\frac{\cos(2n+2)\eta}{4n+4}-\\&-\sum_{r=1}^{\infty}A_{2r+1}e^{-(2n+2r+2)\xi}\frac{\cos(2n+2r+2)\eta}{2n+2r+2}\Big]\\&\qquad(n=1,2,3,\ldots).\end{aligned} \tag{11}$$

It is not to be expected that the general skew-symmetric motion can be expanded in terms of these sets, since at infinity the motion consists of regular wave trains travelling away from the origin, whereas each $\phi_{2n+1}(\xi, \eta)$ vanishes at infinity.

The set is completed by the addition of the potential Φ and stream-function Ψ describing a horizontal dipole at the origin (cf. ref. **2**). In particular, the stream-function Ψ is given by

$$\begin{aligned}\Psi &= \Psi_c(\xi, \eta)\cos\sigma t + \Psi_s(\xi, \eta)\sin\sigma t \\ &= \mathrm{Im}\left[2Kcie^{iKz-i\sigma t} + \frac{2}{\pi}\sin\sigma t \int_0^\infty \frac{kce^{-kz}\,dk}{k+iK}\right] \\ &= \mathrm{Im}\left[2Kcie^{iKz-i\sigma t} + \frac{2}{\pi}\frac{c}{z}\sin\sigma t + \right. \\ &\quad \left. + \frac{2}{\pi}\sin\sigma t\left\{iKc(\gamma + \log iKz)\sum_{r=0}^{\infty}\frac{(iKz)^r}{r!} - iKc\sum_{r=1}^{\infty}\frac{(iKz)^r}{r!}\left(\frac{1}{1}+\ldots+\frac{1}{r}\right)\right\}\right]. \end{aligned} \tag{12}$$

4. Rolling oscillations of small amplitude about the origin

The process which is employed to determine the coefficients of $\psi_{2n+1}(\xi, \eta)$, $n = 1, 2, 3, \ldots$ in the expansion of ψ is best illustrated by an example. Consider a cylinder whose equation is $\xi = \xi_0$ and suppose that it is rolling about the origin, the angular displacement at time t being

$$\theta = \theta_0 \cos\sigma t, \tag{13}$$

where θ_0 is small.

The boundary condition is (ref. **3**, Art. 72)

$$\psi = \frac{1}{2}\frac{d\theta}{dt}(x^2+y^2) + F(t), \tag{14}$$

on the cylinder, where $F(t)$ is a function of t only; for small θ_0 this condition may be replaced by

$$\psi = \frac{1}{2}\frac{d\theta}{dt}(x^2+y^2) + F(t) \quad \text{on} \quad \xi = \xi_0. \tag{15}$$

(For other skew-symmetrical motions x^2+y^2 is replaced by some other even function of η, to which all the following considerations may be applied.) Suppose that ψ is multiplied by a constant so as to make the coefficient of Ψ unity; A is a function of θ_0 and the period. Then,

$$\begin{aligned} A\psi = {} & \Psi_c(\xi, \eta)\cos\sigma t + \Psi_s(\xi, \eta)\sin\sigma t - \\ & - \sum_{r=1}^{\infty} p_{2r+1}(Kc, \xi_0)\psi_{2r+1}(\xi, \eta)\cos\sigma t - \\ & - \sum_{r=1}^{\infty} q_{2r+1}(Kc, \xi_0)\psi_{2r+1}(\xi, \eta)\sin\sigma t, \end{aligned} \tag{16}$$

and p_{2r+1}, q_{2r+1} must be determined in such a way that on $\xi = \xi_0$ the stream-function ψ differs from a multiple of x^2+y^2 by a function of t only, that is

$$\Psi_c(\xi_0, \eta)\cos\sigma t + \Psi_s(\xi_0, \eta)\sin\sigma t - \\ - \sum_1^\infty p_{2r+1}(Kc, \xi_0)\psi_{2r+1}(\xi_0, \eta)\cos\sigma t - \\ - \sum_1^\infty q_{2r+1}(Kc, \xi_0)\psi_{2r+1}(\xi_0, \eta)\sin\sigma t \\ = C(t)(x^2+y^2)_0 + F(t). \tag{17}$$

There must be no source-singularities on the cylinder, i.e. ψ is continuous in the range $0 \leqslant \eta \leqslant \frac{1}{2}\pi$. It is therefore assumed that the series (16) converges uniformly in η on $\xi = \xi_0$.

Suppose that the beam of the cylinder is $2a$ and that the draught is b. Put $\eta = \frac{1}{2}\pi$ and subtract the new equation from (17), thus eliminating $F(t)$,

$$[\Psi_c(\xi_0, \eta) - \Psi_c(\xi_0, \tfrac{1}{2}\pi)]\cos\sigma t + [\Psi_s(\xi_0, \eta) - \Psi_s(\xi_0, \tfrac{1}{2}\pi)]\sin\sigma t - \\ - \sum_1^\infty p_{2r+1}[\psi_{2r+1}(\xi_0, \eta) - \psi_{2r+1}(\xi_0, \tfrac{1}{2}\pi)]\cos\sigma t - \\ - \sum_1^\infty q_{2r+1}[\psi_{2r+1}(\xi_0, \eta) - \psi_{2r+1}(\xi_0, \tfrac{1}{2}\pi)]\sin\sigma t \\ = C(t)(x^2+y^2-a^2)_0 \\ = (p_1\cos\sigma t + q_1\sin\sigma t)\left(\frac{x^2+y^2-a^2}{b^2-a^2}\right)_0, \quad \text{say;} \tag{18}$$

that is

$$\Psi_c(\xi_0, \eta) - \Psi_c(\xi_0, \tfrac{1}{2}\pi) \\ = p_1\left(\frac{x^2+y^2-a^2}{b^2-a^2}\right)_0 + \sum_1^\infty p_{2r+1}[\psi_{2r+1}(\xi_0, \eta) - \psi_{2r+1}(\xi_0, \tfrac{1}{2}\pi)], \tag{19}$$

$$\Psi_s(\xi_0, \eta) - \Psi_s(\xi_0, \tfrac{1}{2}\pi) \\ = q_1\left(\frac{x^2+y^2-a^2}{b^2-a^2}\right)_0 + \sum_1^\infty q_{2r+1}[\psi_{2r+1}(\xi_0, \eta) - \psi_{2r+1}(\xi_0, \tfrac{1}{2}\pi)]. \tag{20}$$

These equations must be solved for the infinite set of unknowns p_{2r+1}, q_{2r+1}. One approximate method is to fit a finite set of polynomials by least squares, as was done for the case of the heaving circular cylinder in ref. **1**. However, in this paper the solution of the set of equations will be considered only under the condition that Kce^{ξ_0} is small and that a and b are of the same order of magnitude.

The expansion in power series of Kc of the functions $\Psi_c(\xi, \eta)$, $\Psi_s(\xi, \eta)$

suggests that

$$p_{2r+1} = \sum_{n=0}^{\infty} P_{n,2r+1}(Kc)^n \tag{21}$$

$$q_{2r+1} = \sum_{n=0}^{\infty} Q^{(1)}_{n,2r+1}(Kc)^n + \log Kc \sum_{n=1}^{\infty} Q^{(2)}_{n,2r+1}(Ks)^n, \tag{22}$$

since the expression in square brackets on the right-hand side of (19) and (20) involves only $(Kc)^0$ and $(Kc)^1$. It is therefore possible to determine the coefficients $P_{n,2r+1}$, $Q^{(1)}_{n,2r+1}$, $Q^{(2)}_{n,2r+1}$ recursively by equating coefficients of $(Kc)^n$ and $(Kc)^n \log Kc$ on the two sides of (19) and (20). It is assumed that the resulting power series defining p_{2r+1}, q_{2r+1} converge for sufficiently small values of Kc. This is known to be true for the heaving motion of the circular cylinder.

Now, if $(Kc)^2 \log Kc$ is negligible,

$$\Psi_c(\xi, \eta) = 2Kc, \tag{23}$$

$$\Psi_s(\xi, \eta) = \mathrm{Im}\left[\frac{2c}{\pi z} + \frac{2}{\pi} iKc(\gamma + \log iKz)\right], \tag{24}$$

$$\Psi_c(\xi_0, \eta) - \Psi_c(\xi_0, \tfrac{1}{2}\pi) = 0, \tag{25}$$

$$\begin{aligned}\Psi_s(\xi_0, \eta) - \Psi_s(\xi_0, \tfrac{1}{2}\pi) &= \mathrm{Im}\left(\frac{2c}{\pi z_0}\right) + \frac{2}{\pi} Kc \log\left|\frac{z_0}{a}\right| \\ &= \mathrm{Im}\left(\frac{2c}{\pi z_0}\right) + O(Kc),\end{aligned} \tag{26}$$

and $$\psi_{2r+1}(\xi_0, \eta) - \psi_{2r+1}(\xi_0, \tfrac{1}{2}\pi) = e^{-(2r+1)\xi_0} \cos(2r+1)\eta + O(Kc). \tag{27}$$

It follows that $$P_{0,2r+1} = P_{1,2r+1} = Q^{(2)}_{1,2r+1} = 0 \tag{28}$$

and $Q^{(1)}_{0,2r+1}$ is given by

$$\mathrm{Im}\left(\frac{2c}{\pi z_0}\right) = Q^{(1)}_{0,1}\left(\frac{x^2+y^2-a^2}{b^2-a^2}\right)_0 + \sum_{r=1}^{\infty} Q^{(1)}_{0,2r+1} e^{-(2r+1)\xi_0} \cos(2r+1)\eta. \tag{29}$$

The amplitude of the motion of the cylinder is determined to the first order by $Q^{(1)}_{0,1}$, which may be found by multiplying (29) by $\cos\eta$ and integrating from 0 to $\frac{1}{2}\pi$. But

$$\mathrm{Im}\left(\frac{2c}{\pi z_0}\right) = \sum_{n=0}^{\infty} a_{2n+1} e^{-(2n+1)\xi} \cos(2n+1)\eta \quad (\xi \geqslant \xi_0), \tag{30}$$

from the theory of harmonic functions, where only a_1 is required in the calculation of $Q^{(1)}_{0,1}$.

Multiply both sides of (30) by e^{ξ} and let ξ tend to infinity. For large ξ,

$$x \sim \tfrac{1}{2} c e^{\xi} \sin\eta, \tag{31}$$

$$y \sim \tfrac{1}{2} c e^{\xi} \cos\eta. \tag{32}$$

In the limit the equation (30) reduces to

$$-(4/\pi)\cos\eta = a_1\cos\eta,$$

or

$$a_1 = -4/\pi. \tag{33}$$

On carrying out the multiplication and integration,

$$-\frac{4}{\pi}e^{-\xi_0} = Q^{(1)}_{0,1}\frac{4}{\pi}\int_0^{\frac{1}{2}\pi}\left(\frac{x^2+y^2-a^2}{b^2-a^2}\right)_0\cos\eta\,d\eta. \tag{34}$$

On the cylinder, the stream-function is given approximately by

$$A\psi = Q^{(1)}_{0,1}\sin\sigma t\left(\frac{x^2+y^2-a^2}{b^2-a^2}\right)_0 = -\tfrac{1}{2}A\theta_0\,\sigma\sin\sigma t(x^2+y^2-a^2)_0, \tag{35}$$

where A is a normalizing constant, and at positive infinity

$$A\psi = 2Kce^{-Ky}\cos(Kx-\sigma t) = \frac{gAB}{\sigma}e^{-Ky}\cos(Kx-\sigma t), \tag{36}$$

where $|B|$ is the amplitude at infinity. Hence

$$B = \frac{K^2c\theta_0(b^2-a^2)}{Q^{(1)}_{0,1}} = K^2ce^{\xi_0}\theta_0\int_0^{\frac{1}{2}\pi}(a^2-x^2-y^2)_0\cos\eta\,d\eta. \tag{37}$$

As an example consider the elliptic cylinder

$$x = c\cosh\xi_0\sin\eta, \qquad y = c\sinh\xi_0\cos\eta$$
$$a = c\cosh\xi_0, \qquad b = c\sinh\xi_0. \tag{38}$$

Here

$$(a^2-x^2-y^2)_0 = (a^2-b^2)\cos^2\eta \tag{39}$$

and the amplitude $|B|$ is

$$K^2ce^{\xi_0}\theta_0\int_0^{\frac{1}{2}\pi}|a^2-b^2|\cos^3\eta\,d\eta = \tfrac{2}{3}K^2\theta_0(a+b)^2|a-b|. \tag{40}$$

It can be shown that this formula is valid whether a is greater or less than b. The calculation shows that the error is $O(K^3a^4)$, which is negligible if Ka is small. When $Q^{(1)}_{0,1}$ has been found, $Q^{(1)}_{0,2r+1}$ is obtained by multiplying (29) by $\cos(2r+1)\eta$ and integrating from 0 to $\frac{1}{2}\pi$.

5. The boundary condition $\partial\phi/\partial y = 0$ $(y = 0)$

There is another way of approaching the problem, which is suggested by the boundary condition

$$K\phi + \frac{\partial\phi}{\partial y} = 0 \quad (y = 0). \tag{41}$$

As K tends to zero, the boundary condition tends formally to

$$\frac{\partial\phi}{\partial y} = 0 \quad (y = 0). \tag{42}$$

It is not unreasonable to expect a close relationship between the first approximation to the wave problem and the complete solution ψ_R of the problem with boundary condition (42). (Cf. ref. **10**.) One way of solving the latter is to expand the stream-function in terms of the set

$$\psi_{2n+1,R} = e^{-(2n+1)\xi}\cos(2n+1)\eta, \tag{43}$$

to which is added the dipole function

$$\Psi_R = \mathrm{Im}\left(\frac{2c}{\pi z}\right). \tag{44}$$

Then the determination of the coefficients in this expansion is clearly the same as the determination of $Q^{(1)}_{0,2r+1}$. Expansion of $\mathrm{Im}(2c/\pi z)$ leads to the following

THEOREM 1. *Suppose that in the skew-symmetric wave-problem ψ is prescribed (except for an additive constant) on the cylinder $\xi = \xi_0$, and that at the mean free surface $y = 0$*

$$K\phi + \frac{\partial\phi}{\partial y} = 0.$$

To obtain the wave amplitude at infinity when Ka is small, solve the simpler problem, in which ψ is prescribed as before on $\xi = \xi_0$, but the free surface is replaced by a rigid plane and

$$\frac{\partial\phi}{\partial y} = 0 \quad (y = 0).$$

If the solution to this latter problem is written in the form

$$\psi_R = \sum_{r=0}^{\infty} B_{2r+1}\, e^{-(2r+1)\xi}\cos(2r+1)\eta \sin\sigma t,$$

where

$$B_{2r+1}\, e^{-(2r+1)\xi_0} = O\left(\frac{1}{r^2}\right). \tag{45}$$

Then for the original problem the waves at infinity are described by

$$\psi = -\tfrac{1}{2}\pi B_1 Kc e^{-Ky}\cos(K|x| - \sigma t). \tag{46}$$

The error in ψ is small of order $K^2a^2B_1$ when $B_1 \neq 0$.

A similar investigation for symmetrical motions, using a source function and a set of polynomials $\psi_{2r}(\xi, \eta)$ (cf. ref. **1**), leads to

THEOREM 2. *If the solution of the problem modified as in Theorem 1 is written in the form*

$$\psi_R = \left[C_0\,\eta + \sum_{r=1}^{\infty} C_{2r}\, e^{-2r\xi}\sin 2r\eta\right]\sin\sigma t, \tag{47}$$

where C_0 is adjusted to make

$$C_{2r}\, e^{-2r\xi_0} = O\left(\frac{1}{r^2}\right),$$

then for the original problem the waves at infinity are described by

$$\psi = \pi C_0 e^{-Ky} \sin(K|x| - \sigma t), \tag{48}$$

the error in ψ being of order $K^2a^2C_0 \log Ka$, when $C_0 \neq 0$.

6. The pressure on the cylinder

The pressure at any point in the fluid is connected with the velocity potential by the relation

$$p = g\rho y - \rho \frac{\partial \phi}{\partial t} + F(t),$$

where $F(t)$ is a function of time to be determined from the condition that at the free surface the pressure is zero. In the skew-symmetric motion ϕ is considered as the superposition of the non-orthogonal polynomials, defined by equation (10), and the dipole potential taken in the form

$$\Phi = \text{Real part of } \left[2Kcie^{iKz - i\sigma t} + \frac{2}{\pi} \sin \sigma t \int_0^\infty \frac{kce^{-kz}\, dk}{k + iK} \right]. \tag{49}$$

The non-orthogonal set tends to zero as $|z|$ tends to infinity, (49) reduces to the potential describing a regular wave train for which the pressure is given by

$$p = g\rho y - \rho \frac{\partial \Phi}{\partial t} = 0 \quad \text{on the surface.} \tag{50}$$

Hence without loss of generality $F(t)$ may be taken as zero. A simple calculation gives

THEOREM 3. *If in the modified skew-symmetrical motion*

$$[\partial \phi_R / \partial y = 0, \quad y = 0]$$

$$\psi_R = \sum_{r=0}^{\infty} B_{2r+1} e^{-(2r+1)\xi} \cos(2r+1)\eta \sin \sigma t,$$

where

$$B_{2r+1} e^{-(2r+1)\xi_0} = O\left(\frac{1}{r^2}\right), \tag{51}$$

then in the original motion the hydrodynamic pressure $-\rho \dfrac{\partial \phi}{\partial t}$ near the cylinder can be obtained approximately from

$$\phi_R = -\sum_{r=0}^{\infty} B_{2r+1} e^{-(2r+1)\xi} \sin(2r+1)\eta \sin \sigma t. \tag{52}$$

The error in the pressure is of order $Kc\rho\, \partial \phi_R / \partial t$. A rather more complicated calculation shows that if the modified symmetrical motion is given by

$$\psi_R = \left[C_0 \eta + \sum_{r=1}^{\infty} C_{2r} e^{-2r\xi} \sin 2r\eta \right] \cos \sigma t, \quad \text{where} \quad C_{2r} e^{-2r\xi_0} = O\left(\frac{1}{r^2}\right) \tag{53}$$

then the hydrodynamic pressure $-\rho\dfrac{\partial\phi}{\partial t}$ *is obtained from*

$$\phi_R = \left[-C_0(\gamma+\log\tfrac{1}{2}Kc+\xi)+\sum_{r=1}^{\infty} C_{2r}\,e^{-2r\xi}\cos 2r\eta\right]\cos\sigma t+\pi C_0\sin\sigma t. \quad (54)$$

7. Applications

The theory which has been given in the previous sections may be applied to a variety of problems concerning the motion of cylinders, and under suitable conditions to the discussion of the motion of ships of long parallel middle body. If numerical computation is to be avoided, the parameter Ka must be so small that the first approximation is valid. This condition is usually fulfilled when a long ship is given a slow forced rolling motion, but not for a heaving motion. Also, the error in the calculation of a symmetrical motion is of order $Ka\log Ka$, and is larger than for a skew-symmetrical one. For these reasons most of the calculations will be made for cases of rolling motions. The section of the cylinder will first be taken as elliptical, so that direct comparison with experiments on ships will not be possible. The extension to other sections involves rather tiresome calculations which, though simple in principle, would obscure the ideas underlying the work. However, the calculation of the amplitude of waves generated by the rolling of a cylinder of nearly rectangular section will be given in detail.

For convenience the modified motion in which the free surface is supposed to be replaced by a rigid plate $\left(\dfrac{\partial\phi}{\partial y}=0,\ y=0\right)$ will be described as the R-motion set up by the motion of the cylinder.

(A) *The roll axis of a cylinder of elliptic section*

When a ship executes a slow rolling motion in still water, there is a point of least movement, called the tranquil point, about which the rolling motion may be supposed to take place. The position of the roll axis in the corresponding two-dimensional motion will now be investigated.

Consider a ship the immersed part of which is a cylinder of semi-elliptic section with its centre in the mean free surface, and consider the skew-symmetrical forced rolling motion about any axis parallel to the axis of the cylinder and lying in the plane of symmetry. For slow rolling the first approximation is adequate; also, the damping is so small that during a roll period there is little difference between free and forced rolling. To maintain a motion at constant amplitude a small amount of energy must be supplied per unit time, most conveniently by a couple. In general there will be an oscillatory reaction on the roll axis, but when this axis coincides with the axis of free rolling, the reaction will be small. For small

angles of roll, the rolling motion about a fixed axis can be considered as made up of a rolling motion about the centre, together with an oscillatory horizontal displacement of the centre in phase with the rolling motion. As the cylinder rolls, the fluid exerts a varying pressure on the cylinder, given by

$$p = g\rho y - \rho\frac{\partial\phi}{\partial t}, \tag{55}$$

the first term representing the hydrostatic, the second the hydrodynamic pressure. The potential is adjusted in accordance with Theorem 3. By the principle of Archimedes the total hydrostatic force is vertical and depends only on the displacement, which is constant (to the first order in θ_0) during the rolling motion and equal to the weight of the ship.

The horizontal forces acting on the cylinder are:

(1) the resultant force due to the hydrodynamic pressure;

(2) the reaction of the roll axis.

The resultant of these two forces is equal to the product of the ship's mass and the horizontal acceleration of the centre of gravity. When the roll axis is the axis of the free rolling motion, the second force will be neglected. An equation is thus obtained to determine the roll axis.

Let d be the depth of the centre of gravity and l that of the roll axis below the water-line. It is assumed that the horizontal axis is the major axis. Suppose that the inclination of the ship at time t is

$$\theta = \theta_0 \sin\sigma t, \tag{56}$$

then the horizontal displacement of the centre of the ellipse is

$$-l\theta = -l\theta_0 \sin\sigma t.$$

It follows, as in ref. (**3**), that on the ellipse $\xi = \xi_0$

$$\begin{aligned}\psi &= -\tfrac{1}{4}\theta_0\sigma c^2(1+\cos 2\eta)\cos\sigma t - l\theta_0\sigma c\sinh\xi_0\cos\eta\cos\sigma t \\ &= -\frac{4}{\pi}\theta_0\sigma c^2\cos\sigma t\sum_{r=0}^{\infty}\frac{(-1)^{r-1}}{(2r-1)(2r+1)(2r+3)}\cos(2r+1)\eta - \\ &\qquad - l\theta_0\sigma c\sinh\xi_0\cos\eta\cos\sigma t.\end{aligned} \tag{57}$$

The solution for the corresponding R-motion is clearly

$$\begin{aligned}\psi_R = -\frac{4}{\pi}\theta_0\sigma c^2\cos\sigma t\sum_{r=0}^{\infty}\frac{(-1)^{r-1}}{(2r-1)(2r+1)(2r+3)}e^{-(2r+1)(\xi-\xi_0)}\cos(2r+1)\eta - \\ - l\theta_0\sigma c\sinh\xi_0 e^{-(\xi-\xi_0)}\cos\eta\cos\sigma t.\end{aligned} \tag{58}$$

By Theorem 3, the corresponding potential function is

$$\begin{aligned}\phi_R = \frac{4}{\pi}\theta_0\sigma c^2\cos\sigma t\sum_{r=0}^{\infty}\frac{(-1)^{r-1}}{(2r-1)(2r+1)(2r+3)}e^{-(2r+1)(\xi-\xi_0)}\sin(2r+1)\eta + \\ + l\theta_0\sigma c\sinh\xi_0 e^{-(\xi-\xi_0)}\sin\eta\cos\sigma t\end{aligned} \tag{59}$$

near the cylinder.

The horizontal force per unit length opposing the motion is

$$-\int_{-\frac{1}{2}\pi}^{\frac{1}{2}\pi} p\frac{\partial y}{\partial \eta}d\eta = 2\rho\int_{0}^{\frac{1}{2}\pi}\frac{\partial \phi}{\partial t}\frac{\partial y}{\partial \eta}d\eta \quad (\xi = \xi_0)$$

$$= \rho c\sigma \sinh\xi_0[\tfrac{2}{3}\theta_0\sigma c^2 + \tfrac{1}{2}\pi\theta_0\sigma cl\sinh\xi_0]\sin\sigma t. \tag{60}$$

The horizontal displacement of the centre of gravity is

$$(d-l)\theta_0\sin\sigma t.$$

Now the horizontal force per unit length is equal to the product of the mass M per unit length and the horizontal acceleration of the centre of gravity:

$$M\sigma^2(d-l)\theta_0\sin\sigma t = \rho c\sigma\sinh\xi_0\sin\sigma t[\tfrac{2}{3}\theta_0\sigma c^2 + \tfrac{1}{2}\pi\theta_0\sigma cl\sinh\xi_0] \tag{61}$$

i.e. (with $c\cosh\xi_0 = a$, $c\sinh\xi_0 = b$),

$$M(d-l) = \rho b[\tfrac{2}{3}c^2 + \tfrac{1}{2}\pi bl],$$

so

$$l = \frac{Md - \frac{2}{3}\rho bc^2}{M + \frac{1}{2}\pi\rho b^2}. \tag{62}$$

But the cylinder is in equilibrium in its mean position, so that

$$M = \tfrac{1}{2}\pi\rho ab,$$

$$l = \frac{ad - \frac{4}{3}\pi(a^2 - b^2)}{a+b}. \tag{63}$$

To this approximation the position of the roll axis is independent of the frequency. It follows that (63) also gives the position of the roll axis for the case of free slow rolling, which can be expressed as the superposition of a number of undamped forced oscillations with periods lying in a narrow band near the mean rolling period. Equation (62) was first derived by R. Brard (ref. **10**), who compared it with experiments and found satisfactory agreement.

When the semi-axes a and b are nearly equal,

$$l = \tfrac{1}{2}d. \tag{64}$$

This formula is in agreement with the experimental results mentioned by Sir William White (ref. **8**, p. 169) for rolling without bilge keels. It appears that the position of the roll-axis depends critically on the difference $(a-b)$ of the semi-axes. When higher terms are included in the calculation, it is no longer permissible to assume that the two skew-symmetrical motions are in phase. Under these conditions, i.e. when the diameter of the ellipse is not small compared with the wave-length, there is no roll-axis; the instantaneous centre of rotation is not confined to a small region.

(B) *The added mass in a slow heaving motion*

Suppose that an elliptic cylinder is given a forced heaving motion

$$y = l \sin \sigma t.$$

Then on the cylinder $\xi = \xi_0$

$$\psi = -l\sigma c \cosh \xi_0 \sin \eta \cos \sigma t$$

$$= -l\sigma c \cosh \xi_0 \left[\frac{2}{\pi} \eta + \frac{2}{\pi} \sum_1^\infty \frac{(-1)^{r-1}}{r(4r^2-1)} \sin 2r\eta \right] \cos \sigma t. \tag{65}$$

It follows that in the corresponding R-motion

$$\psi_R = -l\sigma c \cosh \xi_0 \left[\frac{2}{\pi} \eta + \frac{2}{\pi} \sum_1^\infty \frac{(-1)^{r-1}}{r(4r^2-1)} e^{-2r(\xi-\xi_0)} \sin 2r\eta \right] \cos \sigma t. \tag{66}$$

By Theorem 3, the corresponding potential function ϕ is

$$-l\sigma c \cosh \xi_0 \left[-\frac{2}{\pi} (\gamma + \log \tfrac{1}{2} Kc + \xi) + \frac{2}{\pi} \sum_1^\infty \frac{(-1)^{r-1}}{r(4r^2-1)} e^{-2r(\xi-\xi_0)} \cos 2r\eta \right] \cos \sigma t -$$

$$- 2l\sigma c \cosh \xi_0 \sin \sigma t. \tag{67}$$

The vertical hydrodynamic force opposing the motion of the cylinder is

$$\int_{-\frac{1}{2}\pi}^{\frac{1}{2}\pi} p \frac{\partial x}{\partial \eta} d\eta = -2\rho \int_0^{\frac{1}{2}\pi} \frac{\partial \phi}{\partial t} \frac{\partial x}{\partial \eta} d\eta \quad (\xi = \xi_0), \tag{68}$$

$$= 2\rho c \cosh \xi_0 \, l\sigma^2 c \cosh \xi_0 \left[\frac{2}{\pi} (\gamma + \log \tfrac{1}{2} Kc + \xi_0) \int_0^{\frac{1}{2}\pi} \cos \eta \, d\eta \sin \sigma t - \right.$$

$$\left. - \frac{2}{\pi} \sum_1^\infty \frac{(-1)^{r-1}}{r(4r^2-1)} \int_0^{\frac{1}{2}\pi} \cos 2r\eta \cos \eta \, d\eta \sin \sigma t + 2 \int_0^{\frac{1}{2}\pi} \cos \eta \, d\eta \cos \sigma t \right]$$

$$= 2\rho l a^2 \sigma^2 \left[\frac{2}{\pi} \left(\gamma + \log \frac{Kce^{\xi_0}}{2} \right) \sin \sigma t - \frac{2}{\pi} \sin \sigma t \sum_1^\infty \frac{1}{r(4r^2-1)^2} + 2 \cos \sigma t \right] \tag{69}$$

$$= 2\rho l a^2 \sigma^2 \left[-\frac{2}{\pi} \left(\log \frac{1}{K(a+b)} + 0{\cdot}23 \right) \sin \sigma t + 2 \cos \sigma t \right], \tag{70}$$

where the numerical constant $0{\cdot}23 = 1{\cdot}5 - \log 2 - \gamma$ approximately, and γ is Euler's constant.

Here the first term is 180 degrees out of phase with the acceleration and so represents the effect of added mass. The second term is in quadrature with the acceleration; the work done by it is accounted for by wave damping.

Let M' be the mass per unit length of a semicircular cylinder of radius a, i.e.

$$M' = \tfrac{1}{2}\pi\rho a^2.$$

Then the inertia force per unit length represented by the first term can be written in the form

$$\frac{8}{\pi^2}M'\left[\log\frac{1}{K(a+b)}+0{\cdot}23\right]\frac{d^2y}{dt^2}, \tag{71}$$

whence the added mass per unit length is to the first order

$$\frac{8}{\pi^2}M'\left[\log\frac{1}{K(a+b)}+0{\cdot}23\right]. \tag{72}$$

It may be noted that the ratio of the inertia force (71) to the hydrostatic restoring force per unit length $2\rho alg$ is of order $Ka\log Ka$, which is assumed to be small.

(C) *Motion of a ship in a sea-way*

Suppose that a ship of the type described in (A) is placed in a progressive train of waves advancing from positive infinity

$$\psi = \frac{gA}{\sigma}e^{-Ky}\sin(Kx+\sigma t) = \frac{gKA}{\sigma}(x\cos\sigma t - y\sin\sigma t)+G(t) \tag{73}$$

(near the origin to the first order); and suppose that as a result the coordinates of the centre of the cylinder at time t are

$$x = L\cos(\sigma t+\alpha), \qquad y = l\sin(\sigma t+\beta),$$

and that the inclination of the minor axis at time t is

$$\theta = \theta_0\cos(\sigma t+\delta).$$

Then, on the ellipse $\xi = \xi_0$,

$$\psi = -l\sigma c\cosh\xi_0\sin\eta\cos(\sigma t+\beta) - L\sigma c\sinh\xi_0\cos\eta\sin(\sigma t+\alpha)+ \\ +\tfrac{1}{4}\theta_0\sigma c^2\sin(\sigma t+\delta)[1+\cos 2\eta]. \tag{74}$$

The stream-function satisfying this condition is

$$\psi = \frac{gA}{\sigma}e^{-Ky}\sin(Kx+\sigma t) - \\ -\frac{gA}{\sigma}Kc\cosh\xi_0\cos\sigma t\left[\frac{2}{\pi}\eta+\frac{2}{\pi}\sum_1^\infty\frac{(-1)^{r-1}}{r(4r^2-1)}e^{-2r(\xi-\xi_0)}\sin 2r\eta\right] - \\ -l\sigma c\cosh\xi_0\cos(\sigma t+\beta)\left[\frac{2}{\pi}\eta+\frac{2}{\pi}\sum_1^\infty\frac{(-1)^{r-1}}{r(4r^2-1)}e^{-2r(\xi-\xi_0)}\sin 2r\eta\right]+ \\ +\frac{gA}{\sigma}Kc\sinh\xi_0\,e^{-(\xi-\xi_0)}\cos\eta\sin\sigma t - L\sigma c\sinh\xi_0\,e^{-(\xi-\xi_0)}\cos\eta\sin(\sigma t+\alpha)+ \\ +\frac{4}{\pi}\theta_0\sigma c^2\sin(\sigma t+\delta)\sum_0^\infty\frac{(-1)^{r-1}}{(2r-1)(2r+1)(2r+3)}e^{-(2r+1)(\xi-\xi_0)}\cos(2r+1)\eta. \tag{75}$$

Whence the potential function is to the first order

$$\phi = \frac{gA}{\sigma} e^{-Ky} \cos(Kx+\sigma t) -$$
$$- \left[g\frac{KAa}{\sigma} \cos\sigma t + l\sigma a \cos(\sigma t+\beta) \right] \left[-\frac{2}{\pi}\left(\gamma + \log\frac{Kc}{2} + \xi\right) + \right.$$
$$\left. + \frac{2}{\pi} \sum_{1}^{\infty} \frac{(-1)^{r-1}}{r(4r^2-1)} e^{-2r(\xi-\xi_0)} \cos 2r\eta \right] -$$
$$- 2\left[g\frac{KAa}{\sigma} \sin\sigma t + l\sigma a \sin(\sigma t+\beta) \right] -$$
$$- g\frac{AKb}{\sigma} e^{-(\xi-\xi_0)} \sin\eta \sin\sigma t + L\sigma b e^{-(\xi-\xi_0)} \sin\eta \sin(\sigma t+\alpha) -$$
$$- \frac{4}{\pi}\theta_0 \sigma c^2 \sin(\sigma t+\delta) \sum_{0}^{\infty} \frac{(-1)^{r-1}}{(2r-1)(2r+1)(2r+3)} e^{-(2r+1)(\xi-\xi_0)} \sin(2r+1)\eta. \tag{76}$$

From this velocity potential valid near the cylinder the force and the couple acting on the cylinder can be found, the expression for the pressure being

$$p = g\rho y - \rho\frac{\partial\phi}{\partial t}.$$

When the forces are equated to the product of mass and acceleration in the direction of the force, these equations, with a similar equation for the couple, are sufficient to determine the quantities l, L, θ_0; α, β, δ. For example, consider the heaving motion which is independent of the skew-symmetrical motions.

The force opposing the motion is (correct to the *second* order)

$$2\rho gAa \sin\sigma t[1-\tfrac{1}{4}\pi Kb] -$$
$$- \frac{4}{\pi}\rho a^2\sigma^2 \left[\log\frac{1}{K(a+b)} + 0{\cdot}23 \right] [A \sin\sigma t + l \sin(\sigma t+\beta)] +$$
$$+ \frac{4}{\pi}\rho a^2\sigma^2 [A \cos\sigma t + l \cos(\sigma t+\beta)] + 2\rho gla \sin(\sigma t+\beta),$$

which is to be equated to $\quad \tfrac{1}{2}\pi\rho lab\sigma^2 \sin(\sigma t+\beta) \qquad (77)$

since the mass of the ship is equal to $\frac{1}{2}\pi\rho ab$ by the principle of Archimedes.

It follows that to the second order

$$\beta = 0, \qquad l+A = 0 \tag{78}$$

(taking account of the equation $gK = \sigma^2$), so that the ship moves with the wave.

The reflection from the ship's side due to heaving can be shown to be zero, to this order.

8. The problem of roll resistance in still water

The damping of the rolling motion is known to be mainly due to three different causes: (1) skin friction, (2) wave-making, (3) eddy-making by keels. It is agreed that skin friction does not account for more than a small fraction of the rolling decrement (ref. **2**). The waves generated in the rolling motion of a ship are of the order of one inch in height and rather difficult to measure. Nevertheless, naval architects have arrived at tentative conclusions about the relative importance of (2) and (3). For instance, G. S. Baker has developed an approximate theory (ref. **4**) from which he deduces that wave-making should account in some cases for more than half the energy lost by the ship. According to Baker, (2) and (3) should make comparable contributions to the damping for any section of rectangular shape with rounded corners. The contribution from eddies is increased when the ship is under way.

The mechanism of wave-damping is independent of the viscosity of the fluid. A reasonable estimate of its magnitude may probably be obtained by assuming that the fluid is frictionless. If the ship has a long parallel middle body of length at least as great as the wave-length set up by the rolling motion, the two-dimensional theory worked out in this paper may be applied. Moreover, the parameter Ka is small; in most cases its value is about 0·1 (ref. **2**). It is therefore sufficient to consider the first approximation. The calculation is unchanged when a uniform flow parallel to the axis of the cylinder is superposed.

It will now be shown that hydrodynamical theory does not support the empirical formulae hitherto put forward. In the next section the waves generated by a cylinder rolling about a point in the mean surface will be calculated. (The tranquil point is usually near the mean surface.) It will be shown that there is at least one nearly rectangular section for which the wave amplitude is zero, so that the damping may be overestimated by Baker's formulae. It is hoped to arrange experiments to check the theory.

9. Determination of the waves made by a conventional section

The formula (37) for the wave amplitude requires that x and y should be of the form (5, 6), with $\xi = \xi_0$.

Transformations are known expressing a rectangle with rounded corners in this form (ref. **5**), but for practical purposes it is necessary to use finite expressions

$$x_N(c, \xi_0) = c\cosh\xi_0 \sin\eta + c\sum_1^{2N} A_{2r+1,N}\, e^{-(2r+1)\xi_0}\sin(2r+1)\eta, \qquad (79)$$

$$y_N(c, \xi_0) = c\sinh\xi_0 \cos\eta - c\sum_1^{2N} A_{2r+1,N}\, e^{-(2r+1)\xi}\cos(2r+1)\eta, \qquad (80)$$

for which $x_N^2+y_N^2$ can be found without a prohibitive amount of computation. Equations (79, 80) will represent a roughly rectangular curve if contact with its tangents at $\eta = 0$ and $\eta = \frac{1}{2}\pi$ is of the highest order possible:

$$\left(\frac{\partial}{\partial\eta}\right)^{2s} y_N = 0, \qquad \eta = 0 \quad (s = 1, 2, \ldots, N), \tag{81}$$

$$\left(\frac{\partial}{\partial\eta}\right)^{2s} x_N = 0, \qquad \eta = \tfrac{1}{2}\pi \quad (s = 1, 2, \ldots, N). \tag{82}$$

The equations for $A_{2r+1,N}$ are

$$\sinh\xi_0 = \sum_{r=1}^{2N} A_{2r+1,N}\, e^{-(2r+1)\xi_0}(2r+1)^{2s} \quad (s = 1, 2, \ldots, N), \tag{83}$$

$$\cosh\xi_0 = \sum_{r=1}^{2N} A_{2r+1,N}\, e^{-(2r+1)\xi_0}(-1)^{r-1}(2r+1)^{2s} \quad (s = 1, 2, \ldots, N). \tag{84}$$

By addition and subtraction,

$$\tfrac{1}{2}e^{\xi_0} = \sum_{r=1}^{N} A_{4r-1}\, e^{-(4r-1)\xi_0}(4r-1)^{2s} \quad (s = 1, 2, \ldots, N), \tag{85}$$

$$-\tfrac{1}{2}e^{-\xi_0} = \sum_{r=1}^{N} A_{4r+1}\, e^{-(4r+1)\xi_0}(4r+1)^{2s} \quad (s = 1, 2, \ldots, N). \tag{86}$$

Each of these systems is of the form

$$\sum_{r=1}^{N} B_{r,N}\, b_r^s = 1 \quad (s = 0, 1, \ldots, N-1) \tag{87}$$

the solution of which is

$$B_{r,N} = \prod_{\substack{s=1 \\ s\neq r}}^{N} \left(\frac{b_s-1}{b_s-b_r}\right). \tag{88}$$

The equations (83, 84) thus have the solutions

$$A_{4r-1,N}\, e^{-(4r-1)\xi_0}(4r-1)^2 = \tfrac{1}{2}e^{\xi_0} \prod_{\substack{s=1 \\ s\neq r}}^{N} \left[\frac{(4s-1)^2-1}{(4s-1)^2-(4r-1)^2}\right], \tag{89}$$

$$A_{4r+1,N}\, e^{-(4r+1)\xi_0}(4r+1)^2 = -\tfrac{1}{2}e^{\xi_0} \prod_{\substack{s=1 \\ s\neq r}}^{N} \left[\frac{(4s+1)^2-1}{(4s+1)^2-(4r+1)^2}\right]. \tag{90}$$

As N tends to infinity each coefficient tends to a limit corresponding to the limiting rectangle. Small values of N give satisfactory sections, some of which are shown in Fig. 1. The parameter ξ_0 determines the shape, the parameter c the scale. It is necessary to verify in each case that there is a $(1, 1)$ correspondence between points on the boundary and the coordinates ξ or η.

In the subsequent calculation N will be taken as unity. Then the

parametric equations of the cylinder are

$$x = \tfrac{9}{16}(a+b)\sin\eta + \tfrac{25}{48}(a-b)\sin\eta + \tfrac{1}{16}(a+b)\sin 3\eta - \tfrac{1}{48}(a-b)\sin 5\eta, \quad (91)$$

$$y = \tfrac{9}{16}(a+b)\cos\eta - \tfrac{25}{48}(a-b)\cos\eta - \tfrac{1}{16}(a+b)\cos 3\eta + \tfrac{1}{48}(a-b)\cos 5\eta, \quad (92)$$

also $$ce^{\xi_0} = \tfrac{9}{8}(a+b).$$

The amplitude at infinity has been shown to be, by (37),

$$K^2\theta_0 ce^{\xi_0}\left|\int_0^{\frac{1}{2}\pi}(a^2-x^2-y^2)\cos\eta\, d\eta\right|.$$

In this case

$$x^2+y^2-a^2 = -\tfrac{67}{128}(a^2-b^2)(1+\cos 2\eta) +$$

$$+\tfrac{1}{1152}[25(a-b)^2+81(a+b)^2](1-\cos 4\eta)+\tfrac{3}{128}(a^2-b^2)(1+\cos 6\eta), \quad (93)$$

whence

$$\frac{4}{\pi}\int_0^{\frac{1}{2}\pi}(x^2+y^2-a^2)\cos\eta\, d\eta = -\frac{278}{105\pi}(a^2-b^2)+\frac{1}{270\pi}[25(a-b)^2+81(a+b)^2]$$

$$= -\frac{2{\cdot}25}{\pi}(a-1{\cdot}26b)(a+1{\cdot}05b) \quad (94)$$

and the amplitude at infinity is, to the first order,

$$0{\cdot}63K^2\theta_0(a+b)(a+1{\cdot}05b)|a-1{\cdot}26b|. \quad (95)$$

When a and b are equal the amplitude is

$$\tfrac{27}{40}K^2\theta_0 a^3. \quad (96)$$

This may be compared with $\frac{2}{3}K^2\theta_0 a^3$ for a thin plate (ref. **9**). But when $a = 1{\cdot}26b$, the first order amplitude vanishes. It may be deduced that for this ratio of a to b, the amplitude, and therefore also the wave-damping, is very small. The corresponding section is shown in Fig. 1.

For reference the amplitude is given for the same class of cylinders turning about an axis at height H above the water surface. It is

$$0{\cdot}63K^2\theta_0(a+b)[(1{\cdot}26b-a)(1{\cdot}05b+a)+0{\cdot}015H(a+26b)]. \quad (97)$$

10. Discussion

That wave-making might account for the damping of the rolling motion of ships was first suggested by W. Froude (ref. **7**). Assuming that the angular displacement satisfied a differential equation of the second degree with constant coefficients, he was able to give the damping decrement in terms of the characteristics of the ship and the wave height at infinity (see also ref. **2**). A considerable advance was made by Havelock (ref. **2**), who not only corrected an error in Froude's calculation but also attempted to find the wave height at infinity in terms of the characteristics of the

ship. For this purpose he considered the motion as two-dimensional and evaluated the waves made by the rolling about a vertical mean position of a completely submerged thin plate whose width was small compared with the length of surface waves it generated. Comparison with Baker's experiments showed that the calculated amplitude was too small. This was to be expected, since there is a flow between the surface and a submerged cylinder, which tends to reduce the amplitude, and which cannot

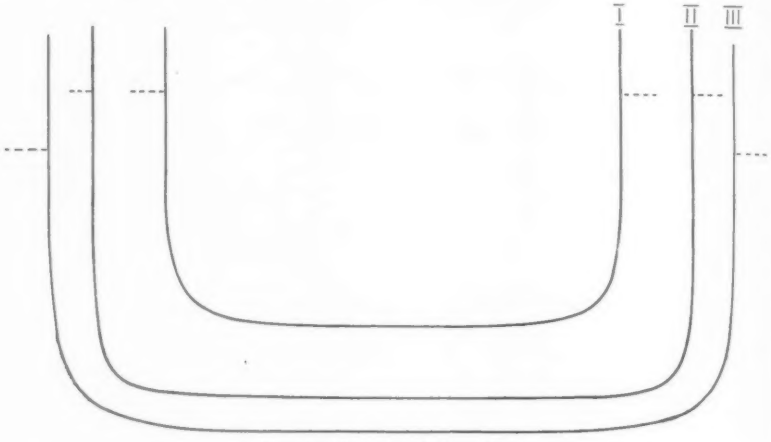

FIG. 1. Some typical sections.

Parametric equations:

I. $x = \frac{a}{8}(9\sin\eta + \sin 3\eta)$,

$y = \frac{a}{8}(9\cos\eta - \cos 3\eta)$. (Minimum radius of curvature $0{\cdot}25a$.)

II. $x = \frac{49a}{640}\left(15\sin\eta + 2\sin 3\eta - \frac{3}{49}\sin 7\eta\right)$,

$y = \frac{49a}{640}\left(15\cos\eta - 2\cos 3\eta + \frac{3}{49}\cos 7\eta\right)$. (Minimum radius of curvature $0{\cdot}16a$.)

III. $x = \frac{9}{16}(a+b)\sin\eta + \frac{25}{48}(a-b)\sin\eta + \frac{1}{16}(a+b)\sin 3\eta - \frac{1}{48}(a-b)\sin 5\eta$,

$y = \frac{9}{16}(a+b)\cos\eta - \frac{25}{48}(a-b)\cos\eta - \frac{1}{16}(a+b)\cos 3\eta + \frac{1}{48}(a-b)\cos 5\eta$,

where $a = 1{\cdot}26b$. When this section is forced to roll about the origin the wave amplitude of the resulting fluid motion vanishes to the first order.

take place when the cylinder is in the surface. This effect was calculated by the present writer, who gave an explicit expression for the waves generated by a thin plate oscillating about the vertical and not completely submerged. Comparison with experiment showed excellent agreement (ref. **9**).

In those calculations it was assumed that it would be sufficiently accurate to replace a cylinder by a thin plate of width equal to the draught of the ship. When the finite section of the cylinder is taken into account, formula (95) is obtained. Baker's experimental results, as quoted by Havelock, belong to a ship in which $a = 1{\cdot}31b$ in the centre section (ref. **4**), so that the good agreement with the earlier formula cannot be explained on any two-dimensional theory. Dr. Baker has informed the present writer that the model ship on which he made experiments did not possess a long parallel middle body, so that two-dimensional theory could not be expected to apply. No detailed comparison of theory and experiment is possible until experiments are made on suitable models.

11. Acknowledgement

I am indebted to the Admiralty for permission to publish this paper.

REFERENCES

1. F. Ursell, see above, p. 218.
2. T. H. Havelock, *Phil. Mag.* **29** (1940), 407.
3. H. Lamb, *Hydrodynamics* (6th edition, Cambridge, 1932).
4. G. S. Baker, *Trans. N.E. Coast Inst. Eng. and Shipbuilders*, **56** (1939), 25.
5. W. M. Page, *Proc. London Math. Soc.* **11** (1913), 313.
6. J. D. Cockcroft, *Journal Inst. Elect. Eng.* **66** (1928), 385.
7. W. Froude, *Naval Science*, **1** (1872), 411.
8. Sir W. White, *Naval Architecture* (5th edition, London, 1900).
9. F. Ursell, *Quart. J. Mech. and Applied Math.* **1** (1948), 246.
10. R. Brard, *Bull. Assoc. Maritime et Aéronautique*, **43** (1939), 231.

THE YAWED DELTA WING AT INCIDENCE AT SUPERSONIC SPEEDS

By GWENDOLEN M. ROPER (*Imperial College, London*)

[Received 27 April 1948; revised 8 February 1949]

SUMMARY

Three cases of the yawed delta wing at incidence have been considered: (1) the case when both leading edges lie inside the Mach cone of the vertex; (2) the case when both leading edges lie outside the Mach cone of the vertex; (3) the case when one leading edge lies inside, and one leading edge lies outside, the Mach cone of the vertex. In each case the wing has two leading edges, and the trailing edge lies outside the Mach cones of the base vertices. The formulae for the disturbance velocities in the regions outside and inside the Mach cone of the vertex have been obtained. Hence the pressure distribution on the isosceles delta wing has been deduced for each case, and the total lift calculated. Some numerical results are exhibited graphically.

I. Introduction

1. In a previous paper (**1**) we have considered the flat delta wing at incidence at supersonic speeds, when the leading edges lie outside the Mach cone of the vertex (hereinafter termed simply 'the Mach cone'), the wing being symmetric to the direction of flow.

The present paper deals with three cases of the yawed delta wing, with the leading edges outside or inside the Mach cone.

The analysis for the case when both leading edges lie within the Mach cone is reduced, by a suitable transformation, to that for the symmetric delta wing with the leading edges within the Mach cone given by H. J. Stewart (**2**).

For the cases when one or both leading edges lie outside the Mach cone, the methods of the complex variable are used to obtain the induced velocity components inside the Mach cone. The conditions outside and on the Mach cone are quoted from known solutions.

For each case, the pressure distribution on the wing and the total lift are found.

II. Formulation of the problems

2. In each case the x-axis is taken through the vertex of the wing, parallel to the undisturbed stream, the axes of y and z to complete a right-handed orthogonal system, the y-axis being in the plane of the wing. The speed of the undisturbed stream is U, its Mach number M, and the Mach angle $\mu = \operatorname{cosec}^{-1} M$. The angles between the leading edges of the

wing and the x-axis are ω_1, $-\omega_2$, and the (small) angle of incidence is α; in applying the boundary conditions, z is put equal to zero.

The velocity components of the disturbance in the x, y, z directions respectively are denoted by u, v, w. The thickness of the wing is ignored.

The equations used are those used for the symmetric case, (**2**), (**1**), that is, the Prandtl–Glauert equation of the linear perturbation theory

$$\beta^2 \frac{\partial^2 P}{\partial x^2} = \frac{\partial^2 P}{\partial y^2} + \frac{\partial^2 P}{\partial z^2}, \tag{2.1}$$

where P is any one of the velocity components u, v, w, and β denotes $(M^2-1)^{\frac{1}{2}}$, and the irrotational relations

$$\frac{\partial w}{\partial y} = \frac{\partial v}{\partial z}, \qquad \frac{\partial u}{\partial z} = \frac{\partial w}{\partial x}, \qquad \frac{\partial v}{\partial x} = \frac{\partial u}{\partial y}. \tag{2.2}$$

The condition to be satisfied on the wing, that is on

$$z = 0, \quad x > 0, \quad -x \tan \omega_2 < y < x \tan \omega_1,$$

is that $\tan \alpha = -w/(U+u)$, or to our order of approximation,

$$w = -U\alpha. \tag{2.3}$$

3. In the previous paper on the flat delta wing (**1**) it was deduced from equations (2.1), (2.2) that the equation to be satisfied by the induced velocity components, inside the Mach cone, is

$$\frac{\partial^2 P}{\partial \sigma^2} + \frac{\partial^2 P}{\partial \theta^2} = 0, \tag{3.1}$$

where

$$\left.\begin{aligned} \operatorname{sech} \sigma &= \frac{\beta(y^2+z^2)^{\frac{1}{2}}}{x} = \beta \tan \omega, \\ \theta &= \tan^{-1}(z/y), \end{aligned}\right\} \tag{3.2}$$

and that the equation to be satisfied by the induced velocity components, outside the Mach cone, is

$$\frac{\partial^2 P}{\partial \chi^2} - \frac{\partial^2 P}{\partial \theta^2} = 0, \tag{3.3}$$

where

$$\left.\begin{aligned} \sec \chi &= \frac{\beta(y^2+z^2)^{\frac{1}{2}}}{x} = \beta \tan \omega, \\ \theta &= \tan^{-1}(z/y). \end{aligned}\right\} \tag{3.4}$$

ω, θ are the normal spherical polar angular coordinates, σ is real within the Mach cone, and is zero on the Mach cone, χ is real outside the Mach cone, and is zero on the Mach cone.

Solutions of the equation (3.1), for the region inside the Mach cone, will now be obtained for the yawed delta wing for the cases ($\omega_1 > \omega_2$):

(*a*) $0 < \omega_1 < \mu$, $0 < \omega_2 < \mu$, that is, both leading edges within the Mach cone.

(*b*) $\omega_1 > \mu$, $\omega_2 > \mu$, that is, both leading edges outside the Mach cone.

(*c*) $\omega_1 > \mu$, $0 < \omega_2 < \mu$, $\omega_1 - \omega_2 < \pi - 2\mu$, that is, one leading edge outside the Mach cone, and one leading edge inside the Mach cone, and the trailing edge outside the Mach cones of the base vertices.

Solutions of equation (3.3) can be found and the constant velocities outside and on the Mach cone deduced mathematically; or it can be argued, on physical grounds, that the conditions correspond to those for the infinite yawed wing. Since these conditions are well known, the results will be quoted.

III. The yawed delta wing, when the leading edges of the wing lie within the Mach cone of the vertex

4. For the region inside the Mach cone the velocity components u, v, w satisfy the equation

$$\frac{\partial^2 P}{\partial \sigma^2} + \frac{\partial^2 P}{\partial \theta^2} = 0. \tag{3.1}$$

Therefore, the complex functions $\mathbf{U} = u + i\bar{u}$, $\mathbf{V} = v + i\bar{v}$, $\mathbf{W} = w + i\bar{w}$, are taken as analytic functions of the complex variable $\vartheta = \theta + i\sigma$. It has been shown (**1**) that

$$\frac{d\mathbf{V}}{d\vartheta} = \cot\vartheta \frac{d\mathbf{W}}{d\vartheta} \tag{4.1}$$

and

$$\frac{d\mathbf{U}}{d\vartheta} = -\frac{1}{\beta}\operatorname{cosec}\vartheta \frac{d\mathbf{W}}{d\vartheta}. \tag{4.2}$$

Inside the Mach cone, $0 < \sigma < \infty$, on the Mach cone, $\sigma = 0$, $-\pi < \theta < \pi$, and on the leading edges of the wing,

$$\operatorname{sech}\sigma = \operatorname{sech}\sigma_1 = \beta\tan\omega_1 \quad (\theta = 0),$$

$$\operatorname{sech}\sigma \equiv \operatorname{sech}\sigma_2 = \beta\tan\omega_2 \quad (\theta = \pi).$$

Therefore, on the wing,

$$\theta = 0, \qquad \sigma_1 \leqslant \sigma < \infty,$$

or

$$\theta = \pm\pi, \quad \sigma_2 \leqslant \sigma < \infty.$$

On the ϑ-plane, the Mach cone is represented by the θ-axis, from $\theta = -\pi$ to $\theta = +\pi$, and the upper surface of the wing by the two semi-infinite lines $\theta = 0$ ($\sigma_1 \leqslant \sigma < \infty$), $\theta = \pi$ ($\sigma_2 \leqslant \sigma < \infty$).

The transformation

$$\zeta \equiv \xi + i\eta = d + A/(f + \cos\vartheta), \tag{4.3}$$

where $-d$, $-f$, A are positive constants, and $f < 1$, transforms the semi-infinite region bounded by the lines $\theta = 0$, $\theta = \pi$ $(\sigma > 0)$; $\sigma = 0$ $(0 \leqslant \theta \leqslant \pi)$ in the ϑ-plane, into the region $\eta > 0$ in the ζ-plane. The

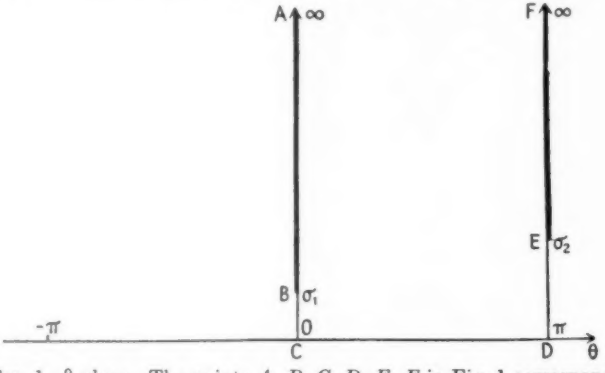

FIG. 1. ϑ-plane. The points A, B, C, D, E, F in Fig. 1 correspond to points A, B, C, D, E, F in Fig. 2.

boundary is mapped on the whole ξ-axis. The values of d, f, A are chosen so that, in the ζ-plane, the points corresponding to points $(\pi, 0)$, (π, σ_2), $(0, \sigma_1)$, $(0, 0)$ in the ϑ-plane, are the points -1, $-k$, k, 1 on the ξ-axis. It is easy to show that these values of d, f, A are given by:

$$\left.\begin{aligned} -f = -d &= \sinh \tfrac{1}{2}(\sigma_2 - \sigma_1)\operatorname{cosech} \tfrac{1}{2}(\sigma_2 + \sigma_1), \\ A = 1 - f^2 &= \sinh\sigma_1 \sinh\sigma_2 \operatorname{cosech}^2 \tfrac{1}{2}(\sigma_2 + \sigma_1), \end{aligned}\right\} \tag{4.4}$$

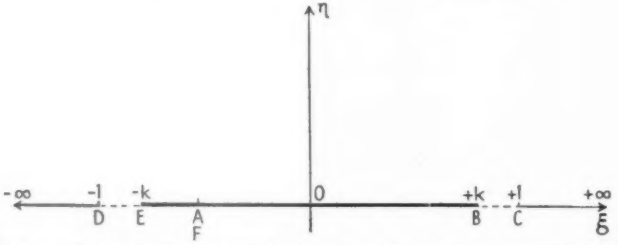

FIG. 2. ζ-plane. The points A, B, C, D, E, F in Fig. 2 correspond to points A, B, C, D, E, F in Fig. 1.

and therefore $$k = \cosh \tfrac{1}{2}(\sigma_2 - \sigma_1)\operatorname{sech} \tfrac{1}{2}(\sigma_2 + \sigma_1). \tag{4.5}$$

The transformation

$$\zeta' = -\int_{\zeta}^{\infty} \frac{d\zeta}{[(\zeta^2 - 1)(\zeta^2 - k^2)]^{\frac{1}{2}}}, \tag{4.6}$$

that is $\zeta = -\mathrm{ns}\,\zeta'$, modulus k, maps the region $\eta > 0$, in the ζ-plane, into the rectangle having its corners at points $\zeta' = \pm K,\ \pm K + iK'$ on the ζ'-plane, K, iK' being the quarter-periods of the Jacobian elliptic functions, modulus k. The points $\zeta = -1,\ -k,\ k,\ 1,\ \infty$ in the ζ-plane correspond to the points $K,\ K+iK',\ -K+iK',\ -K,\ 0$ respectively in the ζ'-plane.

H. J. Stewart (**2**) has shown that the conditions for W are satisfied by

$$\frac{d\mathbf{W}}{d\zeta'} = iD\,\mathrm{cd}^2(\zeta'), \quad D \text{ being a constant,} \tag{4.7}$$

where

$$-U\alpha = \mathrm{Re}\int_0^{iK'} \frac{d\mathbf{W}}{d\zeta'}\,d\zeta', \tag{4.8}$$

and therefore

$$D = \frac{k^2 U\alpha}{E'}, \tag{4.9}$$

where E' is the complete elliptic integral of the second kind, with modulus $k' = (1-k^2)^{\frac{1}{2}}$. Therefore

$$\frac{d\mathbf{W}}{d\zeta} = \frac{d\mathbf{W}}{d\zeta'}\frac{d\zeta'}{d\zeta} = -\frac{ik^2 U\alpha}{E'}\frac{(\zeta^2-1)^{\frac{1}{2}}}{(\zeta^2-k^2)^{\frac{1}{2}}}. \tag{4.10}$$

Hence, using equation (4.2),

$$\frac{d\mathbf{U}}{d\zeta} = \frac{ik^2 U\alpha}{\beta E'(1-f^2)^{\frac{1}{2}}}\left(\frac{f-\zeta}{(\zeta^2-k^2)^{\frac{1}{2}}}\right) \tag{4.11}$$

and

$$\mathbf{U} = \frac{iU\alpha}{\beta E'(1-f^2)^{\frac{1}{2}}}\left\{\frac{k^2}{(\zeta^2-k^2)^{\frac{1}{2}}} - \frac{f\zeta}{(\zeta^2-k^2)^{\frac{1}{2}}}\right\}. \tag{4.12}$$

There is no integration constant, since, on the Mach cone, $\sigma = 0$, $u = 0$.

On the upper surface of the wing, $\tan\omega = y/x$, $\mathrm{sech}\,\sigma = |\beta\tan\omega|$, $\theta = 0$ or π, $\eta = 0$, and

$$\zeta \equiv \xi_0 = \frac{\pm f\cosh\sigma + 1}{\pm\cosh\sigma + f} = \frac{f+\beta\tan\omega}{1+f\beta\tan\omega}. \tag{4.13}$$

Therefore, on the wing, on the upper surface,

$$u = \frac{U\alpha}{\beta E'(1-f^2)^{\frac{1}{2}}}\left\{\frac{k^2 - f\xi_0}{(k^2-\xi_0^2)^{\frac{1}{2}}}\right\}. \tag{4.14}$$

When $\omega_2 = \omega_1$, $\sigma_2 = \sigma_1$, $f = 0$, $k = \mathrm{sech}\,\sigma_1 = \beta\tan\omega_1$, and on the wing, $\zeta = \beta\tan\omega$, and therefore

$$u = \frac{U\alpha\tan^2\omega_1}{E'(\tan^2\omega_1 - \tan^2\omega)^{\frac{1}{2}}}, \tag{4.15}$$

which is Stewart's result for the symmetric wing.

From equation (4.1),

$$\frac{d\mathbf{V}}{d\zeta} = -\frac{ik^2 U\alpha}{E'(1-f^2)^{\frac{1}{2}}}\left\{\frac{f\zeta - 1}{(\zeta^2-k^2)^{\frac{1}{2}}}\right\},$$

and hence
$$\mathbf{V} = \frac{-U\alpha}{E'(1-f^2)^{\frac{1}{2}}}\left\{\frac{\zeta - fk^2}{(k^2-\zeta^2)^{\frac{1}{2}}}\right\}. \tag{4.16}$$

There is no integration constant, since $v = 0$ on the Mach cone.

When $\omega_2 = \omega_1$, on the upper surface of the wing,
$$v = \frac{-U\alpha \tan\omega}{E'(\tan^2\omega_1 - \tan^2\omega)^{\frac{1}{2}}},$$
which is also the value obtained by integrating Stewart's expression for $d\mathbf{V}$ in the symmetric case.

5. *The lift of the yawed delta wing, when both leading edges lie within the Mach cone of the vertex*

If the disturbance velocities u, v, w are small compared with the undisturbed stream velocity U, and their first powers only are retained, the pressure on a surface element of the wing may be calculated by Bernoulli's equation
$$\int \frac{dp}{\rho} + \tfrac{1}{2}q^2 = \text{constant},$$
and we obtain $p - p_1 \equiv \Delta p = -\rho U u$, ρ being the density of the undisturbed stream.

Hence, on the upper surface of the wing
$$\Delta p = -\frac{\rho U^2\alpha}{\beta E'(1-f^2)^{\frac{1}{2}}}\left\{\frac{k^2 - f\xi_0}{(k^2-\xi_0^2)^{\frac{1}{2}}}\right\}. \tag{5.1}$$

Since the pressure variation on the under surface of the wing has the opposite sign, the pressure difference is $2|\Delta p|$.

To find the total lift, the pressure difference is integrated over the surface of the isosceles delta wing. On the wing, $R^2 \equiv x^2 + y^2$, $\tan\omega = y/x$ and c is the maximum chord of the wing, measured perpendicular to the trailing edge. The angle between the chord c and the x-axis is
$$\lambda = (\omega_1 - \omega_2)/2, \tag{5.2}$$
and the total lift is
$$\frac{2\rho U^2\alpha}{\beta E'(1-f^2)^{\frac{1}{2}}}\left[\int_{-\omega_2}^{\omega_1} \frac{k^2 - f\xi_0}{(k^2-\xi_0^2)^{\frac{1}{2}}}\, d\omega \int_{R=0}^{c\sec(\omega-\lambda)} R\, dR\right]$$
$$= \frac{\rho U^2\alpha c^2(1-f^2)^{\frac{1}{2}}}{E'} \int_{-k}^{k} \frac{(k^2 - f\xi_0)\, d\xi_0}{(k^2-\xi_0^2)^{\frac{1}{2}}(H_1\xi_0 - H_2)^2}, \tag{5.3}$$
where $H_1 = \beta f\cos\lambda - \sin\lambda$, $H_2 = \beta\cos\lambda - f\sin\lambda$.

Hence, the total lift is
$$\frac{\rho U^2\alpha c^2(1-f^2)^{\frac{1}{2}}k^2\pi}{E'} \frac{(H_2 - H_1 f)}{(H_2^2 - H_1^2 k^2)^{\frac{1}{2}}}, \tag{5.4}$$

whilst the lift coefficient based on area is

$$C_L = \frac{2\pi\alpha\beta k^2(1-f^2)^{\frac{1}{2}}\cos\lambda}{E'\tan\frac{1}{2}(\omega_1+\omega_2)(H_2^2-H_1^2k^2)^{\frac{1}{2}}} \tag{5.5}$$

$$= \frac{\pi\alpha\cos\lambda}{E'\cos\mu\cos\gamma}\big[\cos 2\lambda-\cos 2\mu\cos 2\gamma- \\ -2\{\sin(\mu+\gamma+\lambda)\sin(\mu+\gamma-\lambda)\sin(\mu-\gamma+\lambda)\sin(\mu-\gamma-\lambda)\}^{\frac{1}{2}}\big]^{\frac{1}{2}}, \tag{5.6}$$

where the semi-angle of the wing is $\gamma = (\omega_1+\omega_2)/2$, and μ is the Mach angle.

When $\omega_2 = \omega_1$ the total lift is

$$\frac{\pi\rho U^2\alpha c^2\tan^2\omega_1}{E'} \quad \text{and} \quad C_L = \frac{2\pi\alpha\tan\omega_1}{E'}, \tag{5.7}$$

which are the results obtained by H. J. Stewart for the symmetric case.

When $\omega_1 = \mu$, $\sigma_1 = 0$, $k = 1$, $f = -1$, so that

$$1-f^2 = 0 \quad \text{and} \quad H_2^2-H_1^2k^2 = 0.$$

But

$$\lim_{\omega_1\to\mu}\left(\frac{1-f^2}{H_2^2-H_1^2k^2}\right) = \frac{1}{\beta}\tan(\mu-\lambda)$$

and therefore

$$C_L \to \frac{4\alpha\cos\lambda}{\beta^{\frac{1}{2}}}\left[\frac{1-\beta\tan\lambda}{\beta+\tan\lambda}\right]^{\frac{1}{2}} = 4\alpha\cos\lambda[\tan(\mu-\lambda)\tan\mu]^{\frac{1}{2}}, \tag{5.8}$$

which gives the lift coefficient for the delta wing with one leading edge within the Mach cone, and one leading edge in the Mach cone. This value agrees with that given later in (11.7).

IV. The yawed delta wing, with both leading edges outside the Mach cone of the vertex

6. *Solution for the region outside the Mach cone*

The equation to be satisfied by the velocity components u, v, w for the region outside the Mach cone is

$$\frac{\partial^2 P}{\partial\chi^2}-\frac{\partial^2 P}{\partial\theta^2} = 0. \tag{3.3}$$

χ is real outside the Mach cone, and is zero on the Mach cone, and

$$\sec\chi = |\beta\tan\omega|.$$

On the leading edges,

$$\left.\begin{aligned}\sec\chi \equiv \sec\chi_1 &= \beta\tan\omega_1 \quad (\theta = 0),\\ \sec\chi \equiv \sec\chi_2 &= \beta\tan\omega_2 \quad (\theta = \pi).\end{aligned}\right\} \tag{6.1}$$

It can be shown that the values of u, v, w for the regions outside, and on, the Mach cone are given by:

$$(0 \leqslant |\theta| \leqslant \pi/2,\ 0 \leqslant \chi \leqslant \chi_1;\quad \pi/2 \leqslant |\theta| \leqslant \pi,\ 0 \leqslant \chi \leqslant \chi_2),$$

$$\left.\begin{array}{rlll} 0 < \theta < \chi_1 - \chi, & u = u_1, & v = v_1, & \\ \pi - (\chi_2 - \chi) < \theta < \pi, & u = u_2, & v = -v_2, & \\ -(\chi_1 - \chi) < \theta < 0, & u = -u_1, & v = -v_1, & \\ -\pi < \theta < -[\pi - (\chi_2 - \chi)], & u = -u_2, & v = -v_2, & \end{array}\right\} w = -U\alpha. \tag{6.2}$$

$$\chi_1 - \chi < |\theta| < \pi - (\chi_2 - \chi), \qquad u = 0, \qquad v = 0, \qquad w = 0,$$

where

$$\left.\begin{array}{ll} u_1 = U\alpha/(\beta \sin \chi_1), & v_1 = -U\alpha \cot \chi_1, \\ u_2 = U\alpha/(\beta \sin \chi_2), & v_2 = -U\alpha \cot \chi_2. \end{array}\right\} \tag{6.3}$$

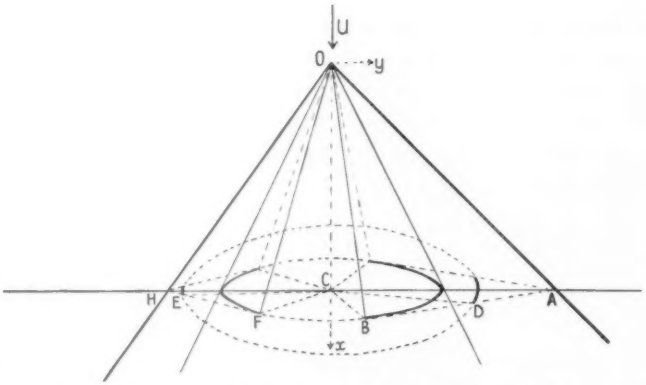

FIG. 3. AOB, HOF are the Mach planes of the leading edges OA, OH of the wing. From the geometry of the figure, the angles subtended at the axis OC, of the Mach cone of the vertex, by the Mach planes AOB, HOF, are given by

$$1/\beta \equiv \tan \mu = \tan \omega_1 \cos ACB = \tan \omega_2 \cos HCF.$$

Therefore angle $ACB = \chi_1$, and angle $HCF = \chi_2$, since $\beta \tan \omega_1 = \sec \chi_1$, and $\beta \tan \omega_2 = \sec \chi_2$. Angle $ACD = \chi_1 - \chi$ and angle $HCE = \chi_2 - \chi$.

7. *Solution for the region inside the Mach cone*

The equations used for the solution inside the Mach cone are equations (3.1), (4.1), (4.2).

Inside the Mach cone, $0 < \sigma < \infty$, on the Mach cone, $\sigma = 0$, $-\pi < \theta < \pi$; and on the wing, $\theta = 0$ or $\pm\pi$.

On the ϑ-plane the Mach cone is represented by the θ-axis from $\theta = -\pi$

to $\theta = +\pi$, and the upper surface of the wing inside the Mach cone, by the semi-infinite lines $\theta = 0$, $\theta = \pi$ ($\sigma > 0$).

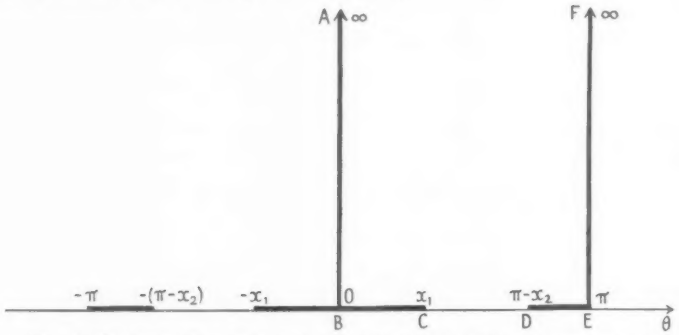

FIG. 4. ϑ-plane. The points A, B, C, D, E, F in Fig. 4 correspond to points A, B, C, D, E, F in Fig. 5.

The transformation $$\zeta \equiv \xi + i\eta = -\cos\vartheta \tag{7.1}$$ transforms the semi-infinite region bounded by the lines $\theta = 0$, $\theta = \pi$ ($\sigma > 0$); $\sigma = 0$ ($0 \leqslant \theta \leqslant \pi$) in the ϑ-plane, into the region $\eta > 0$ in the ζ-plane. The boundary is mapped on the whole ξ-axis. The points -1, $-\cos\chi_1$, $+\cos\chi_2$, $+1$ on the ξ-axis correspond to the points 0, χ_1, $\pi-\chi_2$, π on the θ-axis.

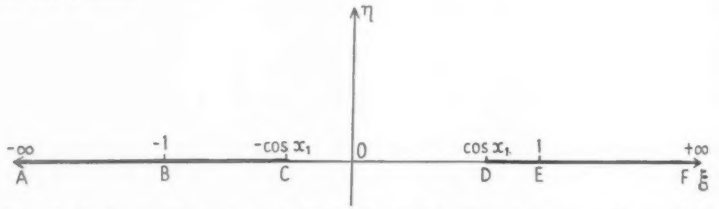

FIG. 5. ζ-plane. The points A, B, C, D, E, F in Fig. 5 correspond to points A, B, C, D, E, F in Fig. 4.

The conditions to be satisfied by w inside the Mach cone are

$$w \equiv w_0 = -U\alpha$$

on the wing, and

$$\left.\begin{aligned} 0 \leqslant |\theta| \leqslant \chi_1, \\ \pi-\chi_2 < |\theta| \leqslant \pi, \\ \chi_1 < |\theta| < \pi-\chi_2, \end{aligned}\right\} \quad \left.\begin{aligned} w = w_0 = -U\alpha \\ w = 0. \end{aligned}\right\} \text{ on the Mach cone.} \tag{7.2}$$

Therefore, for the region considered here, the conditions to be satisfied are:

$$\left.\begin{aligned} -\infty < \xi < -\cos\chi_1, \\ \cos\chi_2 < \xi < +\infty, \\ -\cos\chi_1 < \xi < \cos\chi_2, \end{aligned}\right\} \quad \left.\begin{aligned} w = -U\alpha \\ w = 0. \end{aligned}\right\} \text{ on the } \xi\text{-axis.} \tag{7.3}$$

There is a discontinuity in the value of w when $\xi = -\cos\chi_1$ and when $\xi = \cos\chi_2$.

Conditions (7.3) are satisfied by

$$\mathbf{W} = w_0 + \frac{w_0 i}{\pi}\log\left(\frac{\zeta-\cos\chi_2}{\zeta+\cos\chi_1}\right), \tag{7.4}$$

the principal values of the logarithms being taken. Therefore, on the upper surface of the wing,

$$\mathbf{W} = w_0 + \frac{w_0 i}{\pi}\log\left(\frac{-\cos\vartheta-\cos\chi_2}{-\cos\vartheta+\cos\chi_1}\right). \tag{7.5}$$

Hence
$$\frac{d\mathbf{W}}{d\vartheta} = \frac{w_0 i}{\pi}\left[\frac{\sin\vartheta}{\cos\vartheta-\cos\chi_1} - \frac{\sin\vartheta}{\cos\vartheta+\cos\chi_2}\right], \tag{7.6}$$

and using relation (4.2),

$$\frac{d\mathbf{U}}{d\vartheta} = -\frac{w_0 i}{\beta\pi}\left[\frac{1}{\cos\vartheta-\cos\chi_1} - \frac{1}{\cos\vartheta+\cos\chi_2}\right]. \tag{7.7}$$

Integrating (7.7),

$$\mathbf{U} = -\frac{U\alpha i}{\beta\pi}\left[\frac{1}{\sin\chi_1}\log\frac{\tan(\chi_1/2)-\tan(\vartheta/2)}{\tan(\chi_1/2)+\tan(\vartheta/2)} - \right.$$
$$\left. -\frac{1}{\sin\chi_2}\log\frac{\cot(\chi_2/2)-\tan(\vartheta/2)}{\cot(\chi_2/2)+\tan(\vartheta/2)}\right] + C, \tag{7.8}$$

the principal values of the logarithms being taken and C being a constant.

Above the wing, $0 < \theta < \pi$, and the conditions to be satisfied by u are:

$$\left.\begin{array}{rll} 0 < \theta < \chi_1, & u = \text{constant} = u_{1m}, & \\ \pi-\chi_2 < \theta < \pi, & u = \text{constant} = u_{2m}, & \\ \chi_1 < \theta < \pi-\chi_2, & u = 0. & \end{array}\right\} \quad \text{for } \sigma = 0. \tag{7.9}$$

Therefore, for $0 < \theta < \pi/2$,

$$u = \frac{U\alpha}{\beta\pi}\left[\frac{1}{\sin\chi_1}\left\{\tan^{-1}\left(\frac{-\sinh\sigma}{\tan(\chi_1/2)(\cos\theta+\cosh\sigma)-\sin\theta}\right)-\nu-\right.\right.$$
$$\left.\left. -\tan^{-1}\left(\frac{\sinh\sigma}{\tan(\chi_1/2)(\cos\theta+\cosh\sigma)+\sin\theta}\right)\right\}-$$
$$-\frac{1}{\sin\chi_2}\left\{\tan^{-1}\left(\frac{-\sinh\sigma}{\cot(\chi_2/2)(\cos\theta+\cosh\sigma)-\sin\theta}\right)-\right.$$
$$\left.\left. -\tan^{-1}\left(\frac{\sinh\sigma}{\cot(\chi_2/2)(\cos\theta+\cosh\sigma)+\sin\theta}\right)\right\}\right]+C,$$

where $\nu = 0$ for $0 < \theta < \chi_1$, and $\nu = \pi$ for $\chi_1 < \theta < \pi/2$.

For $\pi/2 < \theta < \pi$,

$$u = \frac{U\alpha}{\beta\pi}\Big[\frac{1}{\sin\chi_1}\Big\{\tan^{-1}\Big(\frac{-\sinh\sigma\tan(\chi_1/2)}{\tan(\chi_1/2)\sin\theta-(\cosh\sigma-\cos\theta)}\Big)-\pi- \\ -\tan^{-1}\Big(\frac{-\sinh\sigma\tan(\chi_1/2)}{\tan(\chi_1/2)\sin\theta+(\cosh\sigma-\cos\theta)}\Big)\Big\}- \\ -\frac{1}{\sin\chi_2}\Big\{\tan^{-1}\Big(\frac{-\sinh\sigma\cot(\chi_2/2)}{\cot(\chi_2/2)\sin\theta-(\cosh\sigma-\cos\theta)}\Big)-\nu- \\ -\tan^{-1}\Big(\frac{-\sinh\sigma\cot(\chi_2/2)}{\cot(\chi_2/2)\sin\theta+(\cosh\sigma-\cos\theta)}\Big)\Big\}\Big]+C,$$

where $\nu = \pi$ for $\pi-\chi_2 < \theta < \pi$, and $\nu = 0$ for $\pi/2 < \theta < \pi-\chi_2$. Hence

$$C = \frac{U\alpha}{\beta\sin\chi_1}, \qquad u_{1m} = \frac{U\alpha}{\beta\sin\chi_1}, \qquad u_{2m} = \frac{U\alpha}{\beta\sin\chi_2}. \tag{7.10}$$

Therefore, on the upper surface of the wing, for $\theta = 0$,

$$u = \frac{2U\alpha}{\beta\pi}\Big[\frac{1}{\sin\chi_1}\sin^{-1}\frac{\tan(\chi_1/2)}{\{\tan^2(\chi_1/2)+\tanh^2(\sigma/2)\}^{\frac{1}{2}}}+ \\ +\frac{1}{\sin\chi_2}\sin^{-1}\frac{\tan(\chi_2/2)}{\{\tan^2(\chi_2/2)+\coth^2(\sigma/2)\}^{\frac{1}{2}}}\Big] \\ = \frac{2U\alpha}{\beta\pi}\Big[\frac{1}{\sin\chi_1}\sin^{-1}\frac{1}{(1+t_1^2)^{\frac{1}{2}}}+\frac{1}{\sin\chi_2}\sin^{-1}\frac{1}{(1+t_2'^2)^{\frac{1}{2}}}\Big], \tag{7.11}$$

where

$$t_1 = \cot(\chi_1/2)\tanh(\sigma/2), \qquad t_2' = \cot(\chi_2/2)\coth(\sigma/2),$$

and for $\theta = \pi$,

$$u = \frac{2U\alpha}{\beta\pi}\Big[\frac{1}{\sin\chi_1}\sin^{-1}\frac{1}{(1+t_1'^2)^{\frac{1}{2}}}+\frac{1}{\sin\chi_2}\sin^{-1}\frac{1}{(1+t_2^2)^{\frac{1}{2}}}\Big], \tag{7.12}$$

where

$$t_2 = \cot(\chi_2/2)\tanh(\sigma/2), \qquad t_1' = \cot(\chi_1/2)\coth(\sigma/2).$$

On the under surface of the wing, u has the same numerical values, but the opposite signs.

Using the relation (4.1),

$$\frac{d\mathbf{V}}{d\vartheta} = \frac{w_0 i}{\pi}\Big[\frac{\cos\chi_1}{\cos\vartheta-\cos\chi_1}+\frac{\cos\chi_2}{\cos\vartheta+\cos\chi_2}\Big]. \tag{7.13}$$

Therefore

$$\mathbf{V} = \frac{U\alpha i}{\pi}\Big[\cot\chi_1\log\frac{\tan(\chi_1/2)-\tan(\vartheta/2)}{\tan(\chi_1/2)+\tan(\vartheta/2)}+ \\ +\cot\chi_2\log\frac{\cot(\chi_2/2)-\tan(\vartheta/2)}{\cot(\chi_2/2)+\tan(\vartheta/2)}\Big]+D, \tag{7.14}$$

the principal values of the logarithms being taken, D being a constant.

The conditions to be satisfied by v above the wing are:

$$\left.\begin{aligned} 0 < \theta < \chi_1, \quad & v = \text{constant} = v_{1m}, \\ \pi - \chi_2 < \theta < \pi, \quad & v = \text{constant} = v_{2m}, \\ \chi_1 < \theta < \pi - \chi_2, \quad & v = 0. \end{aligned}\right\} \text{ for } \sigma = 0. \tag{7.15}$$

Therefore

$$D = -U\alpha \cot \chi_1, \quad v_{1m} = -U\alpha \cot \chi_1, \quad v_{2m} = +U\alpha \cot \chi_2. \tag{7.16}$$

Hence, on the upper surface of the wing, for $\theta = 0$,

$$v = -\frac{2U\alpha}{\pi} \cot \chi_1 \sin^{-1} \frac{1}{(1+t_1^2)^{\frac{1}{2}}} + \frac{2U\alpha}{\pi} \cot \chi_2 \sin^{-1} \frac{1}{(1+t_2'^2)^{\frac{1}{2}}},$$

and for $\theta = \pi$,

$$v = -\frac{2U\alpha}{\pi} \cot \chi_1 \sin^{-1} \frac{1}{(1+t_1'^2)^{\frac{1}{2}}} + \frac{2U\alpha}{\pi} \cot \chi_2 \sin^{-1} \frac{1}{(1+t_2^2)^{\frac{1}{2}}}.$$

On the under surface of the wing, v has the same numerical values, but the opposite signs.

8. *The lift of the yawed delta wing when both leading edges lie outside the Mach cone*

It has been shown, in § 5, that the pressure variation on a surface element of the wing is given by

$$\Delta p = -\rho U u,$$

where ρ is the density of the undisturbed stream.

Therefore, on the upper surface of the wing, for $\theta = 0$,

$$\Delta p = -\frac{2\rho U^2 \alpha}{\beta\pi}\left[\frac{1}{\sin \chi_1} \sin^{-1} \frac{1}{(1+t_1^2)^{\frac{1}{2}}} + \frac{1}{\sin \chi_2} \sin^{-1} \frac{1}{(1+t_2'^2)^{\frac{1}{2}}}\right] \tag{8.1}$$

inside the Mach cone, and

$$\Delta p = -\frac{\rho U^2 \alpha}{\beta \sin \chi_1} \tag{8.2}$$

outside the Mach cone.

For $\theta = \pi$,

$$\Delta p = -\frac{2\rho U^2 \alpha}{\beta\pi}\left[\frac{1}{\sin \chi_1} \sin^{-1} \frac{1}{(1+t_1'^2)^{\frac{1}{2}}} + \frac{1}{\sin \chi_2} \sin^{-1} \frac{1}{(1+t_2^2)^{\frac{1}{2}}}\right] \tag{8.3}$$

inside the Mach cone, and

$$\Delta p = -\frac{\rho U^2 \alpha}{\beta \sin \chi_2} \tag{8.4}$$

outside the Mach cone.

The pressure variation on the under surface of the wing has the opposite sign. Therefore the pressure difference is $2|\Delta p|$.

To find the total lift, the pressure difference is integrated over the surface of the isosceles delta wing.

It can be shown that the total lift is

$$\frac{2\rho U^2 \alpha c^2}{(\beta^2-\tan^2\lambda)^{\frac{1}{2}}} \tan(\omega_1+\omega_2)/2, \tag{8.5}$$

where $\lambda = (\omega_1-\omega_2)/2$ is the angle between the chord c and the x-axis. Hence the lift coefficient, based on area, is given by

$$C_L = \frac{\text{total lift}}{\frac{1}{2}\rho U^2 c^2 \tan(\omega_1-\lambda)} = \frac{4\alpha}{(\beta^2-\tan^2\lambda)^{\frac{1}{2}}} \tag{8.6}$$

$$= \frac{4\alpha \sin\mu \cos\lambda}{[\cos(\mu+\lambda)\cos(\mu-\lambda)]^{\frac{1}{2}}}. \tag{8.7}$$

It is seen from (8.7) that the lift coefficient C_L depends on the angle of yaw λ, but is independent of the angle of the wing. When $\omega_2 = \omega_1$, $\lambda = 0$, and the total lift is

$$\frac{2\rho U^2 \alpha c^2}{\beta} \tan\omega_1 = \frac{2\rho U^2 \alpha c^2}{\beta^2 \cos\chi_1} \tag{8.8}$$

and the lift coefficient is $4\alpha/\beta$.

These are the results obtained for the symmetric case.

V. The yawed delta wing when one leading edge lies inside, and one leading edge lies outside, the Mach cone of the vertex

9. *Solution for the region outside the Mach cone*

As in § 6, the velocity components u, v, w for the region outside the Mach cone satisfy the equation (3.3).

On the leading edge, outside the Mach cone,

$$\sec\chi \equiv \sec\chi_1 = \beta\tan\omega_1. \tag{9.1}$$

It can be shown that, for the regions outside and on the Mach cone,

$$\begin{aligned} 0 < \theta < \chi_1-\chi, &\quad u = U\alpha/(\beta\sin\chi_1), &\quad v = -U\alpha\cot\chi_1 \\ -(\chi_1-\chi) < \theta < 0, &\quad u = -U\alpha/(\beta\sin\chi_1), &\quad v = U\alpha\cot\chi_1 \\ \chi_1-\chi < |\theta| < \pi, &\quad u = 0, &\quad v = 0. \end{aligned} \tag{9.2}$$

10. *Solution for the region inside the Mach cone*

Equations (3.1), (4.1), (4.2) are used for the solution inside the Mach cone.

Inside the Mach cone, $0 < \sigma < \infty$ and on the Mach cone, $\sigma = 0$, $-\pi < \theta < \pi$. On the leading edge of the wing, inside the Mach cone,

$$\operatorname{sech}\sigma \equiv \operatorname{sech}\sigma_2 = \beta\tan\omega_2 \quad (\theta = \pm\pi).$$

On the wing,

$$\theta = 0, \qquad 0 \leqslant \sigma < \infty,$$

$$\theta = \pm\pi, \quad \sigma_2 \leqslant \sigma < \infty.$$

On the ϑ-plane the Mach cone is represented by the θ-axis from $\theta = -\pi$

to $\theta = +\pi$, and the upper surface of the wing inside the Mach cone by the two semi-infinite lines $\theta = 0$ $(0 \leqslant \sigma < \infty)$, $\theta = \pi$ $(\sigma_2 \leqslant \sigma < \infty)$.

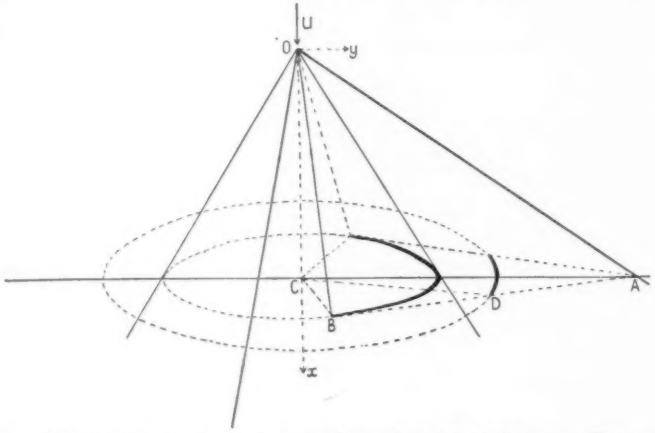

FIG. 6. AOB is a Mach plane of the leading edge OA of the wing. From the geometry of the figure, as in Fig. 3, angle $ACB = \chi_1$. Angle $ACD = \chi_1 - \chi$.

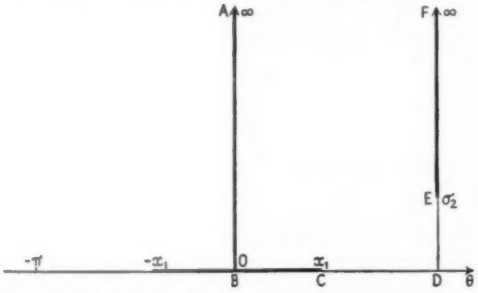

FIG. 7. ϑ-plane. The points D, E in Fig. 7 correspond to points D, E in Fig. 8.

The transformation
$$\zeta = d + \frac{1}{\cos\vartheta - \cos\chi_1} \tag{10.1}$$
transforms the semi-infinite region bounded by the lines $\theta = 0$, $\theta = \pi$ $(\sigma > 0)$; $\sigma = 0$ $(0 \leqslant \theta \leqslant \pi)$ in the ϑ-plane, into the region $\eta > 0$ in the ζ-plane. The boundary is mapped on the ξ-axis. The values of d, k are chosen so that the points corresponding to $(\pi, 0)$, (π, σ_2) in the ϑ-plane are the points $(-k, 0)$, $(+k, 0)$ in the ζ-plane. These values of d, k are given by:
$$2d = \frac{1}{1+\cos\chi_1} + \frac{1}{\cosh\sigma_2 + \cos\chi_1} \tag{10.2}$$
$$2k = \frac{1}{1+\cos\chi_1} - \frac{1}{\cosh\sigma_2 + \cos\chi_1}. \tag{10.3}$$

The conditions to be satisfied by w in the ζ-plane are:

$$\left.\begin{aligned} -\infty < \xi < -k, \quad & w = 0, \\ k < \xi < +\infty, \quad & w = w_0 = -U\alpha \end{aligned}\right\} \quad (\eta = 0). \tag{10.4}$$

The further transformation

$$\zeta = -k\cos\zeta' \tag{10.5}$$

transforms the region $\eta > 0$ in the ζ-plane into the semi-infinite rectangle, bounded by $\xi' = 0$, $\eta' = 0$, $\xi' = \pi$ $(\eta' > 0)$ in the ζ'-plane.

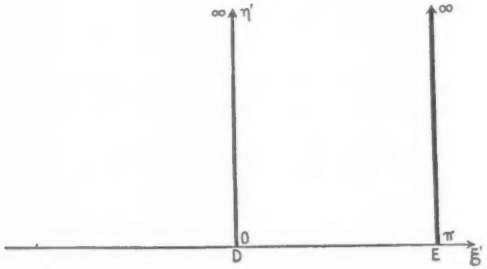

Fig. 8. ζ'-plane. The points D, E in Fig. 8 correspond to points D, E in Fig. 7.

The conditions to be satisfied by w in the ζ'-plane are:

$$\left.\begin{aligned} \xi' = 0, \quad & w = 0, \\ \xi' = \pi, \quad & w = w_0 \end{aligned}\right\} \quad (\eta' > 0). \tag{10.6}$$

The region $\sigma > 0$ $(0 \geqslant \theta \geqslant -\pi)$ in the ϑ-plane maps into the region $\eta < 0$ in the ζ-plane, which is mapped into the semi-infinite rectangle bounded by $\xi' = \pi$, $\eta' = 0$, $\xi' = 2\pi$ $(\eta' > 0)$.

Therefore the region inside the Mach cone is mapped into the basic semi-infinite rectangle bounded by $\xi' = 0$, $\eta' = 0$, $\xi' = 2\pi$ $(\eta' > 0)$ in the ζ'-plane. Since ζ has a period 2π, therefore this pattern is repeated throughout the region $\eta' > 0$ in the ζ'-plane; and $d\mathbf{W}/d\zeta'$ is periodic in the ζ'-plane, with period 2π. The only singularities of $\mathbf{W}$ or $d\mathbf{W}/d\zeta'$ are at the points corresponding to the leading edge inside the Mach cone, that is, at the points congruent to the point $(\pi, 0)$ in the ζ'-plane. Also the value of u given by (4.2) must be finite at all points on the wing, except at the singularity.

These conditions and the conditions (10.6) are satisfied by

$$\frac{d\mathbf{W}}{d\zeta'} = -\frac{w_0}{\pi}\tan^2\frac{\zeta'}{2}. \tag{10.7}$$

Therefore

$$\frac{d\mathbf{W}}{d\vartheta} = \frac{w_0 i}{\pi}\left[\frac{(\cosh\sigma_2 + \cos\chi_1)^{\frac{3}{2}}\sin\vartheta\cos(\vartheta/2)}{\cos(\chi_1/2)(\cos\vartheta - \cos\chi_1)(\cos\vartheta + \cosh\sigma_2)^{\frac{1}{2}}}\right]. \tag{10.8}$$

Using relation (4.2),

$$\frac{d\mathbf{U}}{d\vartheta} = -\frac{w_0 i}{\beta\pi}\left[\frac{(\cosh\sigma_2+\cos\chi_1)^{\frac{1}{2}}\cos(\vartheta/2)}{\cos(\chi_1/2)(\cos\vartheta-\cos\chi_1)(\cos\vartheta+\cosh\sigma_2)^{\frac{1}{2}}}\right]. \qquad (10.9)$$

Integrating (10.9),

$$\mathbf{U} = \frac{w_0 i}{\beta\pi}\left[\frac{(\cosh\sigma_2+\cos\chi_1)^{\frac{1}{2}}\tan\tau}{2^{\frac{1}{2}}\cos(\chi_1/2)\cosh^2(\sigma_2/2)} - \right.$$

$$\left. -\frac{1}{\sin\chi_1}\log\frac{2^{\frac{1}{2}}\sin(\chi_1/2)+(\cosh\sigma_2+\cos\chi_1)^{\frac{1}{2}}\tan\tau}{2^{\frac{1}{2}}\sin(\chi_1/2)-(\cosh\sigma_2+\cos\chi_1)^{\frac{1}{2}}\tan\tau}\right]+C, \qquad (10.10)$$

where $\sin\tau \equiv \sin(\tau_1+i\tau_2) = \operatorname{sech}(\sigma_2/2)\sin(\vartheta/2)$, and C is a constant, the principal values of the logarithms being taken.

The conditions to be satisfied by u, above the wing, are:

$$\left.\begin{array}{ll} 0 \leqslant \theta < \chi_1, & u = \text{constant} = u_{1m}, \\ \chi_1 < \theta \leqslant \pi, & u = 0 \end{array}\right\} \quad \text{for } \sigma = 0. \qquad (10.11)$$

When $\sigma = 0$, $\tau_2 = 0$, $\sin\tau_1 = (\sin\theta/2)/(\cosh\sigma_2/2)$. Therefore when $\sigma = 0$ and $\chi_1 < \theta \leqslant \pi$,

$$0 = u = \frac{w_0(+\pi)}{\beta\pi\sin\chi_1} + C.$$

Hence
$$C = -w_0/(\beta\sin\chi_1) = U\alpha/(\beta\sin\chi_1). \qquad (10.12)$$

When $\sigma = 0$ and $0 \leqslant \theta < \chi_1$, $u = C$, and therefore

$$u_{1m} = U\alpha/(\beta\sin\chi_1). \qquad (10.13)$$

On the upper surface of the wing, for $\theta = 0$,

$$\tau_1 = 0, \qquad \sinh\tau_2 = \sinh(\sigma/2)\operatorname{sech}(\sigma_2/2),$$

for $\theta = \pi$,

$$\tau_1 = \pi/2, \qquad \cosh\tau_2 = \cosh(\sigma/2)\operatorname{sech}(\sigma_2/2) \quad (\sigma > \sigma_2).$$

Therefore on the upper surface of the wing we have, for $\theta = 0$,

$$u = \frac{U\alpha}{\beta\pi}\left[\frac{H}{\cos(\chi_1/2)\cosh^2(\sigma_2/2)} - \frac{1}{\sin\chi_1}\left\{2\tan^{-1}\left(\frac{H}{\sin(\chi_1/2)}\right)-\pi\right\}\right] \qquad (10.14)$$

where
$$H \equiv \frac{(\cosh\sigma_2+\cos\chi_1)^{\frac{1}{2}}\sinh(\sigma/2)}{(\cosh\sigma_2+\cosh\sigma)^{\frac{1}{2}}},$$

and for $\theta = \pi$,

$$u = \frac{U\alpha}{\beta\pi}\left[\frac{H'}{\cos(\chi_1/2)\cosh^2(\sigma_2/2)} - \frac{1}{\sin\chi_1}\left\{2\tan^{-1}\left(\frac{H'}{\sin(\chi_1/2)}\right)-\pi\right\}\right], \qquad (10.15)$$

where
$$H' \equiv \frac{(\cosh\sigma_2+\cos\chi_1)^{\frac{1}{2}}\cosh(\sigma/2)}{(\cosh\sigma-\cosh\sigma_2)^{\frac{1}{2}}}.$$

It can be verified, from (10.13), (10.14), (10.15), that u is continuous

across the surface of the wing, and becomes infinite for $\sigma = \sigma_2$, that is on the leading edge of the wing, inside the Mach cone.

On the under surface of the wing, u has the same numerical values, but the opposite sign.

Using relation (4.1),

$$\frac{d\mathbf{V}}{d\vartheta} = \frac{w_0 i}{\pi}\left[\frac{(\cosh\sigma_2+\cos\chi_1)^{\frac{3}{2}}\cos(\vartheta/2)\cos\vartheta}{\cos(\chi_1/2)(\cos\vartheta-\cos\chi_1)(\cos\vartheta+\cosh\sigma_2)^{\frac{3}{2}}}\right]. \tag{10.16}$$

Therefore

$$\mathbf{V} = \frac{w_0 i}{\pi}\left[\frac{(\cosh\sigma_2+\cos\chi_1)^{\frac{1}{2}}\cosh\sigma_2}{2^{\frac{1}{2}}\cos(\chi_1/2)\cosh^2(\sigma_2/2)}\tan\tau+\right.$$
$$\left.+\cot\chi_1\log\frac{2^{\frac{1}{2}}\sin(\chi_1/2)+(\cosh\sigma_2+\cos\chi_1)^{\frac{1}{2}}\tan\tau}{2^{\frac{1}{2}}\sin(\chi_1/2)-(\cosh\sigma_2+\cos\chi_1)^{\frac{1}{2}}\tan\tau}\right]+D, \tag{10.17}$$

where D is a constant; the principal values of the logarithms being taken.

The conditions to be satisfied by v above the wing are:

$$\left.\begin{aligned} &0 \leqslant \theta < \chi_1, \quad && v = \text{constant} = v_{1m} \\ &\chi_1 < \theta \leqslant \pi, && v = 0 \end{aligned}\right\} \quad \text{for } \sigma = 0. \tag{10.18}$$

Hence

$$D = w_0\cot\chi_1 = -U\alpha\cot\chi_1; \qquad v_{1m} = -U\alpha\cot\chi_1, \tag{10.19}$$

and therefore, on the upper surface of the wing, we have for $\theta = 0$,

$$v = \frac{U\alpha}{\pi}\left[\frac{H\cosh\sigma_2}{\cos(\chi_1/2)\cosh^2(\sigma_2/2)}+\cot\chi_1\left\{2\tan^{-1}\left(\frac{H}{\sin(\chi_1/2)}\right)-\pi\right\}\right], \tag{10.20}$$

and for $\theta = \pi$,

$$v = \frac{U\alpha}{\pi}\left[\frac{H'\cosh\sigma_2}{\cos(\chi_1/2)\cosh^2(\sigma_2/2)}+\cot\chi_1\left\{2\tan^{-1}\left(\frac{H'}{\sin(\chi_1/2)}\right)-\pi\right\}\right]. \tag{10.21}$$

On the under surface of the wing, v has the same numerical values but the opposite signs.

The values of u, v on the Mach cone (10.13), (10.19) agree with those found for the region outside the Mach cone (9.2).

11. *The lift of the yawed delta wing when one leading edge lies inside, and one leading edge lies outside, the Mach cone*

On the upper surface of the wing the pressure difference on a surface element is given by:

$$\Delta p = -\frac{\rho U^2\alpha}{\beta\pi}\left[\frac{H}{\cos(\chi_1/2)\cosh^2(\sigma_2/2)}-\frac{1}{\sin\chi_1}\left\{2\tan^{-1}\left(\frac{H}{\sin(\chi_1/2)}\right)-\pi\right\}\right] \tag{11.1}$$

inside the Mach cone, and by

$$\Delta p = -\frac{\rho U^2 \alpha}{\beta \sin \chi_1} \tag{11.2}$$

outside the Mach cone.

For $\theta = \pi$,

$$\Delta p = -\frac{\rho U^2 \alpha}{\beta \pi}\left[\frac{H'}{\cos(\chi_1/2)\cosh^2(\sigma_2/2)} - \frac{1}{\sin \chi_1}\left\{2\tan^{-1}\left(\frac{H'}{\sin(\chi_1/2)}\right) - \pi\right\}\right]. \tag{11.3}$$

The total lift is found by integrating $2|\Delta p|$ over the surface of the isosceles delta wing.

It can be shown that the total lift is

$$\frac{2\rho U^2 \alpha c^2 \cos\lambda}{\beta^{\frac{1}{2}}\cos(\chi_1/2)}\left(\frac{1-\cot\omega_1 \tan\lambda}{\beta+\tan\lambda}\right)^{\frac{1}{2}} \tan(\omega_1 - \lambda), \tag{11.4}$$

where c is the maximum chord of the wing and $\lambda = (\omega_1 - \omega_2)/2$.

Therefore, the lift coefficient, based on area, is

$$C_L = \frac{\text{total lift}}{\frac{1}{2}\rho U^2 c^2 \tan(\omega_1 - \lambda)} = \frac{4\alpha \cos\lambda}{\beta^{\frac{1}{2}}\cos(\chi_1/2)}\left(\frac{1-\cot\omega_1\tan\lambda}{\beta+\tan\lambda}\right)^{\frac{1}{2}} \tag{11.5}$$

$$= 2^{\frac{1}{2}}\alpha \cos\lambda \sin\mu\left[\frac{\sin\gamma}{\sin(\mu+\gamma+\lambda)\cos(\mu-\lambda)}\right]^{\frac{1}{2}}. \tag{11.6}$$

When $\omega_2 = \omega_1 = \mu$, $\lambda = 0$, and $\chi_1 = 0$, and (11.5) gives $C_L = 4\alpha/\beta$. When $\omega_1 = \mu$, $\chi_1 = 0$, then

$$C_L = \frac{4\alpha\cos\lambda}{\beta^{\frac{1}{2}}}\left(\frac{1-\beta\tan\lambda}{\beta+\tan\lambda}\right)^{\frac{1}{2}} = 4\alpha\cos\lambda[\tan(\mu-\lambda)\tan\mu]^{\frac{1}{2}}. \tag{11.7}$$

(11.7) gives the lift coefficient for the delta wing with one leading edge within the Mach cone, and one leading edge on the Mach cone. The result agrees with the value given in (5.8).

When $\omega_2 = \mu$, $\omega_1 = 2\lambda + \mu$, then

$$C_L = 4\alpha/(\beta^2 - \tan^2\lambda)^{\frac{1}{2}}. \tag{11.8}$$

(11.8) gives the lift coefficient for the delta wing with one leading edge outside the Mach cone, and one leading edge on the Mach cone. The result agrees with the value given in (8.6).

VI. Some numerical results for the isosceles delta wing

12. (i) $\gamma = 45°$, $\mu = 60°$, $0 \leqslant \lambda \leqslant 45°$. (Fig. 9.)

In $0 \leqslant \lambda \leqslant 15°$,

$$C_L/\alpha = \frac{2^{\frac{1}{2}}\pi}{E'}\cos\lambda[\cos 2\lambda - \{\cos(60°+2\lambda)\cos(60°-2\lambda)\}^{\frac{1}{2}}]^{\frac{1}{2}}; \tag{12.1}$$

whilst in $15° \leqslant \lambda \leqslant 45°$,

$$C_L/\alpha = \frac{2^{\frac{5}{2}} 3^{\frac{1}{2}} \cos\lambda}{[\sin(75°-\lambda)\cos(60°-\lambda)]^{\frac{1}{2}}}. \tag{12.2}$$

Formula (12.2) is valid up to $\lambda = 30°$.

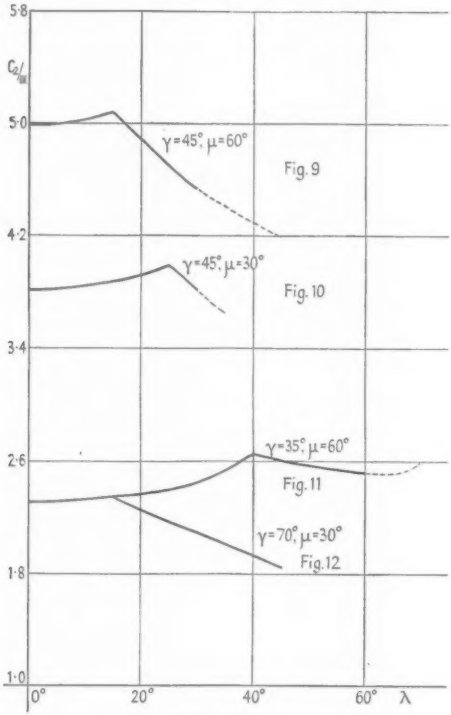

FIGS. 9–12.

(ii) $\gamma = 45°$, $\mu = 30°$, $0 \leqslant \lambda \leqslant 45°$. (Fig. 10.)

In $0 \leqslant \lambda \leqslant 15°$,

$$C_L/\alpha = 2\cos\lambda/[\cos(30°+\lambda)\cos(30°-\lambda)]^{\frac{1}{2}}; \tag{12.3}$$

and in $15° \leqslant \lambda \leqslant 45°$,

$$C_L/\alpha = 2^{\frac{5}{2}} \cos\lambda/[\sin(75°+\lambda)\cos(30°-\lambda)]^{\frac{1}{2}}. \tag{12.4}$$

(iii) $\gamma = 35°$, $\mu = 60°$, $0 \leqslant \lambda \leqslant 35°$. (Fig. 11.)

In $0 \leqslant \lambda \leqslant 25°$,

$$C_L/\alpha = \frac{2\pi\cos\lambda}{E'\cos 35°}[\cos 2\lambda + \tfrac{1}{2}\cos 70° - 2\{\sin(95°-\lambda)\sin(95°+\lambda)\times \times \sin(25°-\lambda)\sin(25°+\lambda)\}^{\frac{1}{2}}]^{\frac{1}{2}}; \tag{12.5}$$

whilst in $25° \leqslant \lambda \leqslant 35°$,

$$C_L/\alpha = 2^{\frac{3}{2}} 3^{\frac{1}{2}} \cos\lambda \left[\frac{\sin 35°}{\sin(85°-\lambda)\cos(60°-\lambda)}\right]^{\frac{1}{2}}. \tag{12.6}$$

Formula (12.6) is valid up to $\lambda = 30°$.

(iv) $\gamma = 70°$, $\mu = 30°$, $0 \leqslant \lambda \leqslant 70°$. (Fig. 12.)

For $0 \leqslant \lambda \leqslant 40°$,

$$C_L/\alpha = 2\cos\lambda/[\cos(30°+\lambda)\cos(30°-\lambda)]^{\frac{1}{2}}; \tag{12.7}$$

whilst for $40° \leqslant \lambda \leqslant 70°$,

$$C_L/\alpha = 2^{\frac{3}{2}} \cos\lambda \left[\frac{\sin 70°}{\sin(80°-\lambda)\cos(30°-\lambda)}\right]^{\frac{1}{2}}. \tag{12.8}$$

Formula (12.8) is valid up to $\lambda = 60°$.

For $\lambda > 30°$ in (i), $\lambda > 30°$ in (iii), and $\lambda > 60°$ in (iv), the trailing edge of the wing lies inside the Mach cones of the base vertices. For $\lambda > 45°$ in (i) and (ii), $\lambda > 35°$ in (iii), and $\lambda > 70°$ in (iv), the edge of the wing, for which $\omega = -\omega_2$, becomes a trailing edge.

Conclusion

The cases when a trailing edge lies inside the Mach cone of any point of it require further investigation. The cases of the flat delta wing when one of the edges through the vertex is a trailing edge, the leading edge lying either inside or outside the Mach cone of the vertex, will be considered in another paper.

Acknowledgement is due to Professor W. G. Bickley for suggesting the subject of this paper, for his continued interest and help, and for many valuable suggestions.

REFERENCES

1. G. M. Roper, 'The flat delta wing, at incidence, at supersonic speeds, when the leading edges lie outside the Mach cone of the vertex': *Quart. J. Mech. and Applied Math.* **1** (1948), 327.
2. H. J. Stewart, 'The lift of a delta wing at supersonic speeds': *Quarterly of Applied Mathematics*, **4** (1946), 246.

SUPERSONIC FLOW PAST THIN WINGS
II. FLOW-REVERSAL THEOREMS

By G. N. WARD

(*Department of Mathematics, The University, Manchester*)

[Received 2 November 1948]

SUMMARY

The results developed in Part I (ref. **1**) are applied to prove that the drag and side forces on a symmetrical wing at zero incidence are unaltered in magnitude when the direction of the flow is reversed, and that, for wings of restricted planform such that the flows over the subsonic edges are independent, the slope of the curve of lift against incidence is unaltered when the direction of the flow is reversed, provided that the Kutta–Joukowski condition is applied at the trailing edge for both stream directions. These results are stated as theorems in § 2, and the possibility of obtaining more general theorems is discussed.

It is also shown that the lift coefficient for a wing, having no subsonic edges and a straight trailing edge, depends only upon the Mach number, the angle of sweep of the trailing edge, and the average incidence over the upper and lower surfaces of the wing, as in (98).

1. Introduction

THE general linearized theory of supersonic flow past thin wings developed in Part I (ref. **1**) is applied to prove some general results for the aerodynamic forces. The notation used is the same as that of Part I and is not re-defined here. The numbering of the equations in this paper follows on consecutively from Part I. A list of the commoner symbols is given in an Appendix.

2. The Flow-reversal theorems

The two following theorems are proved in §§ 3 and 4.

THEOREM I. *If a thin wing, symmetrical about its chord plane, experiences no force normal to its chord plane when placed in a supersonic stream, then a reversal of the direction of the stream leaves the total force on the wing unaltered; the drag component, parallel to the direction of the stream, is unaltered in magnitude and is reversed in direction, and the lateral component, normal to the stream and in the chord plane, is unaltered in magnitude and direction.*

THEOREM II. *If a thin nearly plane wing in a supersonic stream has a planform such that the flows at the subsonic edges (if any) are independent, and if the velocity at the trailing edge satisfies the Kutta–Joukowski condition,*

then a reversal of the direction of the stream leaves the slope of the curve of lift against incidence unaltered, provided that the Kutta–Joukowski condition is satisfied at the trailing edge for the new flow.

The existence of general theorems of this kind was conjectured by Professor S. Goldstein in 1945, and the author is indebted to him for encouragement to prove them.

That part of Theorem I which deals with the drag force has been stated before by W. D. Hayes (ref. **2**) and T. von Kármán (ref. **3**). Hayes has stated a more general theorem for drag which applies to any system to which the linearized theory is applicable, and which includes the drag part of Theorem I as a special case. In general, however, the geometrical configurations of his systems are altered on reversing the flow. Hayes also stated a restricted form of Theorem II, applying only to wings having no subsonic edges ('simple' planforms in his terminology), and mentioned the probability of an extension to other planforms.

Theorem II is very restricted in its scope compared with Theorem I and it is natural to ask whether it can be extended in any respect. This question does not appear to be easy to answer completely, although a partial answer is given here. The theorem is equivalent to a lift-reversal theorem for a *plane* wing of infinitesimal thickness whose planform satisfies the stated conditions, and it is shown later, in § 6, that there is no lift-reversal theorem for a wing of infinitesimal thickness having an arbitrarily warped surface, or a surface such that the local incidence is an arbitrary function of a single coordinate distance, being constant on lines normal to the direction of this coordinate axis. This does not preclude the possibility that there is a lift-reversal theorem for some special surfaces, however, but these do not include the case of a linear variation of incidence. The possibility of removing the restriction on the planform has also been considered by the author, but without positive results.

3. Proof of Theorem I

For the symmetrical case of Part I, it was shown there that the drag force is (equation (60))

$$D = -2\rho U^2 \int_S \int \left(\frac{\partial \phi_0}{\partial z} \frac{\partial \phi_0}{\partial x}\right)_{z=+0} dxdy. \tag{70}$$

Since $(\partial\phi/\partial z)_{z=0} = 0$ on R and T, the integration may be taken over the whole plane $z = +0$ instead of being limited to S. By putting

$$-\frac{1}{2\pi B}\left(\frac{\partial \phi_0}{\partial z}\right)_{z=+0} = f_0(\alpha, \beta), \tag{71}$$

the potential in the plane $z = +0$ is

$$\phi_0 = \int_{-\infty}^{\alpha}\int_{-\infty}^{\beta} \frac{f_0(\alpha',\beta')\,d\alpha'd\beta'}{\sqrt{\{(\alpha-\alpha')(\beta-\beta')\}}}, \tag{72}$$

and the expression for the drag force becomes

$$D = 4\pi\rho U^2 B \int_{-\infty}^{\infty}\int_{-\infty}^{\infty} f_0(\alpha,\beta)\,d\alpha d\beta \left(\frac{\partial}{\partial\alpha}+\frac{\partial}{\partial\beta}\right) \int_{-\infty}^{\alpha}\int_{-\infty}^{\beta} \frac{f_0(\alpha',\beta')\,d\alpha'd\beta'}{\sqrt{\{(\alpha-\alpha')(\beta-\beta')\}}}. \tag{73}$$

If we assume that the wing is of finite extent, then

$$f_0(\pm\infty,\pm\infty) = 0, \tag{74}$$

and by making the further temporary assumption, for simplicity, that $f_0(\alpha,\beta)$ is continuous everywhere, then the differentiations in equation (73) can be carried out to obtain

$$D = 4\pi\rho U^2 B \int_{-\infty}^{\infty}\int_{-\infty}^{\infty} f_0(\alpha,\beta)\,d\alpha d\beta \int_{-\infty}^{\alpha}\int_{-\infty}^{\beta} \frac{(f_{0,\alpha'}+f_{0,\beta'})\,d\alpha'd\beta'}{\sqrt{\{(\alpha-\alpha')(\beta-\beta')\}}}, \tag{75}$$

where $f_{0,\alpha}$ and $f_{0,\beta}$ denote the derivatives of $f_0(\alpha,\beta)$ with respect to α and β respectively.

If the flow is now reversed so that the stream velocity is directed along the negative x-axis, the new force, D', in the direction of x increasing is

$$D' = 4\pi\rho U^2 B \int_{-\infty}^{\infty}\int_{-\infty}^{\infty} f_0(\alpha,\beta)\,d\alpha d\beta \left(\frac{\partial}{\partial\alpha}+\frac{\partial}{\partial\beta}\right) \int_{\alpha}^{\infty}\int_{\beta}^{\infty} \frac{f_0(\alpha',\beta')\,d\alpha'd\beta'}{\sqrt{\{(\alpha'-\alpha)(\beta'-\beta)\}}}. \tag{76}$$

Integration by parts gives

$$D' = -4\pi\rho U^2 B \int_{-\infty}^{\infty}\int_{-\infty}^{\infty} (f_{0,\alpha}+f_{0,\beta})\,d\alpha d\beta \int_{\alpha}^{\infty}\int_{\beta}^{\infty} \frac{f_0(\alpha',\beta')\,d\alpha'd\beta'}{\sqrt{\{(\alpha'-\alpha)(\beta'-\beta)\}}}, \tag{77}$$

and by inverting the order of the double integrations we obtain finally

$$D' = -4\pi\rho U^2 B \int_{-\infty}^{\infty}\int_{-\infty}^{\infty} f_0(\alpha',\beta')\,d\alpha'd\beta' \int_{-\infty}^{\alpha'}\int_{-\infty}^{\beta'} \frac{(f_{0,\alpha}+f_{0,\beta})\,d\alpha d\beta}{\sqrt{\{(\alpha'-\alpha)(\beta'-\beta)\}}}. \tag{78}$$

Comparison of equations (75) and (78) shows that

$$D' = -D. \tag{79}$$

The assumption on the continuity of f_0 can be removed, and discontinuities allowed on a finite number of arcs in the α, β-plane without altering this result, as may be seen by replacing the Riemann integrals by Stieltjes integrals.

Similarly, for the lateral force, Y, in the direction of the positive y-axis,

$$Y = -2\rho U^2 \iint_S \left(\frac{\partial \phi_0}{\partial z}\frac{\partial \phi_0}{\partial y}\right)_{y=+0} dxdy \tag{72}$$

$$= 4\pi\rho U^2 \int_{-\infty}^{\infty}\int_{-\infty}^{\infty} f_0(\alpha,\beta)\, d\alpha d\beta \left(-\frac{\partial}{\partial\alpha}+\frac{\partial}{\partial\beta}\right) \int_{-\infty}^{\alpha}\int_{-\infty}^{\beta} \frac{f_0(\alpha',\beta')\, d\alpha' d\beta'}{\sqrt{\{(\alpha-\alpha')(\beta-\beta')\}}}. \tag{80}$$

If the flow is reversed, the new lateral force, Y', is

$$Y' = -4\pi\rho U^2 \int_{-\infty}^{\infty}\int_{-\infty}^{\infty} f_0(\alpha,\beta)\, d\alpha d\beta \left(-\frac{\partial}{\partial\alpha}+\frac{\partial}{\partial\beta}\right) \int_{\alpha}^{\infty}\int_{\beta}^{\infty} \frac{f_0(\alpha',\beta')\, d\alpha' d\beta'}{\sqrt{\{(\alpha'-\alpha)(\beta'-\beta)\}}}, \tag{81}$$

and by carrying out the same sequences of operations as were used for D and D', we readily obtain the result

$$Y' = Y. \tag{82}$$

This completes the proof of Theorem I.

4. Proof of Theorem II

Theorem II will be proved for the equivalent form mentioned in § 2, that is as a lift-reversal theorem for a plane wing of infinitesimal thickness. Such a wing corresponds to the antisymmetrical case of Part I, with $\lambda(\alpha,\beta) =$ constant. For simplicity the incidence is taken to be such that $\lambda(\alpha,\beta) = 1$; no loss of generality arises since λ depends only upon incidence and Mach number, and these quantities remain unaltered in magnitude when the direction of flow is reversed. The lift on the wing is given by (69) of Part I, which contains only the value of the potential ϕ_1 at points on the trailing edge of the wing for $z = +0$.

Consider the wing whose planform is shown in Fig. 3 (a) of Part I, and let the coordinates of the points N and P (which were left unspecified in Part I) be (α_3,β_3) and (α_4,β_4) respectively. For convenience, the potential $(\phi_1)_{z=+0}$ at the trailing edge is divided into three parts, which are considered separately. These are:

(i) a part ϕ', depending upon the function G_1, arising from the vortex sheet from the subsonic trailing edge T_1N, which is non-zero only on the arc T_1E of C;

(ii) a part ϕ'', depending upon the function G_2, arising from the vortex sheet from the subsonic trailing edge PT_2, which is non-zero only on the arc FT_2 of C;

(iii) a part ϕ''', consisting of terms given in (52) of Part I, which is non-zero only on the arc NP of C.

On the arc T_1N, $\alpha = B_1(\beta)$, and from (50),

$$\phi' = \int_{\beta+\gamma_1}^{B_1(\beta)} \frac{G_1(\alpha'-\beta)}{\sqrt{\{B_1(\beta)-\alpha'\}}} d\alpha' = \int_{\gamma_1}^{B_1(\beta)-\beta} \frac{G_1(\xi)\, d\xi}{\sqrt{\{B_1(\beta)-\beta-\xi\}}}. \tag{83}$$

On the arc NE, $\alpha = B_2(\beta)$, and

$$\phi' = \int_{\beta+\gamma_1}^{B_1(\beta)} \frac{G_1(\alpha'-\beta)}{\sqrt{\{B_2(\beta)-\alpha'\}}} d\alpha' = \int_{\gamma_1}^{B_1(\beta)-\beta} \frac{G_1(\xi)\, d\xi}{\sqrt{\{B_2(\beta)-\beta-\xi\}}}. \tag{84}$$

From (40), when $\lambda = 1$,

$$G_1\{\alpha-A_2(\alpha)\} = 2\sqrt{\{A_2(\alpha)-A_1(\alpha)\}}. \tag{85}$$

Therefore, by putting $\xi = \alpha-A_2(\alpha)$ in (83) and (84), and integrating ϕ' along ET_1 with respect to y, we have

$$\begin{aligned} 2B \int_{ET_1} \phi'\, dy &= 2 \int_{\beta_1}^{\beta_3} [1-B_2'(\beta)]\, d\beta \int_{\alpha_1}^{B_1(\beta)} \sqrt{\left\{\frac{A_2(\alpha)-A_1(\alpha)}{B_2(\beta)-\beta-\alpha+A_2(\alpha)}\right\}} [1-A_2'(\alpha)]\, d\alpha - \\ &\quad - 2 \int_{\beta_1}^{\beta_3} [1-B_1'(\beta)]\, d\beta \int_{\alpha_1}^{B_1(\beta)} \sqrt{\left\{\frac{A_2(\alpha)-A_1(\alpha)}{B_1(\beta)-\beta-\alpha+A_2(\alpha)}\right\}} [1-A_2'(\alpha)]\, d\alpha. \end{aligned} \tag{86}$$

On inverting the order of integration, the integration with respect to β can be carried out, and since $B_1(\beta_3) = B_2(\beta_3)$ and $B_1(A_2(\alpha)) = \alpha$ on the arc NT_1, we have

$$\begin{aligned} 2B \int_{ET_1} \phi'\, dy &= 4 \int_{\alpha_1}^{\alpha_3} \sqrt{\{[A_2(\alpha)-A_1(\alpha)][B_2(A_2(\alpha))-\alpha]\}} [1-A_2'(\alpha)]\, d\alpha \\ &= 4 \int_{\alpha_1}^{\alpha_3} \sqrt{\{[A_2(\alpha)-A_1(\alpha)][B_2(A_2(\alpha))-\alpha]\}}\, d\alpha - \\ &\quad - 4 \int_{\beta_1}^{\beta_3} \sqrt{\{[B_2(\beta)-B_1(\beta)][\beta-A_1(B_1(\beta))]\}}\, d\beta. \end{aligned} \tag{87}$$

In a similar manner we can obtain the result

$$\begin{aligned} 2B \int_{T_2F} \phi''\, dy &= 4 \int_{\beta_2}^{\beta_4} \sqrt{\{[B_2(\beta)-B_1(\beta)][A_2(B_2(\beta))-\beta]\}}\, d\beta - \\ &\quad - 4 \int_{\alpha_2}^{\alpha_4} \sqrt{\{[A_2(\alpha)-A_1(\alpha)][\alpha-B_1(A_1(\alpha))]\}}\, d\alpha. \end{aligned} \tag{88}$$

On the arc NG, from (48) with $\lambda = 1$,

$$\phi''' = 2 \int_{B_1(\beta)}^{B_2(\beta)} \sqrt{\left\{\frac{\beta - A_1(\alpha')}{B_2(\beta) - \alpha'}\right\}}\, d\alpha', \tag{89}$$

and on the arc GP, the expression (52) with $\lambda = 1$ may be expressed in the form

$$\phi''' = 2 \int_{B_1(\beta)}^{B_2(\beta)} \sqrt{\left\{\frac{\beta - A_1(\alpha')}{B_2(\beta) - \alpha'}\right\}}\, d\alpha' - 2 \int_{B_3(\beta)}^{B_2(\beta)} \sqrt{\left\{\frac{\beta - A_1(\alpha')}{B_2(\beta) - \alpha'}\right\}}\, d\alpha' + \\ + 4\sqrt{\{[B_2(\beta) - B_3(\beta)][\beta - A_1(B_2(\beta))]\}}, \tag{90}$$

where $B_3(\beta) = B_1[A_1(B_2(\beta))]$ when $\beta_0 < \beta < A_2(\alpha_0)$. The curve $\alpha = B_3(\beta)$ can be constructed geometrically as illustrated in Fig. 4. This figure is lettered to correspond with the figures in Part I:

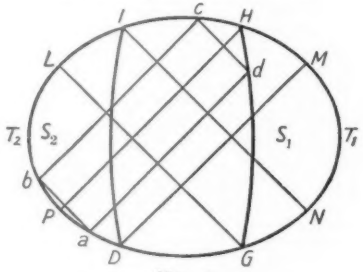

FIG. 4.

All the straight lines are characteristic lines in the plane $z = 0$, a is any point on the arc GP, and $abcd$ is a characteristic parallelogram, b and c lying respectively on PL, LH. As a moves along GP, the locus of d is the curve $\alpha = B_3(\beta)$ or $\beta = A_3(\alpha)$ passing through H and G. That part of S lying to the right of $\alpha = B_3(\beta)$ is denoted by S_1. The curve DI and the area S_2 are defined similarly, by changing left for right. Although the areas S_1, S_2 are shown separated in Fig. 4, they may overlap if the aspect ratio of the wing is sufficiently large.

From (89) and (90) we have

$$2B \int_{PN} \phi'''\, dy = 2 \int_{\beta_4}^{\beta_3} [1 - B_2'(\beta)]\, d\beta \int_{B_1(\beta)}^{B_2(\beta)} \sqrt{\left\{\frac{\beta - A_1(\alpha)}{B_2(\beta) - \alpha}\right\}}\, d\alpha - \\ - 2 \int_{\beta_4}^{A_2(\alpha_0)} [1 - B_2'(\beta)]\, d\beta \int_{B_3(\beta)}^{B_2(\beta)} \sqrt{\left\{\frac{\beta - A_1(\alpha)}{B_2(\beta) - \alpha}\right\}}\, d\alpha + \\ + 4 \int_{\beta_4}^{A_2(\alpha_0)} \sqrt{\{[B_2(\beta) - B_3(\beta)][\beta - A_1(B_2(\beta))]\}}\, [1 - B_2'(\beta)]\, d\beta. \tag{91}$$

After some algebra, the right-hand side of this expression may be written as

$$2\iint_{S_1}\left(\sqrt{\left\{\frac{\beta-A_1(\alpha)}{B_2(\beta)-\alpha}\right\}}+\sqrt{\left\{\frac{B_2(\beta)-\alpha}{\beta-A_1(\alpha)}\right\}}\right)d\alpha d\beta+$$

$$+4\int_{B_1(\beta_4)}^{\alpha_0}\sqrt{\{[A_3(\alpha)-A_1(\alpha)][B_2(A_1(\alpha))-\alpha]\}}\,d\alpha+$$

$$+4\int_{\alpha_0}^{\alpha_4}\sqrt{\{[\alpha-B_1(A_1(\alpha))][A_2(\alpha)-A_1(\alpha)]\}}\,d\alpha-$$

$$-4\int_{0}^{\alpha_3}\sqrt{\{[A_2(\alpha)-A_1(\alpha)][B_2(A_2(\alpha))-\alpha]\}}\,d\alpha+$$

$$+4\int_{\beta_4}^{A_2(\alpha_0)}\sqrt{\{[B_2(\beta)-B_1(\beta)][\beta-A_2(B_2(\beta))]\}}\,d\beta. \tag{92}$$

The results of equations (87), (88), and (92) may now be combined to give

$$2B\int_{T_2T_1}(\phi_1)_{z=+0}\,dy=2\iint_{S_1}\left(\sqrt{\left\{\frac{\beta-A_1(\alpha)}{B_2(\beta)-\alpha}\right\}}+\sqrt{\left\{\frac{B_2(\beta)-\alpha}{\beta-A_1(\alpha)}\right\}}\right)d\alpha d\beta+$$

$$+4\int_{H}^{L}\sqrt{\{[A_3(\alpha)-A_1(\alpha)][B_2(A_1(\alpha))-\alpha]\}}\,d\alpha+$$

$$+4\int_{P}^{G}\sqrt{\{[B_2(\beta)-B_3(\beta)][\beta-A_1(B_2(\beta))]\}}\,d\beta+$$

$$+4\int_{L}^{T_2}\sqrt{\{[A_2(\alpha)-A_1(\alpha)][\alpha-B_1(A_1(\alpha))]\}}\,d\alpha+$$

$$+4\int_{T_2}^{P}\sqrt{\{[B_2(\beta)-B_1(\beta)][A_2(B_2(\beta))-\beta]\}}\,d\beta-$$

$$-4\int_{M}^{T_1}\sqrt{\{[A_2(\alpha)-A_1(\alpha)][B_2(A_2(\alpha))-\alpha]\}}\,d\alpha-$$

$$-4\int_{T_1}^{N}\sqrt{\{[B_2(\beta)-B_1(\beta)][\beta-A_1(B_1(\beta))]\}}\,d\beta, \tag{93}$$

where, for clarity, the limits of the integrations have been specified by the

names of the points given in Fig. 4 rather than by the appropriate coordinates.

If the curve ID in Fig. 4 is given the equation $\alpha = B_4(\beta)$ or $\beta = A_4(\alpha)$, an equivalent expression can be obtained (or written down immediately by using the formal symmetry between α and β) involving an integration over S_2, etc. By taking the average of these two expressions, the last four integrals in (93) cancel with the corresponding terms in the equivalent expression, and we get the more symmetrical result

$$
\begin{aligned}
2B \int_{T_2T_1} (\phi_1)_{z=+0}\, dy = {} & \iint_{S_1} \left(\sqrt{\left\{\frac{\beta - A_1(\alpha)}{B_2(\beta) - \alpha}\right\}} + \sqrt{\left\{\frac{B_2(\beta) - \alpha}{\beta - A_1(\alpha)}\right\}} \right) d\alpha d\beta + \\
& + \iint_{S_2} \left(\sqrt{\left\{\frac{\alpha - B_1(\beta)}{A_2(\alpha) - \beta}\right\}} + \sqrt{\left\{\frac{A_2(\alpha) - \beta}{\alpha - B_1(\beta)}\right\}} \right) d\alpha d\beta + \\
& + 2 \int_H^L \sqrt{\{[A_3(\alpha) - A_1(\alpha)][B_2(A_1(\alpha)) - \alpha]\}}\, d\alpha + \\
& + 2 \int_P^G \sqrt{\{[B_2(\beta) - B_3(\beta)][\beta - A_1(B_2(\beta))]\}}\, d\beta + \\
& + 2 \int_N^D \sqrt{\{[A_2(\alpha) - A_4(\alpha)][\alpha - B_1(A_2(\alpha))]\}}\, d\alpha + \\
& + 2 \int_I^M \sqrt{\{[B_4(\beta) - B_1(\beta)][A_2(B_1(\beta)) - \beta]\}}\, d\beta. \qquad (94)
\end{aligned}
$$

This expression now possesses complete formal symmetry, not only with respect to α and β, but also with respect to the fore and aft on the wing, so that a reversal of the stream direction merely reverses the sign of the lift force without altering its magnitude. This proves Theorem II.

5. The lift of a wing with a straight supersonic trailing edge and no subsonic edges

Before considering the possibility of a more general theorem for lift than Theorem II, it is advantageous to obtain an interesting result for the lift force on wings which have no subsonic edges, and whose trailing edge is straight.

Since the edges of S are supersonic, the flows over the two surfaces are independent. The potential due to an element of area dS at $(x, y, +0)$ on S at a point $(x_1, y_1, +0)$ on the trailing edge and inside the downstream

characteristic cone with its vertex at $(x, y, 0)$ is, from (7) and (13) of Part I,

$$d\phi = \frac{l_1\, dS}{\pi\sqrt{\{(x_1-x)^2 - B^2(y_1-y)^2\}}}. \tag{95}$$

The lift, dL, from this element is obtained by integrating $d\phi$ with respect to y_1 along the relevant portion of the trailing edge. If Θ is the angle of sweep of the trailing edge, it is easy to show that

$$dL = \rho U^2 \frac{l_1 \cos\Theta\, dS}{\sqrt{(M^2\cos^2\Theta - 1)}}. \tag{96}$$

A similar result is obtained for the lower surface. Thus the total lift, L, is

$$\frac{\rho U^2 \cos\Theta}{\sqrt{(M^2\cos^2\Theta - 1)}} \iint_S (l_1 - l_2)\, dS, \tag{97}$$

and the lift coefficient with respect to $\frac{1}{2}\rho U^2$ and the wing area is

$$\frac{4\cos\Theta}{\sqrt{(M^2\cos^2\Theta - 1)}}\, \overline{\tfrac{1}{2}(l_1 - l_2)}, \tag{98}$$

where the bar denotes the average value with respect to the area. The quantity $\overline{\frac{1}{2}(l_1 - l_2)}$ is the average value of the local incidences on the upper and lower surfaces, if the incidence is defined as a right-hand rotation about the y-axis.

Special cases of this result have been noticed before, usually in connexion with plane triangular wings. The special case of this formula (98) for a plane wing is a consequence of Theorem II and the well-known result for the lift coefficient of a 'two-dimensional' swept wing, due to Busemann.

6. The possibility of a more general theorem than Theorem II

By using the result given in (96) it can be shown that there is no general lift-reversal theorem for a wing of infinitesimal thickness having an arbitrarily warped surface. For if there is such a theorem it must be true for special cases, and, in particular, it must be true for a wing having the planform shown in Fig. 5. If the local incidence is varied over an area dS at the point (x, y) shown, which is such that the characteristic lines through it cut only the straight leading and trailing edges, then equation (96) shows that the increments of lift due to this variation are unequal for the two directions of flow, since the angles of sweep of the two supersonic edges are unequal. Thus the theorem cannot be true both before and after the incidence variation, and so there can be no general theorem of this kind.

In a similar way, it can be argued that there is no general lift-reversal theorem for variations of incidence such that the incidence is constant along any set of parallel straight lines and varies arbitrarily in a direction

normal to them. In particular, the incidence cannot be an arbitrary function of x alone, or of y alone.

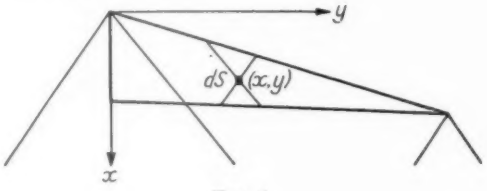

FIG. 5.

For any planform with no subsonic edges, we can write down

$$2B\int_{T_2T_1}(\phi_1)_{z=+0}\,dy=\int_0^{\beta_0}[1-B_2'(\beta)]\,d\beta\int_{B_1(\beta)}^{B_2(\beta)}\frac{d\alpha'}{\sqrt{\{B_2(\beta)-\alpha'\}}}\int_{A_1(\alpha')}^{\beta}\frac{\lambda(\alpha',\beta')\,d\beta'}{\sqrt{(\beta-\beta')}} \tag{99}$$

which, after some transformation,

$$=2\iint_S\left[\left(\sqrt{\left\{\frac{\beta-A_1(\alpha)}{B_2(\beta)-\alpha}\right\}}+\sqrt{\left\{\frac{B_2(\beta)-\alpha}{\beta-A_1(\alpha)}\right\}}\right)\lambda(\alpha,A_1(\alpha))+\right.$$

$$\left.+\int_{A_1(\alpha)}^{\beta}\left(\sqrt{\left\{\frac{\beta-\beta'}{B_2(\beta)-\alpha}\right\}}+\sqrt{\left\{\frac{B_2(\beta)-\alpha}{\beta-\beta'}\right\}}\right)\frac{\partial\lambda}{\partial\beta'}\,d\beta'\right]d\alpha d\beta. \tag{100}$$

The corresponding quantity when the flow is reversed is

$$-2\iint_S\left[\left(\sqrt{\left\{\frac{\beta-A_1(\alpha)}{B_2(\beta)-\alpha}\right\}}+\sqrt{\left\{\frac{B_2(\beta)-\alpha}{\beta-A_1(\alpha)}\right\}}\right)\lambda(B_2(\beta),\beta)-\right.$$

$$\left.-\int_{\alpha}^{B_2(\beta)}\left(\sqrt{\left\{\frac{\alpha'-\alpha}{\beta-A_1(\alpha)}\right\}}+\sqrt{\left\{\frac{\beta-A_1(\alpha)}{\alpha'-\alpha}\right\}}\right)\frac{\partial\lambda}{\partial\alpha'}\,d\alpha'\right]d\alpha d\beta, \tag{101}$$

and it can be verified that, if λ is any linear function of α and β, the magnitudes of these two quantities are unequal in general. Thus it appears probable that Theorem II cannot be generalized in respect of the form of the surface for a general planform.

If we restrict the planform to be symmetrical about the x-axis, then we have at once the almost trivial result that a lift-reversal theorem holds for an incidence variation with y alone and odd in y, since the lift vanishes identically, by symmetry. There appears to be no corresponding result when the incidence is a function of x.

The problem of removing the restriction on the planform has not been solved. The author's personal opinion is that some more general theorem exists for restricted classes of planforms, but that Theorem II is all that is true for general planforms.

Since this paper was written, the theorems of § 2 have been stated by Hayes (ref. **4**). The author has not seen ref. **4**, but he understands that Mr. Hayes has found a counter-example to show that Theorem II is the most general theorem for general planforms.

REFERENCES

1. G. N. Ward, 'Supersonic flow past thin wings, I: General theory', see above, p. 136.
2. W. D. Hayes, *Linearized Supersonic Flow, Thesis for Ph.D. at the California Institute of Technology* (1947), North American Aviation Inc., Report No. AL–222.
3. T. von Kármán, 'Supersonic aerodynamics—principles and applications,' Tenth Wright Brothers Lecture, *J. Aero. Sci.* **14** (1947).
4. W. D. Hayes, 'Reversed flow theorems in supersonic aerodynamics'. *VIIth International Congress of Applied Mechanics*, London (1948).

APPENDIX: LIST OF SYMBOLS

$A_1(\alpha)$, $A_2(\alpha)$	functions defining C, equation (21).
$B_1(\beta)$, $B_2(\beta)$	functions defining C, equation (22).
B	$= \sqrt{(M^2-1)}$.
D, Y, L	rectangular components of the aerodynamic force on the wing.
G_1, G_2	functions depending on the strength of the vortex sheet, equations (40) and (51).
M	Mach number.
U	velocity of the undisturbed stream.
$f(\alpha,\beta)$	$= -\frac{1}{2\pi B}\left(\frac{\partial\phi}{\partial z}\right)_{z=+0}$.
l_1, m_1, n_1	direction cosines of outward normal to upper wing surface ($z = +0$).
l_2, m_2, n_2	direction cosines of outward normal to lower wing surface ($z = -0$).
u, v, w	rectangular components of the disturbance velocity, $U\,\mathrm{grad}\,\phi$.
x, y, z	rectangular Cartesian coordinates.
C	projection of the wing planform boundary on $z = 0$.
R, S, T	regions of the plane $z = 0$ (cf. § 2, Part I).
α, β	$= x \mp By$, characteristic coordinates in $z = 0$.
$(\alpha_0, 0)$, $(0, \beta_0)$, (α_1, β_1), (α_2, β_2), (α_3, β_3), (α_4, β_4)	characteristic coordinates of the points L, M, T_1, T_2, N, P on C respectively (Fig. 1, Part I, or Fig. 4).
$\lambda(\alpha,\beta)$	value of $f(\alpha,\beta)$ on S.
$\mu(\alpha,\beta)$, $\nu(\alpha,\beta)$	values of $f(\alpha,\beta)$ on R.
$\mu_s(\alpha,\beta)$, $\nu_s(\alpha,\beta)$	values of $f(\alpha,\beta)$ on T.
ϕ	potential function such that $(u, v, w) = U\,\mathrm{grad}\,\phi$.
ϕ_0, ϕ_1	parts of ϕ respectively even and odd functions of z.
ρ	density of the undisturbed stream.

Other symbols which do not occur frequently in the text are defined wherever they are used.

ated by
ds that
I is the

above,

lifornia
ort No.

ations,'

VIIth

on the

sheet,

ng sur-

ng sur-

elocity,

N, P

erever